

Flood Forecasting Using Passive Microwave Radiometry in the Zambezi River, Zambia

O.R. Keunen

July 2020



FLOOD FORECASTING USING PASSIVE MICROWAVE RADIOMETRY IN THE ZAMBEZI RIVER, ZAMBIA

A thesis submitted to the Delft University of Technology in partial fulfillment
of the requirements for the degree of

Master of Science in Water Management, Civil Engineering

by

Oscar Rudolf Keunen

July 2020

The work in this thesis was created for the section:



Hydrology
Watermanagement
Faculty of Civil Engineering & Geosciences
Delft University of Technology

Supervisors TU Delft : Ir. Dr. H.C. Winsemius

Ir. Dr. T. Comes

Ir. P. Hulsman

Ir. Dr. R.J. Van der Ent

Supervisors 510.global: Dr. M. Van den Homberg

Dr. S. Giodini

O.R. Keunen: *Flood Forecasting Using Passive Microwave Radiometry in the Zambezi River, Zambia* (2020)

© This work is licensed under the Delft University of Technology

<https://repository.tudelft.nl/islandora/search/?collection=education>.

“Floods are an act of God
but flood damages are acts of Man”

— *Gilbert White, 1945*

ABSTRACT

Humans have always populated in the vicinity of river systems, where the supply of water, nourishment and transportation is obtained from the river. However, inundation is a re-occurring problem and impact of floods are expected to increase due to climate change. Accurate flood forecasting and early warning is critical for disaster risk management. Tackling the problem of forecasting, in data scarce environments, has become increasingly important due to the changing climate. Remotely sensed river monitoring can be an effective, systematic and time-efficient technique to monitor and forecast extreme floods. Conventional flood forecasting systems require extensive data inputs and software to model floods. Moreover, most models rely on discharge data, which is not always available and is less accurate in over-bank flow situations. There is a need for an alternative method which detects riverine inundation, using open-source data and software. This thesis aims to research the use of passive microwave radiometry for the detection, classification and forecasting of inundation.

Brightness temperatures are extracted from the passive microwave radiometry and are converted in a discharge estimator: the C/M-ratio. Surface water has a low emission, thus let the C/M-ratio increase as the surface water percentage in the pixel increases. Sharp increases are observed for over-bank flow conditions. The research combines the identification of inundation with a probability analysis via a quantile regression fit. Flood forecasts can be obtained from an upstream catchment area. In the most ideal situation with a delay of 2,5 hours. This allows for probabilistic early warning decision making, with a lead time up to 14 days. (location specific) Strong Spearman's correlation coefficients between the discharge and C/M-ratio are found (> 0.883). Allowing the model to forecast floods as gauged discharge records do. The model used has a comparable skill to the local GloFas forecast. This research investigated the impact the remote sensed technology could have on the flood forecast, response and warning system. An added model to an Early Action Protocol has the ability to lower uncertainty within decision making and enlarges the intervention window. The advice is to use such a model in combination with other forecasting models such as GloFas.

The challenge using this technology is the integration of hydrological complexity. The method allows for automated, global-covered creation of grid based flood forecasts, independent to cloud coverage. Creating low spatial resolution flood forecasts combined with a probability bound in hours after satellite detection. The method has a high potential for data scarce flood-prone river basins around the world. The future for this technology lies in the global daily availability of the data. With satellite sensors improving, spatial resolution is expected to increase. Allowing for even better flood forecasting ability.

ACKNOWLEDGEMENTS

With the finalizing of this thesis my master Civil Engineering, Water Management at the TU Delft comes to an end. The thesis was part of the graduate internship that was conducted at 510, an initiative of the Netherlands Red Cross.

The graduate internship at 510 allowed me to combine my interest in flood hydrology and remote sensing. With the underlying mindset that research can lead to something bigger. Flood detection in data-scarce environments is hard and, this 'new' method could provide a way of forecasting floods in remote and data-scarce environments. A method which, hopefully, will actually help *the locals* in Zambia to lower their vulnerability to the annual flooding. This motivated me to both make a technological and a social impact for the Red Cross.

Over the course of this thesis I've found myself in quite some strangling situations, to which we had to adapt. Starting with uncertainty about fieldwork in Zambia and eventually the Covid-19 lockdown. But I've enjoyed every single step of the process. I find it incredible how much I've learned over the past 7 months and for that I would like to thank a few:

To start, I would like to show my gratitude for my supervisors at the TU Delft. Hessel Winsemius, my committee chair, has helped and supported me throughout the thesis. With his deep hydrological insights and his technical skill, he always kept me challenged. His ability to motivate and show the worthiness of the research has helped me greatly. Always showing me the positive side of things before our meetings ended. On a more frequent basis I got the chance to discuss the matter and my programming questions with Petra Hulsman. Even in times where we could only meet over Skype, she was able to push me in the right direction. Finally, Tina Comes helped me to structure and finalize the "Follow the Forecast" part of my research. Showing me how to set my work into perspective to the current uses of disaster management in Zambia.

At 510 I had great support for writing my thesis. I would like to thank Marc van den Homberg. His enthusiasm and everlasting "new ideas" helped me to find solutions within my research. Stefania Giodini was a great help in putting this research into perspective in Zambia. During the relatively short time I got to work at 510, I've met a extremely welcoming research community. Who always inspired me to do this research. Especially grateful for the daily "plank" sessions and coffee chats with my fellow interns.

During my *digital* fieldwork in Zambia, I got the chance to meet several people from the Zambian Red Cross Society. I would like to thank Zaitun

Munawar and Wina Wina for their support. They've given me the handles to set this research into perspective in Zambia both in a technical way, but also allowed me to understand the local situation.

In my Master and Bachelor, I've had the privilege to study with close friends. Being able to combine the my educational and social life is a great source of inspiration to me. I would like to show my gratitude to everyone who was a part of that. Lastly, a big thank you and a hug to my family who supported me through-out. Their everlasting support and interest in my research was heartwarming.

Oscar Keunen

July 2020

CONTENTS

	Page
1 INTRODUCTION	1
1.1 Flood risk in Zambia	1
1.2 Disaster Risk Management	2
1.3 Satellite Imagery for Flood protection.....	2
1.4 Passive Microwave Remote Sensing for inundation detection ...	3
1.5 Research Objective	4
1.6 Partners	5
1.7 Reader Guide	6
2 THEORETICAL BACKGROUND	7
2.1 Disaster Risk Management Cycle	7
2.1.1 Early Warning Systems	8
2.1.2 Forecast-based Financing	9
2.2 Prediction Models	10
2.2.1 Probabilistic vs Deterministic Forecasts	10
2.2.2 Lead time & Intervention Window.....	10
2.2.3 Decisions in Flood Forecasting	10
2.2.4 Cost-Benefit of Flood Forecasting & Warning.....	11
2.3 Remote Sensing	11
2.3.1 Remote Sensing for Rivers and Surface water	12
2.4 Microwave Remote Sensing	12
2.4.1 Brightness Temperature	13
2.4.2 Di-electric Constant.....	14
2.4.3 C/M Ratio.....	15
2.5 Current Forecasting Models	17
2.5.1 GloFas.....	17
2.6 Disaster Management analysis	19
3 ZAMBIA & ZAMBEZI RIVER BASIN	23
3.1 General Information.....	23
3.1.1 Climate	23
3.1.2 Population.....	23
3.1.3 Economy.....	24
3.2 Hydrology of the Zambezi River Basin	24
3.2.1 Environmental Characteristics of the Barotse Floodplain	25
3.2.2 Natural Hazards	26
3.3 Area of Interest.....	27
3.4 Early Actions	29
3.5 Zambezi river schematisation.....	30
4 METHODOLOGY.....	33
4.1 Research Input	33
4.1.1 Satellite Imagery	33
4.1.2 Fieldwork data - Online	35
4.1.3 Databases.....	35
4.2 Research Questions - Technology Assessment	36

4.2.1	Identification.....	36
4.2.2	Multi-Annual Analysis.....	38
4.2.3	Timing	39
4.2.4	Skill analysis	42
4.3	Research Question - "Follow the Forecast"	44
4.3.1	"Follow the Forecast" Analysis	44
5	RESULTS	49
5.1	Identification.....	49
5.2	Multi-Annual Analysis.....	53
5.3	Timing	56
5.4	Skill analysis	62
5.4.1	Comparison with GloFas	66
5.5	"Follow the Forecast" Analysis.....	67
5.5.1	Geo-Intelligence workflow	67
5.5.2	Flow of the Forecast	69
5.5.3	Humanitarian Stream Map	71
6	DISCUSSION.....	75
6.1	Hydrological complexities.....	75
6.2	Model	76
6.3	Satellite Data Uncertainty	78
6.4	Decision Making	78
6.5	Implementation	79
6.6	Limitations	80
7	CONCLUSION & RECOMMENDATIONS	81
7.1	Recommendation for further research.....	83
A	POLARISATION COMPARISON.....	89
B	ZAMBEZI RIVER INFORMATION.....	90
C	DISCHARGE VS C/M-RATIO RELATIONSHIP.....	91
D.i	IDENTIFICATION OF UP- AND DOWNSTREAM AREAS	96
D.ii	ROC GRAPHS - SKILL ANALYSIS	98
E	GEO-INTELLIGENCE MODEL STRUCTURE.....	100

ACRONYMS

CSI	Critical Success Rate	43
DMMU	Disaster Management Mitigation Unit	5
DRM	Disaster Risk Management	2
DSS	Disaster Support System	18
EAP	Early Action Protocol	5
EO	Earth Observation	80
ESP	Ensemble Stream-work Prediction	18
EWS	Early Warning System	2
FAR	False Alarm Ratio	43
FBF	Forecast Based Financing	2
FFWRS	Flood Forecasting, Warning and Response Systems	7
GloFas	Global Flood Awareness System	2
GRZ	Government of Republic of Zambia	5
HR	Hit Rate	43
HVS	Humanitarian Value Stream	19
IFRC	International Federation of Red Cross	2
NS	National Society	9
NQT	Normal Quantile Transform	56
OCHA	United Nations Office for Coordination of Humanitarian Affairs	1
PMF	Prinses Margriet Fonds	5
PMRS	Passive Microwave Remote Sensing	3
POD	Probability of Detection	43
POFD	Probability of False Detection	43
RP2	Response Preparedness Phase 2	5
RS	Remote Sensing	7
TWG	Technical Working Group	29
WaSH	WAter Sanitation and Hygiene	71
WARMA	Water Resources Management Authority	5
ZMD	Zambian Meteorological Department	69
ZRCS	Zambian Red Cross Society	4

1

INTRODUCTION

Within the Southern Africa Development Community, Zambia is one of the countries most severely impacted by extreme weather conditions. In fact, it is estimated that 75% of all disasters in Zambia are induced by weather conditions (United Nations, 2016). Floods are the natural hazards with the biggest impact world wide in terms of frequency, geo-spatial distribution and economic impact (United Nations, ISDR, 2017). While both developed and undeveloped countries suffer from the higher frequency of natural disasters (mostly flooding); The low income and undeveloped countries, like Zambia, are hit harder due to the "protection gap" that occurs (UNFCCC). The flood risk of a country is determined by a combination of hazard, exposure and vulnerability. The risk is expected to increase worldwide because of the increase in flood hazard due to climate change. Exposure effects can increase due to the demographic growth. Vulnerability of a specific country can decrease the flood risk, even if the hazard and exposure are increasing. Vulnerability levels are generally high in low-income countries. Therefore it is of utmost importance to lower the vulnerability of low income and developing countries with the effect of a lower flood risk.

1.1 FLOOD RISK IN ZAMBIA

The wet season in Zambia is an annual occurring phenomena. Due to the wet season, an annual frequency in flash and riverine flooding occurs. Effects of the flooding are mostly seen in the displacement and fatalities of the population, loss of agriculture and destruction of infrastructure. Floods in the 2008-2009 season led to one of the most severe impacts, that displaced over 102,000 households, with 31 related deaths. Damaging livelihoods and causing significant threats of waterborne disease in the Western, North – Western provinces (ZRCS, 2019). Floods have a big impact on the agricultural output of the country. In January 2020, United Nations Office for Coordination of Humanitarian Affairs (OCHA) estimated that the Gwembe District recorded a 98% reduction in the maize production, compared to 2018 and the five-year average (OCHA, 2020). The Zambezi is the biggest river in Zambia, covering over 1,390,000 km^2 in Zambia. The Zambezi is one of the largest rivers in Africa. Flood indicative data is scarce due to the limited capacity of data and modelling capacity in developing countries (Schumann et al., 2013).

1.2 DISASTER RISK MANAGEMENT

Disaster Risk Management (DRM) is a program set up to increase the coping capacity of the ones affected by a disaster. It entails the process of implementing the disaster management policy to reduce the risk of a flood. To anticipate to a flood, a well working Early Warning System (EWS) should be in place. An EWS has the goal to give individuals and communities at risk more time to act and reduces the possibility of personal injury, loss of life and damage to property and environment (Teule, 2019). A complete and effective early action system consists of four main pillars: Risk knowledge, Monitoring and warning service, Dissemination and communication and Response capability (Gaillard and Mercer, 2013). There are multiple components in an EWS. First of all, the data collection & monitoring. Continuing, forecasting with the use of hydrological models or local knowledge. Forecasting can be done on different spatial scales and with different lead times. Lastly, there is the decision making, early warning and response. The EWS is best integrated if it enables a multiple-actor and bottom-up approach to the system. Complete and effective early warning systems entail a great interconnectivity between the four pillars (United Nations, ISDR, 2017). EWS's can be implemented on several levels. Global products like Global Flood Awareness System (GloFas) can be used to understand and anticipate on a global scale to disasters. On national scale, products like a linked gauging network or weather linked flood warning systems can be used to obtain more detailed information about a disaster and prevailing flood. A bottom-up example approach is community based disaster risk reduction, supporting and implementing the participation of vulnerable communities in Early Warning. Community based early warning empowers communities with locally developed measures and warning systems to increase coping capacity. The difference between the levels of early warning is large. The attempt of integration of several levels of early warning systems strategies have not resulted in useful products (Šakić Trogrlić et al., 2019). An EWS should lead to a predefined set of early actions. The main problem with the dissemination of early actions is the complex decision making process and the lack of funding for the appropriate action (Šakić Trogrlić and van den Homberg, 2018). Forecast Based Financing (FBF) is a method developed by the International Federation of Red Cross (IFRC) to introduce and place humanitarian funding in the preparation phase to a disaster. The FBF program allows for risk reduction, enhance preparedness and effective DRM and disaster response.

1.3 SATELLITE IMAGERY FOR FLOOD PROTECTION

Satellite imagery is a widely used tool in our society. Daily imagery with a full world coverage is available in all different kind of forms and uses. From the assessment of multi-annual changes of ice coverage on Antarctica to the mapping of deforestation rates in the Amazon, satellite imagery has an enormous power. Remote sensed data is also used in the hydrological sector, for example in the effective measurements of the surface water quantity or

water quality analysis via color spectral insights.

General uses of riverine flood prediction are based on the numerical model type and input data. Basic models run on a numerical 'bucket' model with few input parameters, mostly based on periodically obtained rainfall data and a soil moisture-relation model, like the GloFas model used in Zambia (Alaoui, 2017). Models differ in their complexity. There is a trade-off between the increased spatio-temporal information and the predictive power that is generated. Flood prediction requires quantitative knowledge about infiltration, run-off dynamics and precipitation levels, which are commonly collected at a local or point scale. Scaling this information to a catchment scale comes with a loss of complexity that occurs at catchment scale (Alaoui, 2017).

Current flood warning products used in Zambia are solely based on meteorological data, thus precipitation data, combined with a hydrological and hydraulic model. The latter is used in a global flood model: GloFas. The accuracy of meteorological forecasts varies with lead time, spatial scale of the region of interest and the type of weather being forecasted. Rainfall forecasts can be used to extend the lead time for flood forecasts. However, because forecasts of rainfall for specific locations and timing are not fully accurate, flood forecasts based on rainfall forecasts are often subject to significant uncertainty. Forecast systems such as GloFas are able to give a good indication of extreme discharge peaks in time (ZRCS, 2019). However, their predictive value differs in location, depending on the fit of the hydrological model and the local setting. Insights in, for example, Malawi have shown that the predictive behaviour of GloFas is not sufficient to obtain flood forecasts (Šakić Trogrlić and van den Homberg, 2018).

The question arises, what if this satellite imagery could be used to obtain daily imagery from each catchment worldwide? Optical remote sensing is limited by the effects of cloud cover. As the wavelengths in the optical spectrum are reflected in haze and cloud cover, the predictive capacity of optical imagery is limited.

1.4 PASSIVE MICROWAVE REMOTE SENSING FOR INUNDATION DETECTION

Passive Microwave Remote Sensing (PMRS) is focused on the passive microwave spectrum, which has the advantage of not being blocked by cloud cover. Detecting inundation by means of PMRS has been researched in multiple projects (Brakenridge et al., 2007), (De Groeve and Riva) and (de Groeve, 2010). In the work of Brakenridge et al. the use of the C/M ratio is introduced. The method uses Ka-band radiometry (36,5 GHz, AMSR-E, Horizontally polarized) to obtain the brightness temperature at a given location. The Brightness temperature is converted to the C/M ratio using a correlated cal-

ibration cell to account for diurnal and seasonal fluctuations.

The first result of this research indicates the contrast in brightness temperatures of neighbouring cells (within and outside a floodplain respectively). The results show the ability to obtain inundation in specific areas. Current limitations are seen in the lack of accuracy / resolution, timing and location dependency. The C/M ratio can be related to actual discharge peaks. However, one should keep in mind that the C/M ratio is not able to distinguish between inundation and actual discharge levels. The C/M ratio has not been considered as a predictive flood forecast method yet.

1.5 RESEARCH OBJECTIVE

The ambition of this thesis is to show the opportunities of satellite imagery in flood forecasting on catchment scale. This is done by applying the latter to a use-case as compared to the local possibilities to currently used flood forecasting products: GloFas.

The main objective is to establish and benchmark a forecasting method solely based on upstream PMRS observations for a target area of interest for the Zambian Red Cross Society (ZRCS). By benchmarking it against the current used product, the performance is tested. It can be decided if PMRS could provide additional probabilistic information about flood forecasts next to the current product GloFas. PMRS has been used to monitor floods, but will be used to forecast floods in a probabilistic manner in this thesis. The end-product will consist of a two-fold. On one side, the possibility for integration into a new flood forecasting model is assessed. On the other side, the research is set into perspective by investigating the lead time winning capacity this technology can provide. There are a number of nitpicking research questions that have to be solved in order to find out if this objective can be reached or not.

Main Research Questions:

" Can Satellite Passive Microwave Remote Sensing be used as a trigger for inundation Early Warning System in the Zambezi River, Zambia?"

- **subquestion 1:** Can Passive Microwave Remote Sensing be used to identify inundations?

Although proven in previous research that there is identification capacity, the physical workings of a PMRS model should be tested locally. The correct local areas of interest should be identified and well understood before proceeding to the actual forecasting model.

- **subquestion 2:** To what extent can multi-annual trends in PMRS be related to discharge records?

Multi-annual trends are of importance to test the model and obtain the extreme value analysis of the C/M ratio. The long time-series can be

used to obtain a good understanding of threshold setting using this new method of assessing flooding.

- **subquestion 3:** Could the timing of a flood event be obtained from PMRS?

In flood forecasting, timing is the most important factor when forecasting inundation levels, hence the PMRS model should be creating valid and correct timing outputs. For this, the model is checked to local timing/impact data that verifies how the performance is.

- **subquestion 4:** How does a PMRS based model perform in comparison with GloFas and what skill can a forecast combination with PMRS offer?

The method is tested in comparison to the currently used product. Its performance capacities compared to GloFas are of importance to rate the actual value of the product with the current usage.

- *"Follow the Forecast"*

subquestion 1: How can the lead time of (a combination of) forecasting systems be optimized to enable a maximum implementation time for the actions in an EAP?

In order to set the technology assessment into perspective to the current intervention window of the Early Action Protocol (EAP), an analysis of the timing components in the EAP is executed. The goal is to enlarge the intervention window by either increasing the forecasted lead time with a given uncertainty or optimize the efficiency of the steps within the EAP. Insights into the decision making process are to be obtained.

1.6 PARTNERS

This thesis entails the finalization of the master Water Management with a specialization on Hydrology at the Delft University of Technology. The thesis is written during the graduation internship at 510, an initiative of the Netherlands Red Cross. The research project is part of the integration of the Forecast-based Financing plan for the ZRCS. The project falls within the FBF, Response Preparedness Phase 2 (RP2), Prinses Margriet Fonds (PMF) project, where the aim is to implement an effective EAP for the ZRCS. Within this project, a consortium of partners is working together to realise this EAP, naming a few key partners: Government of Republic of Zambia (GRZ), Water Resources Management Authority (WARMA), Disaster Management Mitigation Unit (DMMU), ZRCS. The project builds on the project ZAMSECUR, in which new methods to monitor and model the Zambezi river are investigated.

1.7 READER GUIDE

For the reader whom is interested or less acquainted with (passive microwave) remote sensing, flood hydrology or disaster management in particular, Chapter 2 provides the technical background supporting this work. In Chapter 3, information about Zambia, the Zambezi river system and the Barotse floodplain are collected. The area of interest is displayed and the reader is informed about the important environmental and hydrological characteristics of the area. Continuing in Chapter 4, where the approach of the research is explained in the Methodology. Chapter 5 contains the main outcomes of the research, backed up by several Appendices to support in visual representation. The results are evaluated and reflected on in Chapter 6. Finally, the conclusion and recommendations for future research are addressed in Chapter 7.

2

THEORETICAL BACKGROUND

This section defines the theoretical background of this thesis. It touches upon the different theoretical backgrounds used. First, introducing some basic concepts of the Disaster Risk Management Cycle. Secondly, introducing the basics of Remote Sensing, the backbone of the C/M ratio (Brakenridge et al., 2007). Furthermore, it provides an insight into early action systems for flood forecasting.

2.1 DISASTER RISK MANAGEMENT CYCLE

The DRM cycle consists of four main stages. Reduction, Readiness, Response and Recovery. The phases can be split into two time frames. The Reduction and Readiness are in the pre-disaster stage. Response and recovery both fit in the post-disaster stage. The pre-disaster stage is focused on activities and measures that ensure an effective coping capacity and response. The post-disaster phase is include rescue, first aid and evacuation practices, but also look at the recovery in the aftermath of a natural disaster (ADPC, 2005). Remote Sensing (RS) data is a viable source of information to decision makers, as it can help to understand the spatial phenomena of the disaster (Joyce et al., 2009). Some concrete examples of the implementation of the DRM cycle focused on floods are:

Reduction phase: Construction of flood control reservoirs or the building of dikes to protect the vulnerable communities.

Readiness: Construction of a meteorological system that can give accurate meteorological data. Creation of an Early Action System in which includes all different aspects of Readiness.

Response: Rescue, first aid and construction of temporal shelters.

Recovery: rehabilitation planning, disaster resistant reconstruction. Funding and resource support for rehabilitation and reconstruction activities (ADPC, 2005).

A disaster management strategy that is commonly adapted is a Flood Forecasting, Warning and Response Systems (FFWRS). A FFWRS enables the user to act in advance of a disaster and create lead time to mitigate the risk (Verkade and Werner, 2011). An FFWRS is used to create time for residents & NGO's or authorities to act (Parker and Fordham, 1996). A FFWRS consists of three main subsystems. The three subsystems are forecasting subsystem, decision subsystem and the warning response subsystem. The subsystems can

be found in Figure 2.1. The forecasting subsystem generates a probabilistic or deterministic forecast from several input parameters. The (hydrological) parameters can be of different types, both deterministic and probabilistic. The second subsystem is the decision subsystem. This subsystem contains the warning protocol and mitigation actions to reduce the losses of floods. Finally there is the warning response subsystem in which the actual implementation of the actions is executed (Parker and Fordham, 1996) & (Verkade and Werner, 2011).

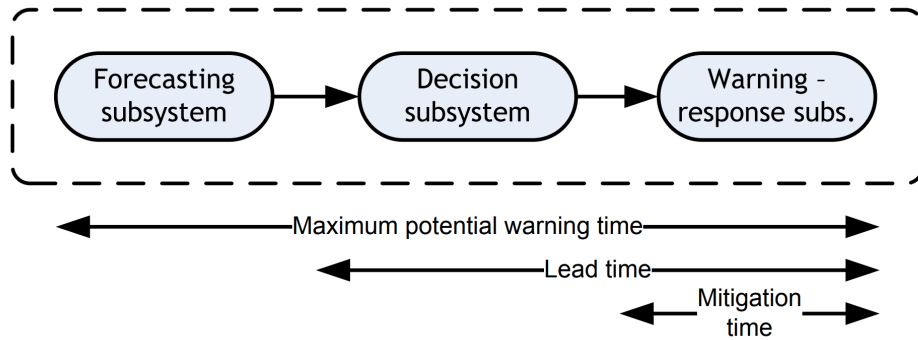


Figure 2.1: FFWRs scheme of a monitoring system in flood forecasting (Verkade and Werner, 2011)

2.1.1 Early Warning Systems

Flood protection measures are in place prevent flooding of people and their assets. If resources for protection are not available the risk can be managed through preparedness, coping capacity and response time. The use of an EAP can improve the preparedness and lower the response time, thus lowering the vulnerability to flood risk. Four main pillars are defined that should be obtained in an effective EAP:

1. Risk Knowledge
2. Monitoring & Warning Service
3. Dissemination and Communication
4. Response Capability (United Nations, ISDR, 2017)

Next to the main pillars, a risk assessment of the vulnerable area should be conducted. Identifying the actual coping capacity of the people in place allows to direct the EAP in the direction of those most in need of help. An EAP should be build up at several levels, from local to district to national. The EWS is based on monitoring and warning from a reliable forecasting source. The need for continuous monitoring to generate accurate warnings is stressed by (United Nations, ISDR, 2017). There are two aspects of this monitoring and warning cycle that have shown to be sensitive to uncertainty namely; 1. the level of uncertainty of a forecast is not represented. 2. The communication of these uncertainty levels with end-users in a simple manner is a challenge.

2.1.2 Forecast-based Financing

Humanitarian organisations aim to respond in the early phase of the DRM. In order to accommodate to this early response the EWEA approach is used. IFRC defines EWEA as *"routinely taking action before a disaster or health emergency happens, making full use of the scientific information on all timescales"* (Rut). Current uses of scientific knowledge, technology and data result in an increase in the quality of the disaster preparedness and anticipation to natural disasters (IFRC, 2008). In 2008, IFRC launched the FbF-pilot to create this new methodology to address the DRM. FbF is explained by the IFRC as *"FbF is an approach which enables access to humanitarian funding for early action, that can be taken based on meteorological forecast information, combined with risk analysis, to prepare for extreme weather events. The goal of FbF is to anticipate disasters, prevent their impact, if possible, and reduce human suffering and losses"* (IFRC, 2008). The new methodology is seen as the new approach to prepare, deliver and respond to natural disasters. The FbF approach is in line with the global goals set by the United Nations, also referred to as the Sustainable Development Goals, as there is a prioritization on investment in water, agriculture and climate change. It is seen merely as a preparedness and reaction strategy but next to the latter also functions as a framework to decrease climate change.

FbF is set up in two main phases. The first phase consists of determining and agreeing on the pre-set activities and roles that play a role when a trigger reaches a threshold. The responsibilities, actions undertaken and regulations set are agreed on and documented in an EAP or Standard Operating Procedure. In setting up these protocols, the IFRC works closely together with national and international parts of the Red Cross and with the local government. The second phase of the FbF consists of ensuring that the resources named are supplied within the correct time-frame. In here the IFRC works as the financial mechanism to fund the activities included in the EAP. The key element of this section is the guaranteed allocation of funds for early action, once the IFRC and the National Society (NS)'s has an approved and validated EAP. Financial allocations are automatically transferred according to a pre-agreed forecast trigger, that indicates the potential for severe negative impacts on the most vulnerable population. The scheme of actions that comprise the FbF methodology are visualised in Figure 2.2



Figure 2.2: Flow of the FbF process. source: media.ifrc.org

2.2 PREDICTION MODELS

Creating a well working FFWRs enables the user to act in advance of the flood disaster. A FFWRs consists of three main subsystems. In order to assess the hydrological skill of a new product, one should assess several aspects of such a system. The following section entails a description of the most important aspects of prediction models and aspects of hydrological modeling.

2.2.1 Probabilistic vs Deterministic Forecasts

The different information source that is used has an effect on the type of forecast that is created. By using information that has an either probabilistic or deterministic nature, the nature of the decision system is determined. Deterministic models rely on thresholds which automatically initiate warning responses. The decision is then dependent on the threshold and system that is designed in the forecast subsystem (Verkade and Werner, 2011). A probability designed system can also be related to a specific threshold. Although this threshold is reached, an additional set of information is provided, namely the probability or probability of exceedance. This extra piece of information allows the user to introduce an optimal probability threshold to initiate a response (Parker and Fordham, 1996). With the extra level of information comes more decision making challenges. Which probabilistic information range is "right"? Or what is the best probability to start early action? (Dale et al., 2014).

2.2.2 Lead time & Intervention Window

The lead time is defined by the Red Cross as: "The length of time between the issuance of a forecast and the occurrence of the disaster is forecasted to happen." (GRC, 2017). The lead time is thus initiated by the moment the forecast is gathered. The lead time can also be linked to a probability of occurrence to inform with more detail about the probability that a specific disaster occurred. Enlarging the lead time is important in early action. A lead times is the time for aid workers time to prepare, disseminate more information and take appropriate action / respond on the emergency. The intervention window is the window of time in which aid workers can make this intervention, given a certain uncertainty. The intervention window is bounded by the time that specific actions take. For example, the decision to evacuate people or livestock can only be made if the time it takes to execute the evacuation is still available. Thus the intervention window is limited.

2.2.3 Decisions in Flood Forecasting

Decisions in flood forecasting are based on the output of the forecasting model. Such a forecasting model could be both probabilistic and deterministic. Decisions can be made based on probability levels, acquired lead time, additional ground truth data or the ability to deploy actions. In most cases a

pre-set manual will make sure the appropriate decision is made for a specific threshold level. There is an important trade-off that occurs in flood forecasting decision making. The trade-off is induced by the increase of certainty when a forecast is given with a lower lead time. The trade-off between a quick response, and dealing with a higher uncertainty. Or waiting for more certainty but having the chance not to be able to introduce the appropriate action (Carsell et al., 2004). Next to the time trade-off, one can also trade-off between cost & benefit for each action.

2.2.4 Cost-Benefit of Flood Forecasting & Warning

Verkade et al. calculated the benefits of flood forecasting from a financial point of view. The goal is to optimize the cost vs. benefit of specific actions that are taken. Four situations were taken into account. A perfect forecast, a deterministic forecast, a probabilistic forecast or no forecast. The result of the forecasted situations gave insight in the optimal way of forecasting from a cost/loss or benefit ratio. There occurs a trade-off between the benefits and losses of the reduction of risk. For all different tested situations the probabilistic forecast resulted in a better flood risk index, and a lower cost to loss ratio (Verkade and Werner, 2011).

2.3 REMOTE SENSING

The process of remote sensing is the gathering and processing of information via devices that are remotely located. This thesis is specified on satellite remote sensing (European Space Agency (ESA), 2015). In satellite remote sensing the electromagnetic radiation is captured by a sensor. Electromagnetic radiation sensors capture signals in a broad range of wavelengths. Depending on the resolution of the electromagnetic radiation sensor. There are three main resolutions that play an important role in remote sensing, namely: spatial resolution, spectral resolution, temporal resolution (Neisingh, W., 2018), (CIMSS, 2015). This thesis is focused on the microwave spectrum (wavelengths: 10^6 nm - 1 m or a frequency: 10^{10} Hz - 10^6 Hz).

Spatial Resolution

Spatial resolution refers to the size of a single cell in an image. The smallest resolution length of a cell is expressed in *m* or *km* depending on the size. A cell resolution of 500 m refers to a cell with the area of $500m \times 500m$. Spatial resolution is of importance as it defines the resolution of a single cell, or input. For Microwave Remote sensing this resolution should be minimized in order to distinguish best between two cells (CIMSS, 2015).

Spectral Resolution

Spectral resolution determines the range and range size of wavelengths measured by the satellite sensor. Wavelengths occur in a huge range, from $1m - 10,000m$ for optical wavelengths and up to $30km$ for micro-wavelengths.

The spectral resolution defines the range in which wavelengths are absorbed / measured by the sensor. Most remote sensing satellites record the energy over multiple wavelengths with varying spectral resolutions. (multi-spectral sensors). Highly advanced new sensors (hyper-spectral sensors) detect hundreds of narrow spectral bands through the electromagnetic spectrum. Introducing a new level of discrimination between target bands with their corresponding spectral response. (CIMSS, 2015)

Temporal Resolution

Temporal resolution defines the timing at which images are captured. The timing between images (frequency of an overpass) defines the timing of which an output of an image can be created. In flood prediction, the temporal resolution of a satellite product defines the timing in which floods can be detected. The time-frame of an overpass is seen as the δT_0 when timing of a product is defined. Ideally, diurnal or semi-diurnal temporal resolution is needed for flood prediction. Temporal resolution differs per satellite and location on earth (CIMSS, 2015).

2.3.1 Remote Sensing for Rivers and Surface water

Applications of RS in rivers or surface waters are mostly based on determining color or temperature of water. Color differences in the optical spectrum are used to allocate water in a specific location. RS are of increasingly important in understanding the spatio-temporal dynamics of water quantity and quality. Applications of RS are used in simulating water management and hydrology scenarios. There are several implementations of the technique which are shortly touched upon, to give an insight in the size and usage of RS (Kawsar, 2015).

One emerging problem in the context of *surface water quantity*, is the lack of temporal and spatial ground data. RS allows the user to look at a multi-temporal timescale to a problem. An example of this is the NDWI (Normalized Difference Water Index), which allows one to visualize, locate and quantify surface water bodies from satellite data (Kawsar, 2015). RS is also used to extract river widths. As discussed in Chapter 4, the software RivWidthCloud, can extract river width changes from RS data (Yang et al., 2019).

2.4 MICROWAVE REMOTE SENSING

Microwave RS comprises two types of remote sensing, namely: passive and active remote sensing. Due to the longer wavelength the microwave radiation can penetrate through clouds, haze, dust and rainfall. The wavelengths are less susceptible to atmospheric scattering than the shorter wavelengths. This entails the big advantage over optical remote sensing, its ability to collect data under all environmental conditions. Passive microwave sensors

detect naturally emitted microwave radiation. Compared to an active system, where the radiation is actively created and the reflection is received (eg. synthetic active radar). The level of natural emitted radiation is related to the temperature and moisture level of the emitant. The emitant in this case is the soil or surface water seen by satellites. Microwave RS has been integrated in the first Landsat missions and on-wards. Therefore a data-set of close to 40 years of daily data is gathered. Passive RS is preferred over active RS due to its more consistent sensor characteristic.

2.4.1 Brightness Temperature

The brightness temperature is the observed parameter measured by the radiometers. It is merely a observational quantity than a physical quantity (Neisingh, W., 2018). The brightness temperature is expressed in units of temperature of an equivalent black body. The brightness temperature of microwave wavelengths is approximated with the Rayleigh-Jeans approximation. (Accurate for radiance much greater than the peak of the black body radiation formula). The Rayleigh-Jeans approximation is given by the following formula:

$$\mathcal{T}_k = \frac{\lambda^4}{2kc} * L_\lambda \quad (2.1)$$

k = Plancks constant, c is speed of light, ϵ is the emissivity, T_k is the kinetic temperature, λ is the wavelength. L is the Luminosity.

The equation is related to the kinetic temperature through the emisivity of the material. I.e. its ability to emit radiation. Passive microwave brightness temperature can be used to monitor temperature changes related to the emissivity property of the soil or water.

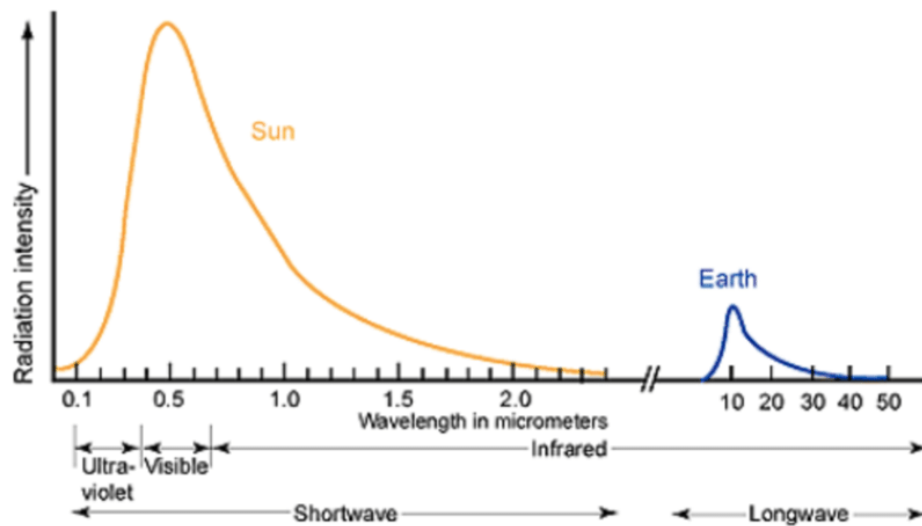
$$T_b = \epsilon * T_k \quad (2.2)$$

The emissivity (ϵ) can be defined as the relative brightness of an object compared to its actual brightness following this formula:

$$\epsilon = \frac{M_e}{M_e^o} \quad (2.3)$$

With M_e being the radiant flux of the surface and M_e^o the radiant flux of a black body with the same temperature as that surface. Materials do not behave like a black body but the property of emissivity does differ per material. This allows the identification between soil or surface water.

$$T_{b,v} = \frac{\lambda}{\kappa} * B_v \quad (2.4)$$



d

Figure 2.3: Thermo-electric black body radiation from the Sun and the Earth. Figure showing the wavelength bands at which the passive radiation is emitted (source: (Macdonald, 2019))

2.4.2 Di-electric Constant

Microwaves are electromagnetic waves, traveling through a space. Satellites gather electromagnetic waves that have traveled through space, the atmosphere and earth's crust. The properties a specific soil has describes how the wave will propagate and interact. In PMRS the important factor to take into account is the electric permittivity or dielectric property of a soil in the earth's crust. Describing the ability of a molecular structure to store or release energy in an electric field.

Solid non-conducting (di-electric) materials found on earth can be explained by their relative permittivity. Surface water has a higher relative permittivity compared to solids, due to its conductive behaviour. The free rotation of a water molecules allows it to align the dipole of the molecule in the electromagnetic field. When a current is applied to water the conductive behaviour allows it to conduct energy. This high di-electric property of water allows it to influence a soil it comes in contact with. When water integrates with a soil the effective di-electric property of the soil enlarges. The di-electric property of a soil or water is an important part of the emission and scattering properties of the soil (De Groeve and Riva, 2009b). showed that passive microwaves are greatly affected by the di-electric properties of a soil. The effect has an impact on the so named: penetration depth of a microwave signal.

Penetration Depth

The penetration depth refers to the ability of a microwave to penetrate the soil to a specific depth. Waves with larger wavelengths penetrate deeper than the shorter wavelengths (Owe and Van de Griend, 1998). The larger

wavelengths have low frequencies while the short wavelengths have a large frequency. In the case of riverine flooding, the aim is not to assess the depth of an inundation. As the inundation might be very shallow. So low penetration depths are required.

2.4.3 C/M Ratio

The C/M-ratio is a measurement quantity of passive microwaves as defined in research of multiple researchers. (Brakenridge et al., 2007), (De Groeve and Riva, 2009b), (De Groeve, 2010). The C/M ratio as defined is the backbone of the thesis, as it is the main tool to use PMRS to observe inundation.

The C/M-ratio is a measurement quantity of passive microwaves as defined in research (Brakenridge et al., 2007). Brakenridge defines the flood prediction method using the Calibration Cell 'C' and Measurement Cell 'M'. These cells are used to estimate the discharge estimator 'HR' (Brakenridge et al., 2007) & (De Groeve and Riva, 2009b).

$$T_{B,measurement\ cell} = (1 - W) * T_{B,land} + W * T_{B,water} \quad (2.5)$$

W resembles the portion of water within the pixel. The T components are defined in [K]. If the physical temperature is constant, changes in brightness temperature are linked to the surface water extent within the pixel. Direct relation between brightness temperature and surface water area cannot be drawn indisputable. Arguments for this relation and its indisputable relation are discussed by (Neisingh, W., 2018). Brightness temperature measurements are influenced by factors like physical temperature, emissivity differences and atmospheric moisture. Their relative contribution cannot be accounted but these factors are assumed to be constant over a large distances. the hypothesis underlying the C/M ratio method is that these influencing factors co-vary enough in the limited space encompassing the "C" and "M" area, that they cancel out when combined. So to cancel this relative contribution of the factors, a division between a 'wet' and 'dry' cell is made.

$$T_{B,measurement\ cell} = T_{B,measurement} * ((1 - w)\epsilon_{land} + W\epsilon_{water}) \quad (2.6)$$

$$T_{B,calibration} = T_{B,land} = T_{B,calibration} * \epsilon_{land} \quad (2.7)$$

The assumption is made that nearby pixels have the same emissivity rate for land (ϵ_{land}), so follows from (de Groeve, 2010):

$$\epsilon_{land,measurement} = \epsilon_{land,calibration} \approx \epsilon_{land},$$

$$T_{B,measurement\ cell} \approx T_{B,calibration\ cell}$$

By comparing to the calibration cell, (Brakenridge et al., 2007), (de Groeve, 2010) integrated a correction for the diurnal and seasonal changes in brightness temperature in a given area. The measurement cell 'M' is defined as a cell that is clearly affected by fluvial change during a period of flood. The measurement cell shows a clear change in brightness temperature when inundated. Also before referred to as the 'wet' cell. The calibration cell 'C' is defined as the cell that is not affected by fluvial change, attributable to surface water changes, thus no expected change in brightness temperature is observed. Referred to as the 'dry' cell. A comparison is also generated by using a pre selected 'C' Cell. This gave no better output.

$$HR_{C/M} = \frac{T_{B,calibration\ cell}}{T_{B,measurement\ cell}} = \frac{M}{C} \quad (2.8)$$

(de Groeve, 2010) defined the magnitude of flooding by comparing the number of standard deviations and mean (average) of the time-series. in eq. 2.9.

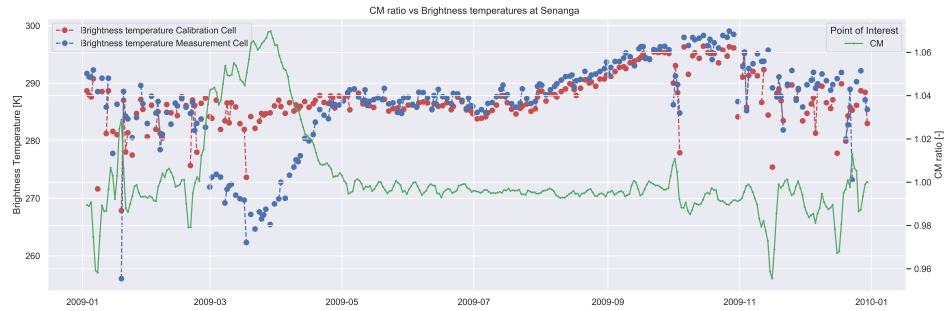


Figure 2.4: Example of the time series of Brightness Temperature at the 'M' measurement location (M) and at the 'C' calibration location (C), combined with the C/M-ratio as defined by (Brakenridge et al., 2007). Data from test location Senanga for the year 2009. Peak of C/M ratio correspond to the true flood disaster in 2009. Location: Senanga (Point of Interest as described in Figure 4.3(own work))

(Brakenridge et al., 2007) & (de Groeve, 2010) & (Neisingh, W., 2018) defined an optimum frequency for the C/M ratio as 36,5-GHz. The incidence angle at which the C/M ratio is determined is 54,8°. The AMSR-E data is used as the profound source of data to do the first test with. AMSR-E data gives a global data set, freely available through the MEaSURES program. This allows the work to be extended to other locations. The H(orizontal) polarization and D(escending) (night) orbit with a spatial resolution of 25 km and a temporal resolution of 1 day (above the 30°latitude) were chosen to be the most optimal conditions. The night overpass occurs at 12:30 - 1:30 AM. The night overpasses have more constant land surface temperature, hence show better differentiation between emissivity differences. In Appendix A, polarisation differences are explained.

(Brakenridge et al., 2007), defined four main indicators for choosing the calibration- and measurement cell.

1. C must be located near M, within the correlation length scale of the physical temperature. This allows the T to be cancelled in the paired ratio.
2. C and M are close there is no time difference in the moments acquired by the satellite sensor.
3. C is an area that is least affected by fluvial change. M is within the range of the specified river. C is unaffected by river width change.
4. M is located in a area that shows a clear change when fluvial change is observed.

(De Groeve and Riva, 2009a) applied an automatic selection of the 'C' alibration cell based on the brightness temperature as the hottest value in neighbouring cells. As the cell with the highest brightness temperature nearby is by definition the 'driest cell, this is the best method for automatic selection of the calibration cell. In the model used in this thesis the highest surrounding brightness temperature is found by finding the surrounding cell with the lowest correlation coefficient. By applying this method item 1, 2 and 3 of the summation above are met. The 'M' easurement cell is handpicked and selected within the permanent river stream to meet requirement 4.

To obtain flood extent information, a 'Wet' input cell can be introduced (Neisingh, W., 2018). In theory this allows the user to interpret the water body by integrating the Digital Elevation Map and the full bank capacity. This is not taken into account since the correctness of using the 'wet' cell only holds for an constant existing water body that is located close to the area of interest. For locations that are too remote from the area of interest, there is a too big difference in physical temperature, emissivity differences and atmospheric moisture to be able to compare to the 'Wet' cell location. For this research location it is found that no 'wet' cell can be obtained in a close enough perimeter to obtain the same physical properties as the area of interest. Therefore the CMC ratio defined by (Neisingh, W., 2018) is not taken into account. Furthermore, the research in this thesis does not need clarification on flood extent as it is focussed on predictions based on up-stream observations.

2.5 CURRENT FORECASTING MODELS

2.5.1 GloFas

Most flood warning or forecasting systems are based on a short term model that can use little amount of inputs to predict discharge levels. GloFas is the current flood forecasting tool used by the Zambian Red Cross to detect floods in Zambia. GloFas is a worldwide flood prediction model. It couples weather forecasts (precipitation data) with a hydrological model on which it provides a hydrograph of all rivers worldwide. GloFas uses the forecast

data from the European Centre for Medium-Range Weather Forecasts. The workings of the system are visualized in Figure 2.5. The input parameters are shown in yellow. Combining the meteorological precipitation data with initial conditions and soil/DEM/topography. The model runs a forecast, hydrological model and post-processing tool (in blue) in order to produce the web interface visualization. GloFas is able to produce 30 day forecasts of flooding, with associated probability of exceedances. The probability of exceedances are calculated by comparing the 30 day forecast with the realtime forecast. The maximum product lead time that is offered is 30 days. But daily forecast data is provided up to 15 days in advance, given a certain probability. GloFas its performance differs per country, as the hydrological model is not country specific. Its function in Zambia is tested upon ground-truth discharge data. The GloFas model is tested with the so called Continuous Ranked Probability Skill Score. This score is calculated against persistence or climatology to give an skill evaluation per lead time (ECMWF, 2019).

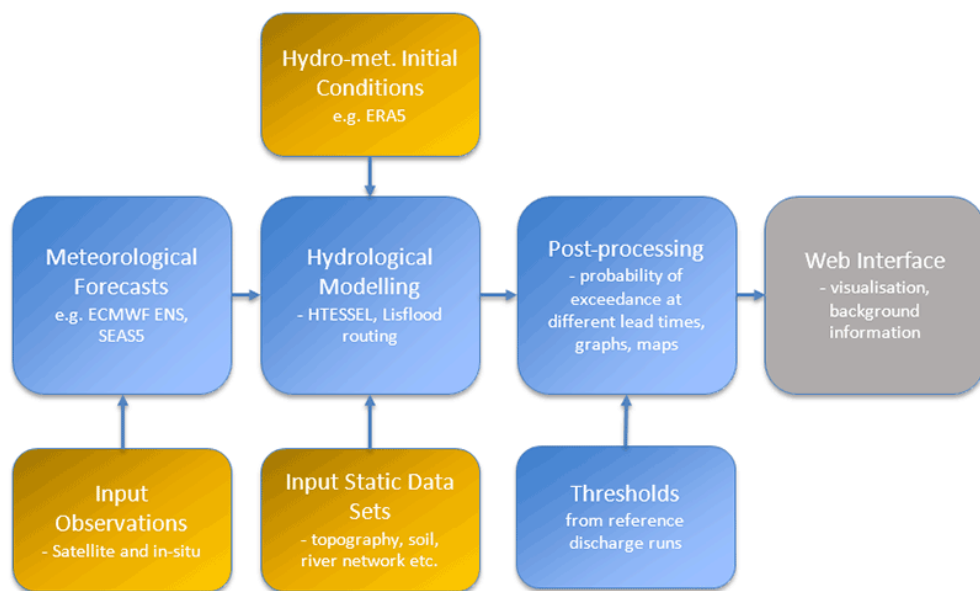


Figure 2.5: GloFas system: input = yellow, model = blue, output = grey
 source: <https://www.globalfloods.eu/>

The EAP in Zambia is based on GloFas. The triggers for this EAP are defined using a multi-annual extreme value analysis. Providing the 60, 70, 80 percentile of the discharge levels. The percentiles are determined from the 10 year returning flood maximum. The linked threshold levels can be used as triggers in the EAP. Medium-time ranged forecasted could reduce flood related losses as they provide a larger intervention window for the decision making processes, compared to shorter, more accurate, forecasts (Thiemig et al., 2015). A high leadtime is connected to a high uncertainty level. To overcome this problem an Ensemble Stream-work Prediction (ESP) can be created. An ESP uses numerical weather productions and a hydrological model to obtain a forecast of the future state of the weather. GloFas is such a system that integrates numerical weather predictions in its model to obtain a forecast. It can be used as the input for the Disaster Support System (DSS) of the Early Action Protocol to determine whether actions, triggers

or funding needs to be applied. The value of an ESP over a single forecast is its ability to generate a probability of occurrence of an extreme weather event. This probabilistic values can be used to identify severeness or interpret thresholds. The performance of GloFas is used as a test benchmark in the hydrological skill assessment, as it is the current product used in Zambia for flood forecasting.

2.6 DISASTER MANAGEMENT ANALYSIS

Several approaches exist in the analysis of disaster management systems. Focusing on different aspects of the disaster management chain, or more focusing on a process or topic. There are three main subsystems of information flow that play a role in the Zambian EAP. The different subsystems as referred to in Figure 2.1, can be analysed by using different techniques.

The forecasting subsystem is entails the whole monitoring and forecasting part of an EAP. There is a rise of online accessible technologies combined with the numerous ways of (pre)-processing functions and the online available geo-spatial data. Solutions to geo-spatial problems require several geo-processing functions and resources, some of which cannot be provided by a single computing system (Ohuru R., 2019). A geo-intelligence workflow is used to create a framework in which the complex geo-processing functions and data sources are combined. The visual representation of the geo-intelligence workflow helped the creation, sharing, understanding and integration of the software processing of geodata (Lemmens et al., 2018). The geo-intelligence workflow allows for organisations to standardize the workflow of a humanitarian process. Evaluating the moment the data comes into the server to the actual release of a trigger.

The decision and response subsystems as displayed in Figure 2.1 contain a timing component that has to be taken into account when analysing the disaster management.

For the FFWRS decision subsystem it is of importance to map the tree of decisions in a system. The so called, forecast information flow diagram which visualizes the flow of information when a trigger is communicated and disseminated. The overview allows the user to identify the decision making tree, flow of information and the target points of improvement of efficiency. In large humanitarian structures it is of importance to visualize the flow of forecast information to create understanding of the system (I.N. Streefkerk, 2020). By assesing the decision framework the nature of the decisions can be evaluated. In disaster decision making there consists a trade-off between uncertainty levels and intervention time (Verkade and Werner, 2011). In this work it is assumed that decisions are solely made based on the forecasted information, policy and procedures in place.

Humanitarian Value Stream (HVS) is a technique to map the chain of a humanitarian stream and quantify its value. It can be implemented in a

range of different humanitarian aid subjects, as to protocols. HVS allows for efficient gathering of operational data and highlights the weaknesses and opportunities of the studied system (Salvadó et al., 2015). HVS entails a field-oriented approach to map the timing and value of each specific segment in the process. The field oriented approach can be organised over Skype as long as the main stakeholders of the humanitarian stream are involved in the interviews. The goal is to improve the organisational structure of the EAP by looking at the four lean principles: Value, Value stream, Flow and Pull. As the value of a step is hard to implement and investigate remotely, an adjusted HVS technique will be implemented in the Methodology.

For improvement in long-term strategies and robustness of the EAP, the following theory is described. Figure 2.6 displays the criteria for a signal monitoring system to support adaptive planning. The three main criteria are: Saliency, Credibility and Legitimacy. Within the main criteria there are a few sub criteria. Saliency: Measureability, Timeliness, Reliability. Credibility: Convincibility and Institutional Connectivity (Haasnoot et al., 2018). By assessing a monitoring system on the later named criteria the robustness of the system as a whole can be tested.

Saliency refers to the actual needs of the end user. With the measureability of the product. The time component that indicates the intervention window that is created. The reliability of the product concerns the probability that the product gives wrong or incorrect signals. The credibility refers to the technical believability of a product. The signal monitoring system should be convinceable in a technical and scientific manner. The user will 'trust' the system more if the Convincibility of the system is high. Institutional connectivity is reached if the system is advocated by the different institutions involved, thus being accepted by a political, social, technological and decision context (Haasnoot et al., 2018).

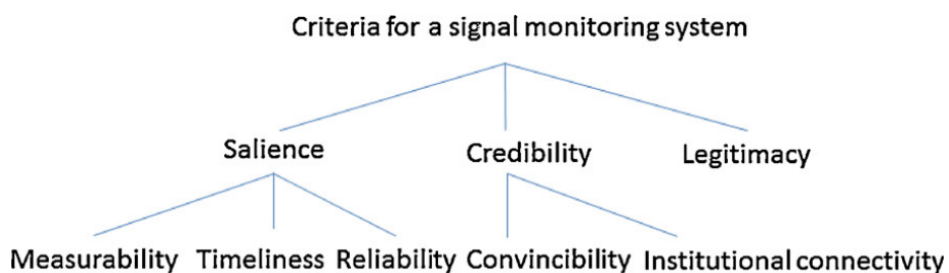


Figure 2.6: Overview of the criteria for signal monitoring within a system. (Haasnoot et al., 2018)

The three theories of analysing the disaster management policy of the EAP can be shortly formulated in Table 2.1:

Geo-intelligence workflow	<i>Covering the 'geo'-intelligence workflow that should be followed to combine the separate data sources and techniques to come to a trigger evaluation.</i>
Forecast Information Flow diagram	<i>Visualizing the flow of information when a trigger is communicated and disseminated</i>
Humanitarian (Value) Stream Mapping	<i>Visualizing the flows of information and goods when a specific action is undertaken.</i>

Table 2.1: Disaster Management Analysis steps

3

ZAMBIA & ZAMBEZI RIVER BASIN

This section entails the general information about Zambia and the Zambezi river Basin. Especially focus is set on the inundation of the flood prone areas of the Zambezi river basin. Further insights in Zambian statistics are displayed in Appendix B

3.1 GENERAL INFORMATION

Zambia is a landlocked country in the south-central part of Africa. The official name of the country is the Republic of Zambia. Zambia is surrounded by eight countries namely; Angola, Namibia, Botswana, Zimbabwe, Mozambique, Malawi, Tanzania and the Democratic Republic of the Congo. The country stretches over an area of 752,618 km^2 .

3.1.1 Climate

The climate of Zambia is classified as predominantly Cwa (Temperate, dry winter, hot summer) following the Köppen-Geiger climate classification. Other classifications do emerge in parts of the country, being; Aw (Tropical Savannah), BSh (Arid, Steppe, Hot) and Cwb (Temperate, dry winter, warm summer) Two dominant seasons regulate the climate pattern. From November to April the rain season occurs, which corresponds to the summer. During the winter, the dry season occurs. Which occurs from May to October. The average annual temperature in the Capital, Lusaka, is 20.3 °C. The average rainfall is 831 mm. Extensive figures about climatology in the Zambezi river system are given in Appendix B.

3.1.2 Population

Zambia has a population of 17,8 million people. The life expectancy is 55,3 years old. The fertility rate is 5,3 births/woman. High levels of inequality occur in Zambia. The inequality is mostly seen in the health care, education and administrative deficiencies. The Barotse floodplain is an area characterized by widespread poverty. The Western provinces is among the most poor of Zambia. The poverty is mostly due to the remoteness, difficult climate and low coping capacity. The diversity of the Zambian population is visualised in the population pyramid in Figure 3.1 (United Nations, 2015).

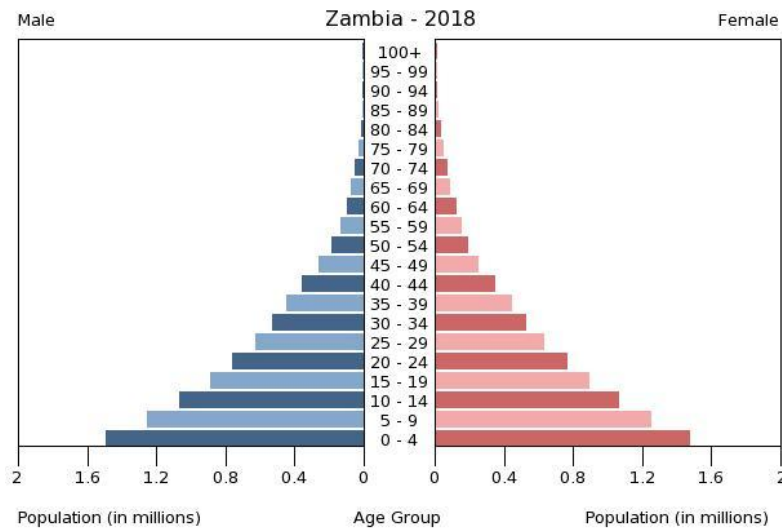


Figure 3.1: Demographic population pyramid of Zambia source: CIA

3.1.3 Economy

The economy of Zambia is based on its mineral and agricultural wealth. In the northern part of Zambia copper, cobalt, uranium ores are mined. Furthermore there is a sub-economy running on gold, diamond and manganese. The GDP per capita of Zambia is 1,491 \$. The economic strengths of Zambia are its export products from agriculture and mining, furthermore there is significant hydroelectric potential in the area. Which is not exploited fully at the moment. Being a landlocked country makes Zambia reliant on the export routes of neighbouring countries. Electricity generation is insufficient and unreliable, putting pressure on the economy. Due to the strong mining sector is a growth of the economy observed and expected to continue in 2020 (Coface, 2020).

3.2 HYDROLOGY OF THE ZAMBEZI RIVER BASIN

The Zambezi river basin originates Northern Zambia, from which it flows through Angola, trans-boundary and eventually back to Zambia. It enters the Indian Ocean at the East coast of Mozambique. The Zambezi connects to three tributaries namely; Dongwe, Kabompo and Lungwebungu. The Zambezi has a total length of over 1,390,000 km^2 . It is classified as the fourth largest river in the African continent, after the Congo, Nile and Niger river basin.

The Zambezi in the Western province is characterised by the Barotse Floodplain. The Barotse Floodplain, also called the Bulozzi floodplain or Zambezi floodplain, is one of the biggest wetlands in Africa. As seen in Figure 3.6d, the Barotse floodplain originates when the Lungwebungu river joins the Zambezi. The end of the floodplain is seen near the city of Senanga. The

Barotse floodplain has a low water area of 537 km^2 and a flooded area of $10,752 \text{ km}^2$.

Zambia is dealing with 2 main flood types namely, flash floods and riverine floods. Flash floods occur when excess rainfall does not infiltrate and continues as runoff in a stream or channel. Due to the dry climate of Zambia, soil is not able to take up large quantities of precipitation and overland flow occurs. Flash floods occur in a short period of time and mostly have a surprising effect. Therefore flash floods often cause greater loss of life than River floods. Riverine flooding occurs in the larger river systems. Mostly in the more wet parts of the country (Zambezi). Excess rainfall collects over a long period of time in the rivers and slow water-level rise occurs over a longer river stretch. When inundated, river flooding can cause great damage as the severe quantity of water is larger compared to flash floods. Riverine floods occur over a longer time period.

3.2.1 Environmental Characteristics of the Barotse Floodplain

The barotse floodplain is located in the Western and North-Western province in Zambia. The Floodplain stretches over an area of approximately 230 km downstream. Within the 30-50 km wide wetland the Upper Zambezi river flows. The Zambezi enters the wetland at Lukulu (where the Kabompo and the Lungwebungu rivers meet) and exists the wetland at Senanga. The main body of the wetland has an area of 5500 km^2 . When flooded the total area of land covered with water is over $10,000 \text{ km}^2$, taking into account the tributaries. Peak in flooding is mostly seen in 2 to 3 months after the peak in the rainy season. (April - May). The wetland is made up of many smaller lagoons, even in periods of dry season. The floodplain is mainly comprised of grasslands. Although trees are largely absent from seasonally flooded areas, there are a number of small wooded areas on higher ground. The western side of the Barotse flood plain is flanked by the plateau of Kalahari sand covered with wood- and grassland (Timberlake, 2000). Species of animals range from various types of fish to large grazers such as wildebeest and zebra's. The Barotse floodplain is the home of the Lozi, a migrating human tribe consisting of over 250,000 people. The Lozi migrate over the plain and move when floods arrive. Their main source of food is supplied by the hunting of fish and land animals (Timberlake, 2000). As the Lozi people are completely dependent on the floodplain climate system, understanding its flooding patterns can be of great importance.

Figure 3.2 illustrates to what extent the Barotse floodplain is filled with water during the wet season. The character of the floodplain shows the high spatial distribution of water in the event of inundation. The water will cover the whole floodplain on a yearly basis. The optical satellite imagery proves the inundation of water over a large area, which is one of the main characteristics that a basin should have when interpreting it using the C/M ratio technique.

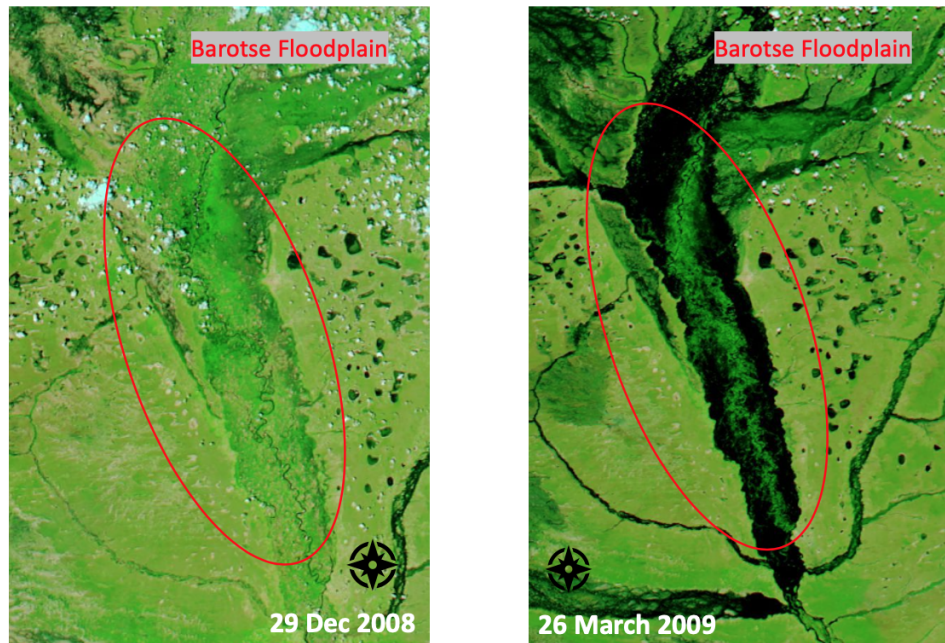


Figure 3.2: MODIS Terra optical imagery showing the inundation process of the Barotse Floodplain. Corrected reflectance filter shows water to appear in black. Clear distinction of the floodplain when inundation occurs (source: EOSDIS Worldview)

3.2.2 Natural Hazards

Zambia is prone to a large range of natural hazards like floods, dry spells, storms, earthquakes and more. Floods and droughts are an annually occurring problem, as in the rest of Sub-Saharan Africa (Šakić Trogrlić and van den Homberg, 2018). The FBF scoping study identified floods as one of the major hazards affecting the country. The annual flooding affected a large amount of people in the livelihoods of the high risk areas. The review of historical hazards can be found in Figure 3.3. The most severe flood occurred in 2008-2009, with a displacement of 102,000 households and 31 related deaths. The disaster caused the bloom of waterborne diseases and due to the displacement over 34,000 households were identified in need of aid (ZRCS, 2019). Most floods are caused by the bursting of riverbanks mainly in the Zambezi River and by heavy rainfall. Due to rainfall there occurs a massive environmental degradation and settlement along the banks. (ZRCS, 2019) Figure 3.3 displays the different types of disasters that occurred in Zambia with their corresponding date. Reviewing this historical data revealed that floods are the hazard type that affected the most people in Zambia. Independent analysis is done by the International Disaster database showed that the floods are the most frequent disasters in Zambia (over 80%), but also were the disasters that have the highest mortality rate and economic loss (UNDRR).

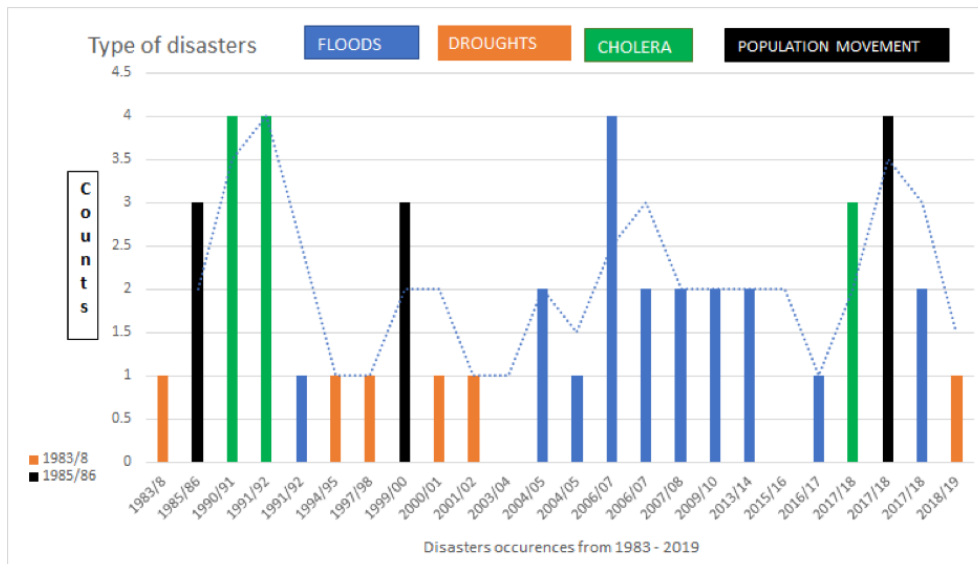


Figure 3.3: Different types of disasters occurring in Zambia within the time period [1983-2019], current information on the Covid-19 disaster count is not yet available. source: (ZRCS, 2019)

3.3 AREA OF INTEREST

Before the analysis is done, an area of interest had to be determined. The area of interest was determined by combining different perspectives of the research. The first perspective was from a humanitarian aid point of view. For this the risk score analysis - and flood risk assessment of the region were used. This assessment was created by the 510, ZRCS and WARMA in preparation of the current EAP. The Risk Score map 3.4 that was created indicates the high risk score of the Western Province in Zambia. The risk score analysis combined the vulnerability, the exposure rate to floods and the capacity to anticipate, cope and recover from the impact of floods. Some general socio-economic, political and physical factors were taken into account. The final product showed a 'high' Risk level of the whole **Western province**. This province is the location of the upper Zambezi river system.

WARMA has created a flood risk map of Zambia for flood forecasting and flood monitoring. Figure 3.5. Three levels of flood risk are identified by

The risk areas as displayed in Figure 3.5 are defined by 510 in consultation with DMMU. The analysis contains information from from four vulnerability indicators: poverty index, literacy level, asset ownership and access to market.

Next to the humanitarian aid perspective, the effectiveness of the technology was taken into account. The technology works best with large floodplains that inundate over a large area when a riverine flood occurs. The products' spatial resolution of 25 km^2 allows only for wide wetlands to give an effective result. The Barotse floodplain was chosen for its wide wetland. The wetland works as an aquifer. When inundation occurs a widespread area of surface water is detected. This layer of surface water is the key for

Senanga

Senanga is a city located in the Southern part of the Barotse floodplain. As Lukulu, Senanaga is classified by the RC as a high risk index region of Zambia. Its flood risk assesment is a lower, but laying in the end of the Barotse Floodplain, Senanga experienced several severe floods. Its remote location makes it a good area of interest, as the coping and recovery capacity of the city is low. See Figure 4.3

3.4 EARLY ACTIONS

In Section 2 the technical use of the EWS in Zambia was described. The triggers following from the EWS lead to a set of pre-described actions. The actions described in the EAP categorized into four main subjects:

1. Shelter provision - Floods typically destroyed a large number of houses. The provision of shelter contributes to the direct first aid needs of the ones most affected. It is the first priority when determining what actions are to be taken. The main objective is to insure that communities are safe and guarded for the imminent effects of floods.
2. Water Sanitation Hygiene (WaSH) - The first need of the ones most affected is the access to clean water and hygiene. Water points are contaminated and the chance of diseases such as Cholera spreading are large. The main objective is to lower the water borne related disease outbreak. From the impact analysis it became clear that these outbreaks where an important death cause during flood season (ZRCS, 2019).
3. Food Security - Due to flooding there is an increase in food insecurity. The main cause is the loss of crops, the poor storage of food and the death or sickness of cattle. By equipping the communities with new sources of food they manage to bridge a period where no food is available.
4. Disease Burden - Malaria outbreak is a burden under the ones most vulnerable. (Children under five, pregnant women and elderly.) Due to the rising water levels the malaria mosquito blooms and the number of infections increase. By reducing the mortality rates due to malaria, the death toll due to preventable diseases goes down.

The four main categories are listed in order of importance. All have a set of actions that are there to be taken by the different institutions. The EAP contains an annex with the Logframe to test the effectivity of each measure. By assigning indicators and defining means of verification, the result of the actions can be mapped. As all actions are yet to be deployed during a disaster, the effectivity has not been properly tested yet (ZRCS, 2019). The decision which action to use is made by the Technical Working Group (TWG). In Section 5, the different variables per action, and the decision to execute a specific action is backed.

3.5 ZAMBEZI RIVER SCHEMATISATION

The following figures display the research area. The schematization of the african continent is displayed, combined with the important attributes in the Zambezi river system. Combined, the four figures entail the main overview of the river system.

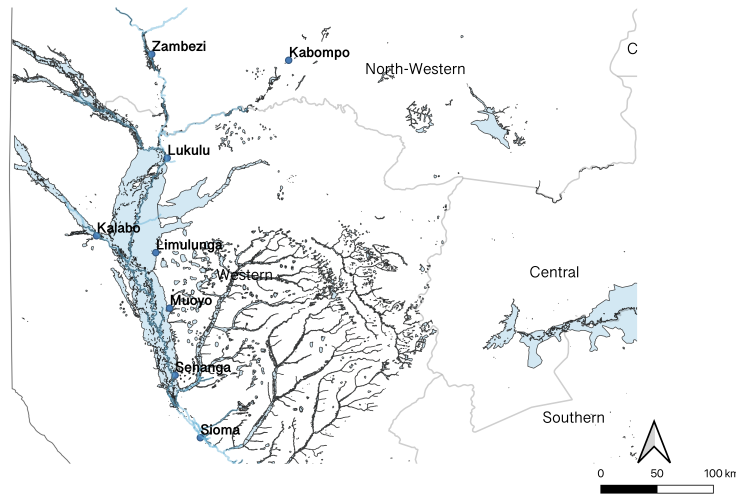
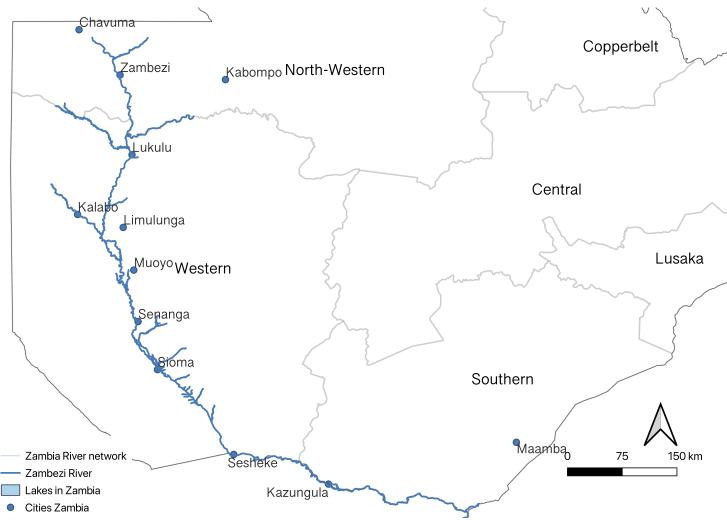
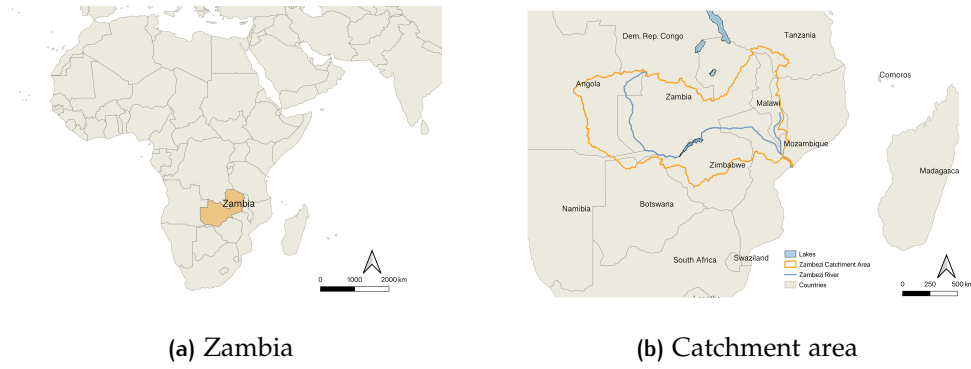


Figure 3.6: Schematisation of the African continent and the geographical location of Zambia, the Zambezi catchment area, the Zambezi river within Zambia and the the Northern part of the Zambezi river in the Barotse Floodplain. (own work)

4 | METHODOLOGY

The methodology entails the working process to create the results. This Chapter displays an overview of the different data, methods and tools used in the thesis. The methodology consists of three parts: the research input, the technology assessment part and the so named "Follow the Forecast"-assessment .

4.1 RESEARCH INPUT

Three main inputs are used to derive the results given in Chapter 5. These are the satellite imagery, fieldwork data and databases. All will be shortly touched upon in the following section. The stigmatization of the workflow can be found in Figure 4.1.

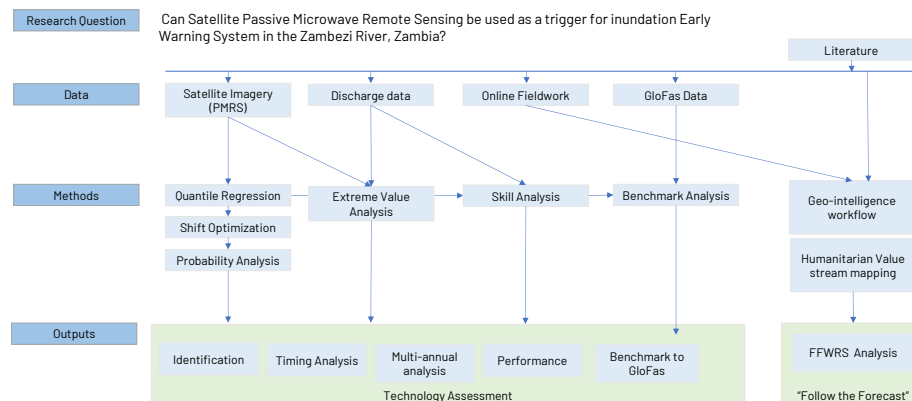


Figure 4.1: Flowchart of the research (source: own work)

4.1.1 Satellite Imagery

As described in Chapter 2, passive microwave remote sensing is the backbone of this thesis. Within this type of satellite imagery, brightness temperature measured by the microwave radiometers is the main parameter used. The data set that was used to obtain the results is gathered by the Advanced Microwave Scanning Radiometer - Earth Observing System (AMSR-E) sensor on NASA's Aqua satellite. The NASA National Snow and Ice Data Center Distributed Active Archive Center (NSIDC DAAC) archives and dis-

tributes daily, weekly, and monthly satellite data products from the AMSR-E sensor. It was launched in May 2002 and finished the operation in December 2011. The data coming from this sensor is in the report referred to as *ASMR-E data*. In NASA's MEaSUREs program, earth system data from different missions is stored. Enabling researches to combine multiple data sources over different time-spans. The datatypes and different satellite types used are found in Table 4.1. A second satellite data set from MEaSUREs was used to obtain a longer data set. This was the data from the SSM-I sensor based on the Defence Meteorological Satellite Program from the United States Air Force. The mission covers data from 1988 until 2017. The instrument measures surface microwave brightness temperature at 19.35, 22.235, 37.0 and 85.5 GHz, All horizontally and vertically polarized. Missions for the DMSP program are named F01-F16. The F15 mission is the current mission providing available data. The current F16 contains newer, more optimized sensors, but their data is not openly available. Table 4.1 illustrates the current available data sets. The technology in regard to flood monitoring are developed by de Groeve et al. (de Groeve, 2010). The data that is used in this report from this second satellite set is referred to as *DSMP data*. Table 4.1 shows that Nimbus data was acquired. Due to the limited temporal resolution this data source is not taken into account.

Satellite	Spatial Resolution	Sensor	Freq.	Temporal Resolution	Availability	Source
Nimbus - 7	3.125 - 25 km	SMMR	37 GHz	1-2 days	1978-1988	NSIDC
DMSP F#	3.125 - 25 km	SSM/I	37 GHz	1-2 days	1987-2017	NSIDC
Aqua	3.125 - 25 km	AMSR-R	37/89 GHz	1-2 days	2002-2011	NSIDC
Landsat	30 m	OLI	optical bands	99 minutes	2002-present	RivWidthCloud

Table 4.1: Satellite types used in the research

Data that was gathered by the satellites is interpreted using software scripts in Python. The brightness temperature data has a flashy character because it is dependent on several physical quantities and environmental conditions. The data is filtered to overcome problems that occurred because of noise in the signal. The method used as a pre-processing filter is the Savitsky Golay filter. The Savitsky Golay is a least-square polynomial filter (Kinoshita and Hogue, 2011). The window width and polynomial fit are determined by assessing the different results based on their coefficient of determination. The best outcomes were gathered with a first-order polynomial and a window length of 21 days. This filtering method was used because it preserves important features of the C/M Ratio data, including peak height and width. It also does not need future data points to apply the filter, which makes it usable for real-time forecasting. This can be compared to filters like a moving average filter which tends to remove these features. The Savitsky Golay filter makes it able to use for forecasting, as you forecast with upstream real-time data. In order to fill the missing values that are obtained in the PMRS data set, a backward fill method is used. The gaps in information occur from slight differences in the overpass that the satellite makes. In the geo-information workflow part of the research an in-depth analysis of the lead time (including overpass time) is given.

Optical imagery was used to verify the location and its inundating floodplain. The condition used for the identification of inundation is that the floodplain clearly inundates when flooded. This is obtained from the four principles of using the C/M ratio as defined by Brakenridge et al (Brakenridge et al., 2007). The type of optical satellite imagery used to identify this inundation are both the MODIS Aqua & Terra missions from NASA. The MODIS imagery allows for liquid water to be detected in the Corrected Reflectance bands (bands 7-2-1). Liquid water on the ground appears dark since it absorbs red color and SWIR. Clear distinction from dry ground can be made as the green color will stand out against the darker black water body. Verification that showed large inundation in the floodplain can be found in Figure 3.2.

4.1.2 Fieldwork data - Online

The main objective of the interviews was to set the technology assessment into retrospective and to answer the *"Follow the forecast"* research question. The online interviews consisted of interviewing national experts that contributed to the EAP. The interviews will be used to fill in the questions that arise when analysing the disaster management system. Mostly focusing on the time frame and decision making network in the system. The interviews are done online via Skype, as the Covid-19 response does not allow for travel to Zambia. The aim was to identify the time components and decision making structure of the EAP.

4.1.3 Databases

Several data sources are used to compare, to validate or set in context the findings. First of all, discharge data supplied by 510 and WARMA was used to validate the lead time forecast gathered by the C/M-ratio. The impact data that was used to assess the impact level in the GloFas analysis was used to allocate the area of interest and its impact level. Demographic data was used to set model performance into context in terms of exposure. In the light of climate change and population growth, the importance of the technique is analysed. This is done using UN demographic data.

The sources of information that are used for Senanga are located in close proximity to each other as visualized in Figure 4.2. The three data input locations are visualized. To be able to correctly compare the three data sources it is of importance for them to be in close proximity.

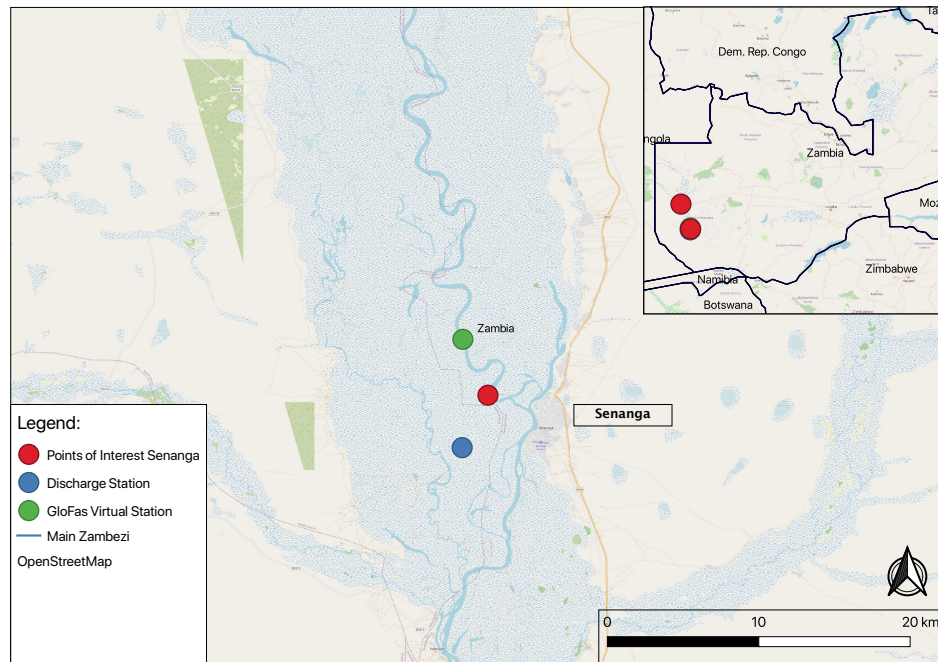


Figure 4.2: Locality of the Discharge, Virtual GloFas and POI Stations at Senanga.

4.2 RESEARCH QUESTIONS – TECHNOLOGY ASSESSMENT

The goal of this technology assessment is to answer the technical aspects of the model. The four questions together create the Technology Assessment Framework — which assesses the use of the PMSR in flood forecasting.

4.2.1 Identification

In research question 1, it is tested if the C/M-ratio provided a reasonable response over several possible points of interest in the floodplain. An upstream point of interest is compared with a downstream point of interest. Their relation can be used to forecast floods downstream. The optical satellite imagery is used to identify the actual inundation. Furthermore the identification is executed by comparing the C/M-ratio's to the discharge values. The timing and onset is an important identification factor. To find the relation between the up- and downstream point the reaction to the C/M-ratio is used.

As described in Table 4.2, several aspects of the floodplain are taken into account when determining the best location for applying the PMRS forecast. The points of interest are assessed by their maximum width, relative upstream area to Senanga, satellite response (maximum C/M ratio). To find the best point of interest, an upstream point has to be selected at Senanga and Lukulu. These points of interest form the input location for the forecast model that is created. The locations are chosen on their response to the C/M ratio, the location in the catchment and the guidelines as defined by Brakenridge et al. (Brakenridge et al., 2007). First of all, the locations

should be located in the catchment so the points entail a representative part of the upstream catchment area. Furthermore, the point should give a good response to the C/M ratio (by using the criteria of (Brakenridge et al., 2007)) and should show enough lead time to the downstream area of interest. In Figure 4.3, all the points are displayed that are assessed for this research. The average width is determined by measuring the width of the floodplain on Google maps. The average width for all point is found. Secondly, the upstream catchment area is measured relative to one another. This is done by looking at the total catchment area and upstream river network. Taken this all into account the location is with the best and worst representative catchment area is ranked. Finally the maximal response to the C/M-ratio is determined by looking at the maximum C/M-ratio that is obtained from the data in a specific high flood year.

Point of Interest	Number of Points used	Average width floodplain [km]	Covered upstream area [3-1]	Max. C/M Response [-]
Senanga (in Barotse Floodplain)
North of Lukulu
Kalabo

Table 4.2: Points of interest that are assessed for identifying the flood forecasting capability of PMRS data. To be filled in the Results. (covered upstream area is measured relative to one another, with 3 = largest upstream area, 1 = smallest upstream area.)

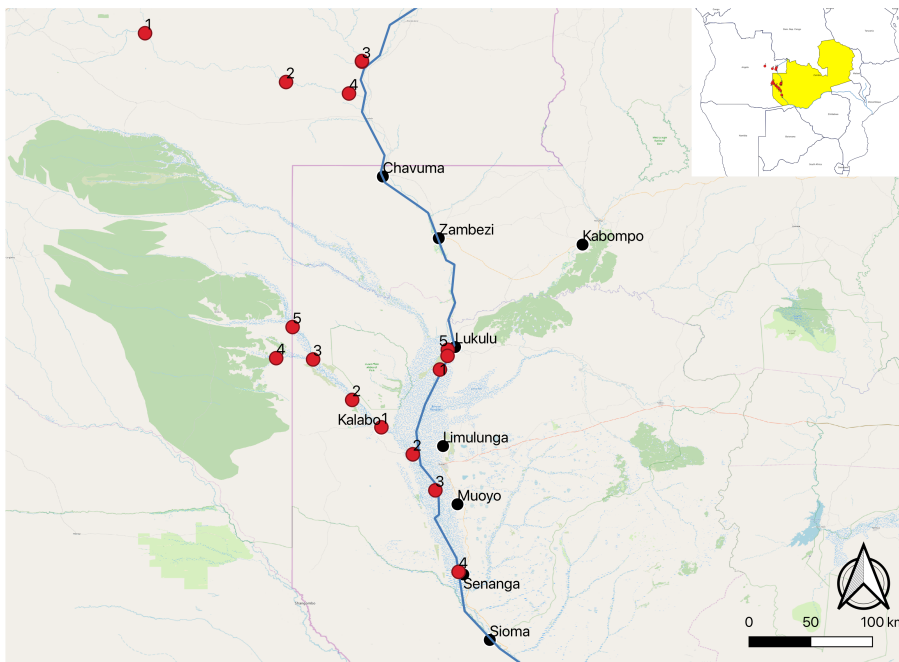


Figure 4.3: All points of interest that are investigated, all the POI's are located in and around the Barotse floodplain, numbers at the points refer to the id number in QGIS

4.2.2 Multi-Annual Analysis

For research question 2, the trends or progression in the multi-annual analysis are found. These form the basis of testing the new PMRS forecasting model. The analysis is done in several steps as discussed below.

Identify Multi-Annual trends

In order to obtain information about the exact occurrence of a flooding and the C/M-ratio threshold level, a multi-annual extreme value analysis is executed. Extreme value analysis is used to analyse C/M-ratio 30 year records. Furthermore, it is done to estimate future occurrence probabilities. The data used in the analysis must be evaluated in terms of the objectives, length of records available and completeness of records. By comparing the C/M-extreme value analysis with the extreme value analysis of the discharge stations, a relation is found between the threshold values of the C/M ratio and the discharge. Using this relation, a threshold of the C/M ratio can be introduced. Two methods are used to identify the multi-annual trend and the relation with the C/M ratio. First of all, a Spearman's rank correlation is executed. Spearman's rank used a Pearson's correlation function on a ranked data set. This rank correlation allowed for correlation of large data sets which are not normally distributed. It helps to mitigate the effect of outliers. A condition to be set for Spearman's rank is that the variables in the data should be in a monotonic relationship with each other. A monotonic relation indicates that the variables should positively or negatively follow each others trend (not necessarily in a linear fashion.) The equation for Spearman's rank can be found in Equation (4.1). To compare, a second correlation function is used to see the effect of the Spearman's rank. This correlation function is the Kendall Tau correlation. While the Spearman's rank is based on errors in deviation, the Kendall Tau correlation is based on calculations on concordant and discordant pairs. It is insensitive to error. The equation for the Kendall Tau correlation can be found in Equation (4.2). Kendall Tau mostly has a better statistical correlation, but, it is widely used on small data sets. It is interesting how the two compare when the extreme value analysis is done.

$$r_s = \rho_{rv_X,rv_Y} = \frac{\text{cov}(rv_X,rv_Y)}{\sigma_{rv_X}\sigma_{rv_Y}} \quad (4.1)$$

ρ denotes the Pearson correlation coefficient, applied to the variable of the C/M ratio. rv implies the ranked variable of the different axis. $\text{cov}(rv_X,rv_Y)$ and $\text{cov}(rv_X,rv_Y)$ displays the co-variance of a the ranked variable and $\sigma_{rv_X}\sigma_{rv_X}$ and $\sigma_{rv_Y}\sigma_{rv_Y}$ are the standard deviations of the rank variables. This formula must be used as the simplified Spearman's rank correlation is applied to an integer input, which the C/M ratio nor the Discharge records are.

$$\tau = \frac{(\text{number of concordant pairs})}{(\text{number of discordant pairs})} \binom{n}{2} \quad (4.2)$$

Where the $\binom{n}{2} = \frac{n(n-1)}{2}$ is a binomial coefficient.

Secondly, a non-linear polynomial fit is done to find the r^2 value or the coefficient of determination. The polynomial has a degree of 2. This r^2 value is the correlation coefficient of the data and it allows to find the level of correlation between the data sets. Values of the r^2 value range between minus infinity to 1. The equation for the coefficient of determination can be found in Equation (4.3). Both are combined to find the threshold levels of the C/M ratio that correspond to the discharge thresholds as set in the EAP.

$$R^2 \equiv 1 - \frac{SS_{res}}{SS_{tot}} \quad (4.3)$$

Where the SS_{res} indicates the residual sum of squares and the SS_{tot} the total sum of squares (the variance of the data).

In hydrological modeling one uses the term return period. The return period, or also called the return interval, is defined by the average estimated time between floods. The return period of the C/M ratio and discharge records for 2, 5 and 10 year return periods was calculated. The model is assessed by different return periods and for different probabilities of exceedance. In research question 4, this output is compared to the performance of GloFas. The return period is calculated using Python. The relationship between flood return period (denoted as T) and the probability of occurrence (p) is given as follows:

$$p = \frac{1}{T} \quad (4.4)$$

Floods with a 10-year return period have a probability of 0.1 or 10% of returning each year. The probability of non-occurrence (q) is calculated by $p + q = 1$. The return period can be calculated by taking the annual maxima of each year of the data set. Sorting and ranking them, and calculating the probability by:

$$p = \frac{(n - i + 1)}{(n + 1)} \quad (4.5)$$

Where p_i entails the probability of a specified ranked flood. i determines the rank and N the number of annual maxima observations.

4.2.3 Timing

For research question 3 the model is evaluated and tested on timing. For this, the inputs of the model are gathered. The probability of exceedance is generated by calculating the Quantile Regression function between the discharge and C/M ratio. (Weerts et al., 2011) defined the use of Quantile Regression

of inundation levels to forecast floods. A probabilistic relation can be simulated between the actual discharge and the related C/M ratio. The data is used to optimize the time shift from the upstream to downstream. Finally, the model is analysed by its performance score in a contingency table.

Normal Quantile Transform

A pre-processing step was used to indicate if the data could be fitted better in the Quantile Regression relation. The Normal Quantile Transform is a form of pre-processing that transforms the C/M ratio values using their quantile position (Weerts et al., 2011). It is checked whether such a pre-processing step could make the relationship better by reducing the impact of outliers.

Quantile Regression

The quantile regression is used to estimate the relationship between the probability distribution of the upstream and downstream C/M Ratio. It is used to estimate the conditional quantiles (Weerts et al., 2011). The degrees of freedom in this quantile regression is kept to a minimum by applying a linear regression for each quantile. The quantiles of interest are deducted from the same probability levels used for GloFas. The quantile regression of the data allows for the points to be distributed within their allocated quantile. This quantile regression plot allowed the user to obtain the probability of a point. The assumption that must hold is that the amount of points must be large enough to assign a probability distribution. Furthermore, the data set should cover the whole spectrum of expected values. This is obtained by also using the DMSP data set, which contained over 30 years of data, with over 10000 samples. Weerts et al. concluded that the use of Quantile Regression provides a simple, efficient and robust way of estimating forecasted water levels with a estimation of the predictive uncertainty. The quantile regression plot is obtained using the QuantReg function in Python, located in the statsmodels package. The regression model is built for each quantile. The response can be describe by Formula (4.6).

$$Q_{\tau}(y_i) = \beta_0(\tau) + \beta_1(\tau)_{x_{i,1}} + \beta_p(\tau)_{x_{i,p}} \quad (4.6)$$

Where $i = 1, \dots, n$ and β_{τ} are found by solving the minimization as given in (4.7).

$$\min_{\beta_0(\tau), \dots, \beta_p(\tau)_{x_{i,p}}} \sum_{i=1}^n \rho_{\tau} \left(y_i - \beta_0(\tau) - \sum_{j=1}^p x_{i,j} * \beta_j(\tau) \right) \quad (4.7)$$

Where each quantile level level is described by τ . Each quantile regression solution to the minimization problem has a distinct set of linear regression coefficients that are plotted (Rodriguez and Yao, 2017).

Shift Optimization

The optimal time water takes to go from the upstream point to the downstream point is calculated by the shift optimization. The shift optimization looked for the “best-fit” quantile regression relationship. The best fit is determined by the optimum of the coefficient of determination in the 50% percentile in the quantile regression. By looping the quantile regression calculation over all time shifts, the best scenario is found. The relationship optimization can be visualised by plotting the different time shifts against their corresponding coefficient of determination.

Probability of Exceedance

The forecasts provided by GloFas have a specific probability. A probabilistic value is assigned to the PMRS forecast via the quantile regression percentile relationships, equivalent to the GloFas probability. The different percentiles correspond to the probabilities of exceedance of the C/M ratio time series. By applying them to the time series, a time series of each specific probability can be obtained and visualized.

Model Set-up

The model compares the upstream “prediction” with the downstream “observation”, both are C/M ratios. The prediction is equipped with the different probabilities as obtained from the quantile regression. The different prediction probabilities are compared to the observation at Senanga. First, a selection in the dataframe is made between the first moment a threshold is reached in the observation. This allowed the model to determine the exact first moment a flood is seen in the observation at Senanga. This is of great importance, as we aim to forecast a flood. Correctly forecasting a threshold is done by looking at the exact **first** moment a threshold is exceeded in the season, which is equivalent to the actual moment a flood wave would cause flooding. Thus the moment when early action is most needed. The ability to forecast ‘on-time’ for the first flood moment will show to be more important in the Chapter 5. The model investigated what happened when a set threshold in the observation was exceeded. If the threshold in the observation was exceeded, the model would see if the prediction would also exceed this specific threshold, given a set time window. This time window is very important because it allows the model to look if the prediction would exceed the threshold within a specific time bound. This time bound is used to determine the lead time that is acquired. To evaluate the performance, the different contingency table characteristics are calculated (Hit, Miss, False Alarm, Correct Negative). This is explained extensively in the next section.

Two important time aspects play a role from the upstream point in the floodplain to the downstream point of interest at Senanga. First of all, the prediction upstream is “shifted” downstream by the shift optimization. This is the initial maximal lead time that is defined. To explain, this is the optimized time it takes from a C/M ratio wave to reach the downstream point in Senanga. Secondly, there is the time window in which the model is allowed

to look for the exceedance of the prediction. This time window has to be deducted from the shift time to obtain the lead time. Another important time consuming source to take into account is the time it takes for the satellite to actually acquire the data. This is further discussed in the methodology about the geo-intelligence workflow. The time windows are visualized in Figure 4.4.

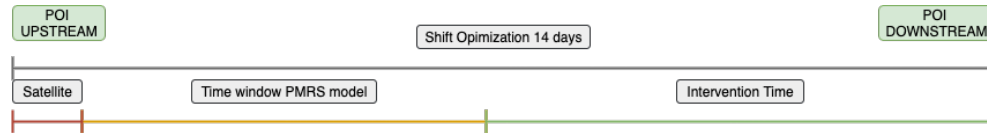


Figure 4.4: Time window of the system explained. Containing the two main time components. (source: own work)

4.2.4 Skill analysis

In research question 4, the skill of the model is assessed and benchmarked against the skill of GloFas. First, the skill of the PMRS product itself is assessed. Then it is benchmarked against the current GloFas product.

In first instance, the performance of the model is tested upon warning thresholds and time windows based on the ROC graphs. The skill is of importance as it describes the predictive value the model has. The model is validated based on different return periods that are obtained from the multi-annual extreme value analysis. The performance of the model is visually assessed based on the ROC curves and contingency table output.

The predictive value of the PMRS model is tested by creating a contingency table. The contingency table includes the hits, misses, false alarms and correct negatives of a model performance. A hit is defined as the number of peaks above a set threshold. The time-frame of analysing the hits is set on one day as the satellite data has a daily availability. The false alarms are defined as the number of peaks above the threshold while the actual data does not reach the threshold value. Misses are the number of flood event days that are not qualified as reaching the threshold while the ground truth data is reaching the threshold. A correct negative is defined as the number of correct negative responses to the threshold, while the observed data observes the same quantification to the threshold value. All these parameters are calculated by a Python script that changes the observed and predicted data to [0] for not reaching a threshold and to [1] when the threshold is reached. The values can be used to compute a contingency table. Displayed in Table 4.3 (Martina et al., 2006).

The output of the contingency table can be used to verify the metrics of the forecast. There are four metrics used to assess the predictive value of the modeled forecast. The metrics that are defined compared to the metrics used by 510 to assess the performance of GloFas. By assessing both models on the same comparisons, the outcomes can be compared when the benchmark

Contingency Table	OBSERVATION		
		[1] - YES	[0] - NO
PREDICTION	[1] - YES	Hits	False Alarms
	[0] - NO	Misses	Correct Negatives

Table 4.3: Example Contingency table source: (Martina et al., 2006)

analysis is performed. The metrics used are: Probability of Detection (POD) or named Hit Rate (HR), Probability of False Detection (POFD), False Alarm Ratio (FAR) and Critical Success Rate (CSI). The metrics are calculated using the following formulas:

$$\text{HR or POD} = \frac{\text{Hits}}{(\text{Hits}) + (\text{Misses})} \quad (4.8)$$

$$\text{POFD} = \frac{\text{False Alarms}}{(\text{False Alarms}) + (\text{Correct Negatives})} \quad (4.9)$$

$$\text{FAR} = \frac{\text{False Alarms}}{(\text{Hits} + \text{False Alarms})} \quad (4.10)$$

$$\text{CSI} = \frac{\text{Hits}}{(\text{Hits}) + (\text{Misses}) + (\text{False Alarms})} \quad (4.11)$$

The metrics can be used to assess the predictive value of the PMRS model. A plot between HR and FAR or POFD for different thresholds shows the predictive value. As all the values of the contingency table contain integers, the metrics are scores between 0 and 1. By varying the input threshold (threshold of C/M ratio at which corresponds to a discharge threshold) the predictive value is changed. The plots below show the increased skill that is reached when the curve moves to the left upper corner in the graph. When the plots occur in the grey area, the model has no skill and the performance is bad. If the plots are made for the different probability of exceedances, the expectation is that the high probability of exceedances plot near the (1,1) point. Vice-versa the low probability of exceedance points will plot on the left side of the plot. As (I.N. Streefkerk, 2020) has shown in the Figure 4.5, there are two locations where the model never or always forecasts an event. As the orange line moves further from the diagonal the skill is increased.

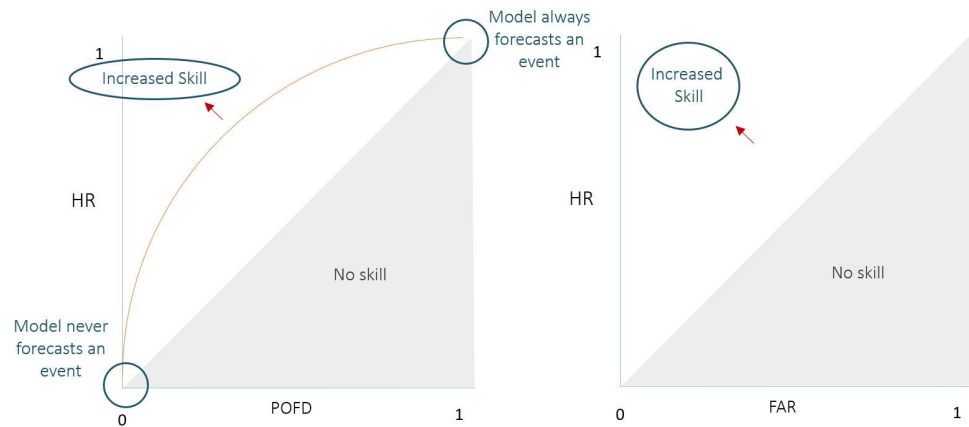


Figure 4.5: Verification analysis as described by (Martina et al., 2006) and visualised by I.N. Streefkerk (2020)

GloFas benchmark

The GloFas product can be benchmarked to the outcomes from the skill analysis from research question 4. The skill GloFas in Zambia is tested for different locations. At every location, the 10 year return period flood with associated probabilities is tested. The skill of GloFas is tested in a slightly different way, **GloFAs!** (**GloFAs!**) is assessed with a different time window methodology. The peaks of the GloFas prediction and the discharge records in the flood season are matched. The peak is evaluated based on the 10 year return period threshold. Therefore, GloFas is tested with the ability to forecast a flood threshold in each wet season. The GloFas model does take into account a time window of three days when determining the skill for the prediction. However, because the peaks are matched, the first moment a flood hits is not taken into account. This is different from the PMRS model as it does not discriminate between the first moment a flood occurs in the season. This difference is key to comparing as the positive outcomes of the contingency table (hits and correct negatives) become more dominant. Their weights overpower the negative outcomes and contingency scores rise. For the comparison to GloFas, we can take this measurement method into account. In this way, the lead time comparison can be taken into account.

For each GloFas virtual gauging station a cut-off is made in the contingency table. A station is classified to have predictive skill as long as the POD exceeds 0.7 and the FAR remains below 0.3. This classification can be used to compare the two contingency tables.

4.3 RESEARCH QUESTION – "FOLLOW THE FORECAST"

4.3.1 "Follow the Forecast" Analysis

For research question 5, the research is focused on three main subsystems: the forecasting subsystem, the decision making subsystem and the response subsystem. These subsystems are the basis of the FFWRs and are described

in Chapter 2. In this section all subsystems are analysed to answer research question 5. The three subsystems are separately analysed using different techniques, appropriate to the different subsystems. The main objective of this section is to optimize the trade-off between confidence of the forecast and the intervention window. For this, the analysis is focused on the "timing" and "decision making" of each subsystem. By combining the information on the analysis of "timing" and "decision making" in all subsystems, a conclusive advice can be drawn on the earlier named trade-off.

The first subsystem, the forecasting subsystem, is analysed using a technique called geo-intelligence workflow. This technique allows the user to map all steps taken in the technical assessment of the forecasting method. The second subsystem, the decision making subsystem, is analysed using a forecast flow diagram this allows the user to map the chain of decision making within the different entities included. Lastly, the response subsystem is analysed using a technique called humanitarian value stream mapping. The HVS measures and maps the stream of actions and its time components. To clarify the structure of the methodology for the "follow the forecast" part of the research, Figure 4.6 provides an overview of the named methods.

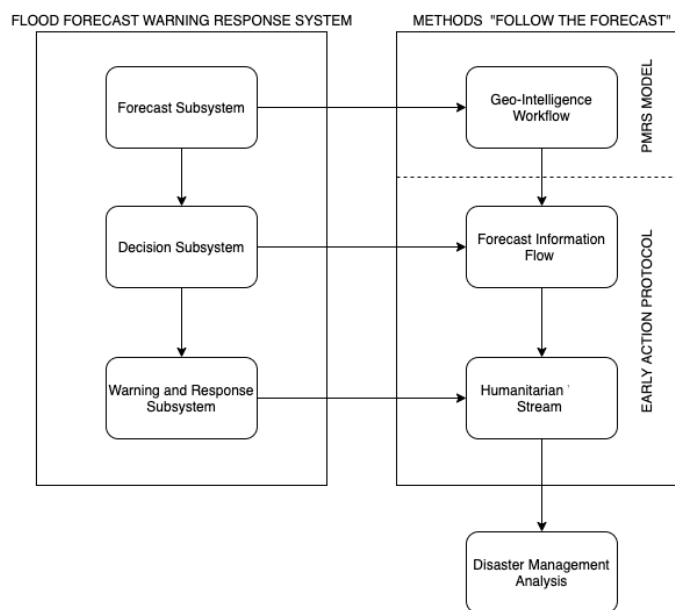


Figure 4.6: Disaster Management Workflow. Based on the FFWRS workflow. (source: own work)

The methodology and result section do not display an investigation in the possibility of integrating an adaptive signal monitoring system. However, in the discussion there is a suggestion for improvement of the EAP based on this theory.

Geo-Intelligence Workflow Mapping

The geo-intelligence workflow is mapped using graphical modelling. In a graphical model the user is allowed to create inputs, tasks and outputs. By streamlining the tasks and the settings needed to obtain the full geo-

intelligence cycle, the overview is generated. By obtaining the mapped workflow, the creation, sharing and understanding of software processing of geo-data is visually represented and made easier (Lemmens et al., 2018). Although a visualization is created, the model should be converted to QGIS or python to create an automated API for the actual implementation. This is not in the scope of this research. What is also mapped are the time intervals that occur in each step. By understanding the time window of the geo-intelligence system, the new technology can be set into perspective. The automated API should be able to do at least the following:

- Extract the daily satellite imagery.
- Run an IDE (Integrated Development Environment) such as python to process the data and run model as described in Appendix E.
- Combine trigger information of multiple sources to come up with a single trigger threshold.
- Run behind the FBF-dashboard to display the triggers.

Forecast flow mapping

The forecast flow is mapped using the inputs from the EAP combined with the interview outputs. A clear organogram is created using the information provided. The visualization leads to clear understanding of the efficiency and decision making process within the protocol. Two main flows of information are mapped: the dissemination of trigger information and the execution of tasks. The set-up and output of this section is intensively discussed during the interviews.

Humanitarian Stream Analysis

The Humanitarian (value) stream entails a field-oriented approach to map the timing of each specific segment in the process. There are three steps that are undertaken to come to the conclusion (Salvadó et al., 2015). First of all, data is collected in order to map the humanitarian stream. Prior to taking interviews, a deep investigation into the "open or available" data was conducted to gather the maximum amount of raw data. It continued by taking interviews of practitioners of the EAP. Humanitarian stream mapping is conducted to effectively gather the information and map the stream. Each interview collected a small part of the humanitarian stream from each practitioners point of view. Combined, these form the basis to map the humanitarian stream. The data is collected using online interviews such as Skype. It is desired to interview multiple stakeholders of the EAP. Due to the limited interview capacity the 'value' is not mapped. The humanitarian stream is mapped and the interviewees gave interesting insights in decision making and timing components of the EAP.



Figure 4.7: Methodology for mapping the Humanitarian value stream (Salvadó et al., 2015)

5 | RESULTS

In this section the main results of the research are described. The result section is structured so it follows the research questions. Additional figures and results are found and can be consulted in the Appendices.

5.1 IDENTIFICATION

The identification section of the results aim to answer research question 1: Can Passive Microwave Remote Sensing be used to identify inundation? To start off, the passive microwave data is downloaded. The signal of the brightness temperature can be found in Figure 5.1. The figure visualized the changing brightness temperatures over a spatial distribution over the floodplain on a given day. The black lines represent the Zambian border. The red dots represent the points of interest that are located within a floodplain. All the points are located in a different brightness temperature cell and thus give a different input to the brightness temperature. This was also seen in the Figure 4.3.

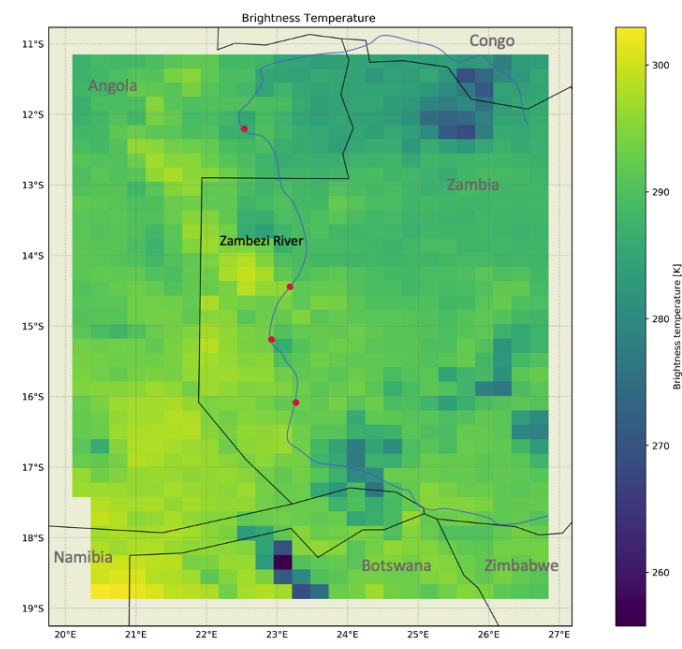


Figure 5.1: Figure showing the different brightness temperatures at 01-08-2007. The red dots represent the four points of interest that have been assigned. The grey/black lines show the outline of the countries surrounding Zambia. (own work)

The different point of interests that are investigated are displayed in Figure 4.3. By extracting the brightness temperatures of the 'C' calibration and 'M' measurement cell, the C/M-ratio is extracted, as described in Section 2.4.3. As stated in Table 5.1, the points of interest are assessed based on different aspects. The final points of interest that are selected are shown in Figure 5.2 and Figure 5.3.

Point of Interest	Number of Points used	Average width floodplain [km]	Covered upstream area [3-1]	Max. C/M Response [-]
Senanga (in Barotse Floodplain)	4	30	3	1.15
North of Lukulu	5	16	1	1.06
Kalabo	5	10	2	1.07

Table 5.1: Points of interest that are assessed for identifying the flood forecasting capability of PMRS data. (covered upstream area is measured relative to one another, with 3 = largest upstream area, 1 = smallest upstream area.)

First of all, the points are selected for their response to the C/M-ratio. The up- and downstream point show similarities in the width, peak and size of the C/M-ratio signal (Figures 5.2 & 5.3). This is of importance as this direct signal will be the main input for the forecast. Secondly, the maximum C/M-ratio values of the up- and downstream point are comparable. When forecasting a flood with a specific return period it is of importance to be able to model the peak moments. Thus, having a comparable signal in the peaks is key to being able to forecast in a good manner. Thirdly, there is a clear lagtime between the up- and downstream point. This lag time, or later referred to as shift, is the first insight into maximum lead time between two points. This is the basis of the forecasting tool. Furthermore, the points are also selected for their contribution to the upstream catchment area. To forecast the flow at Senanga or Lukulu, it is important to model with a point that entails the biggest contributing upstream catchment area. The contributing upstream catchment determines how much of the effective precipitation fallen in the catchment area will actually end up in Senanga or Lukulu. Finally, the contributing width of the upstream and downstream point are comparable in both cases. The contributing width of the floodplain determines how much water can be detected in the tile. The contributing width of the upstream and downstream point should be similar in order to compare C/M-ratio of the the upstream point to the downstream point.

Next to the selected area, all points of interest have been investigated. The outcomes are displayed in Appendix D.i. The selection was based on the previously described selection procedures. The other points of interest that where investigated under-performed to the selected points at Senanga and for Lukulu.

Eventually the detection is verified when the points classify all the criteria of Table 5.1. Next to the criteria the points are checked for the inundation pattern using optical satellite imagery. The inundation pattern in the Barotse Floodplain is checked over a series of identified flood years. To answer the research question, can the C/M-ratio be used to identify flooding, one has to

integrate all aspects as described in the latter. It is possible to identify flooding. The optical satellite imagery identifies the flooding, the readout of the C/M-ratio shows to have the same temporal pattern. The identification and comparison with discharge data in the next research question also confirms the possibility of identification.

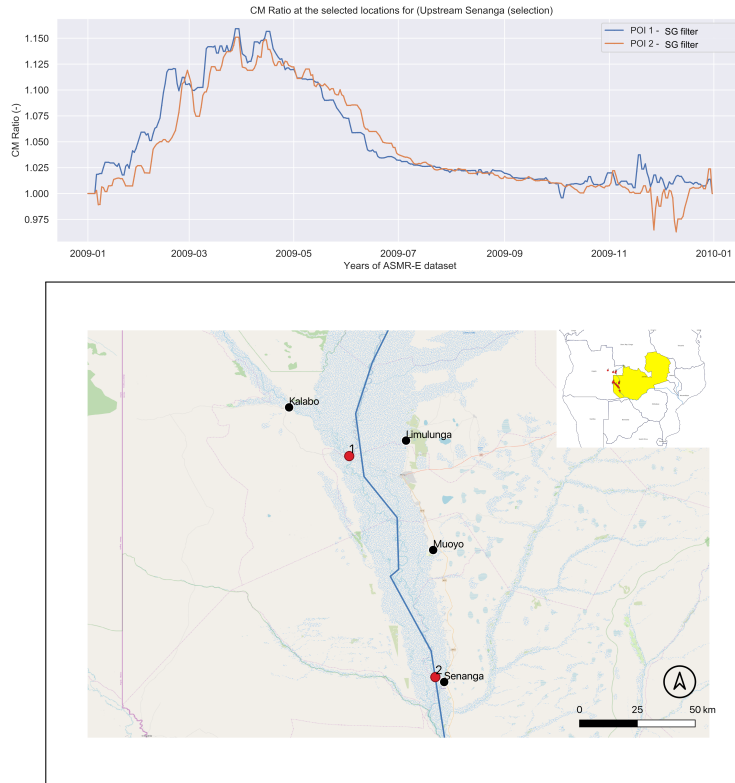


Figure 5.2: Selected points for the model: Upstream POI's North of Senanga (source: own work)

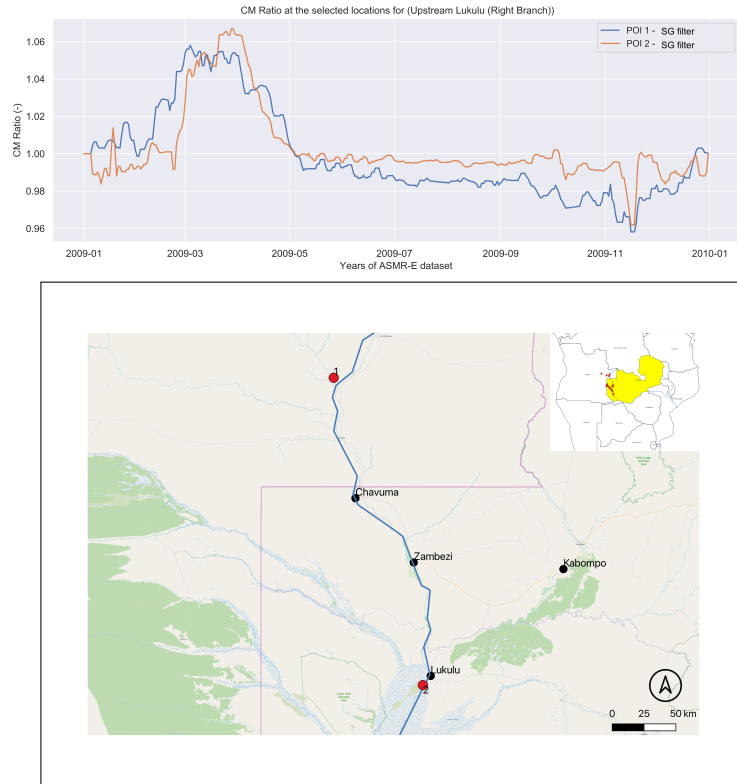


Figure 5.3: Selected points for the model: Upstream POI's North of Lukulu (source: own work)

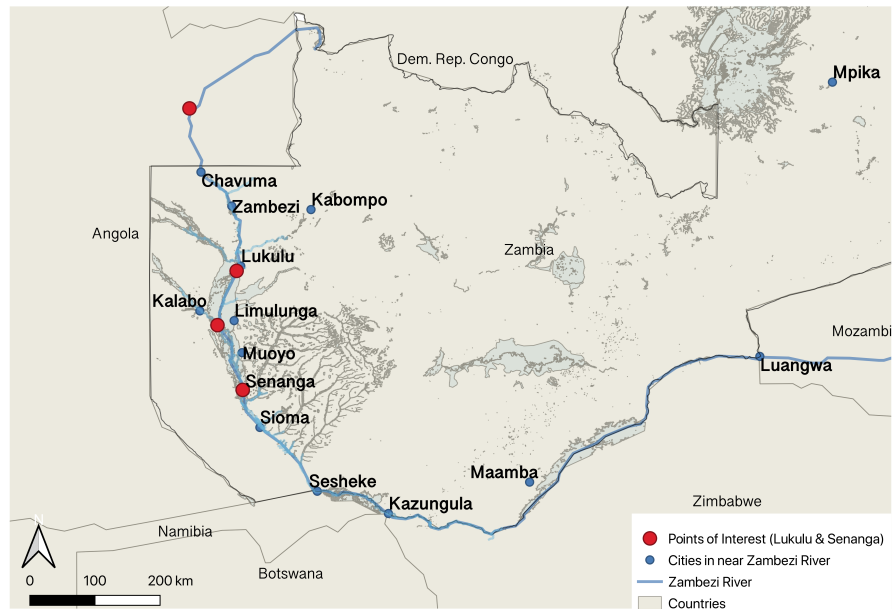


Figure 5.4: Points of interest in the Upper Zambezi River. The points at Lukulu and Senanga are displayed. The points upstream of both areas are identified as points to take the forecast measurement from. (own work)

5.2 MULTI-ANNUAL ANALYSIS

The multi-annual analysis section of the results aim to answer research question 2: To what extent can multi-annual trends in PMRS be related to discharge records? The identification of C/M ratio outputs can only be validated if they are linked to corresponding discharge measurements. First, the discharge records are compared, an extreme value analysis is conducted and finally the return period floods are calculated. The relation between discharge and C/M-ratio is only evaluated for the POI at Senanga. As the Lukulu station did not have sufficient discharge records to compare against the C/M-ratio.

To start off, the C/M-ratio and the discharge at Senanga show similar outputs. An important moment in flood forecasting is the onset of a flood. The actual moment when a threshold level is exceeded for the first time. This is of importance because it is the moment in time when a flood actually occurs. This is the moment one wants to forecast as precise as is required by the mitigation action. Figure 5.5 shows that the C/M-ratio and discharge overlap quite well in the ascending (onset) part of the season. This allows for the C/M-ratio to work as a proxy for flooding. Other years of these time series are visualized in appendix C.

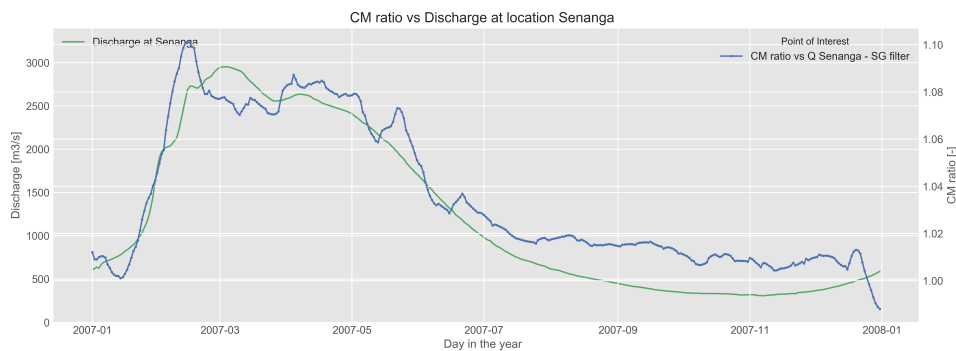


Figure 5.5: Discharge VS C/M ratio plot. Year: 2007 Location: Senanga (source: own work)

The correlation between the discharge and the C/M-ratio is evaluated by fitting a polynomial fit through the scattered data set. This is executed on the hindcast of daily data for 30 years. In Figure 5.1, the polynomial fit is displayed. A clear (close to linear) relation is found between the discharge and the C/M-ratio records. The second order polynomial fit is characterised by Equation (5.1).

$$f(x) = 9.9 * 10^{-09} * x^2 + 9.3 * 10^{-06} * x + 1.0 \quad (5.1)$$

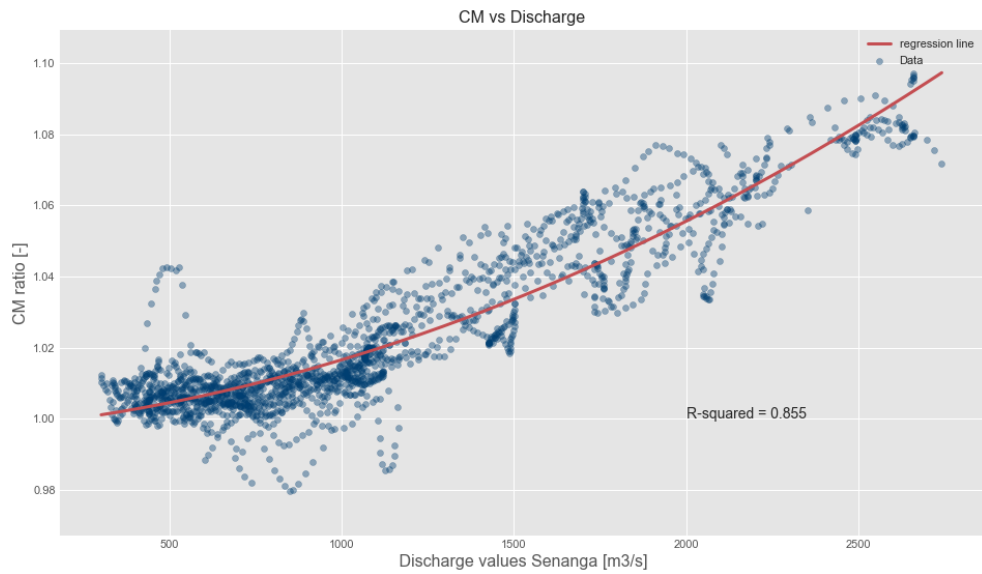


Figure 5.6: Discharge VS C/M ratio scattered. R-Squared value indicates a strong correlation. (source: own work)

The classification of the correlation is done using three different analytical methods. The methods are in depth explained in Chapter 4. The coefficient of determination is 0.855. This indicates a strong correlation between the two data sets. Furthermore, the data is evaluated using the Spearman's rank and Kendall Tau correlation coefficients. Both are displayed in Table 5.2. For the Spearman's Rank, the correlation is classified as strong. For the Kendall Tau, the correlation is classified as medium to strong. Those three methods combined result in the identification of a strong correlation between the discharge and C/M-ratio.

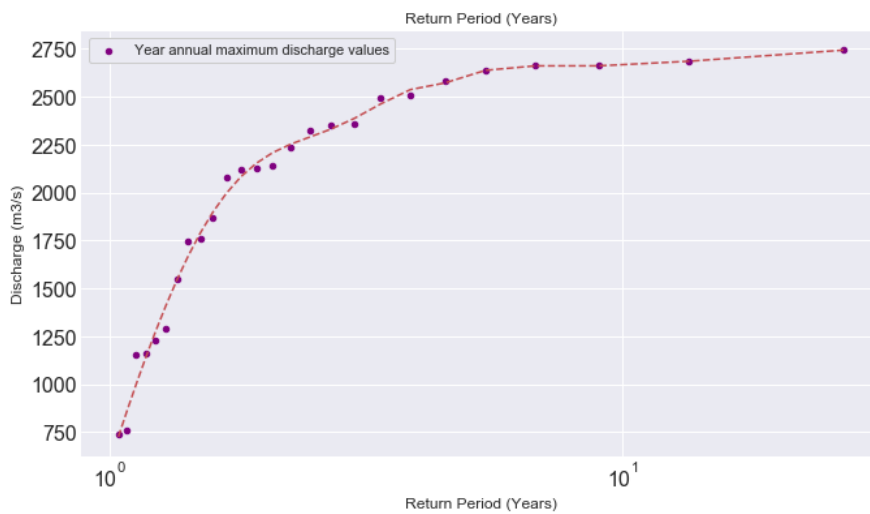
	Correlation Coefficient	p (to reject Ho)	Classification
Spearman's Rank	0,833	0,000	<i>Strong</i>
Kendall Tau	0,654	0,000	<i>Medium - Strong</i>

Table 5.2: Spearman's Rank and Kendall Tau correlation factors. Both show a strong correlation between the discharge values and the C/M-ratio values at Senangna (source: own work)

The two data sets are used to obtain flood return periods. The flood return period will allocate the specific C/M-ratio or discharge level that is allocated to specific flood return period levels. In figures 5.7b & 5.7a, the two return period floods are shown. In Table 5.3 the different return periods are displayed. The discharge return period is calculated and changed into a C/M-ratio by making use of the polynomial found in Figure 5.6. An interesting result that is observed is the difference in return periods for both data sets. Especially the 2 year return period flood differs quite a lot in the two different data sets.

Return periods	Corresponding C/M-Ratio
Discharge - 2 year Return Period	1.062
Discharge - 5 year Return Period	1.088
Discharge - 10 year Return Period	1.093
C/M Ratio - 2 year Return Period	1.074
C/M Ratio - 5 year Return Period	1.090
C/M Ratio - 10 year Return Period	1.108

Table 5.3: Return periods based on C/M-ratio and discharge records at Senanga (source: own work)



(a) Flood return period records based on the extreme value analysis. Based on discharge records - DSMP dataset (source: own work)



(b) Flood return period records based on the extreme value analysis. Based on C/M ratio records - DSMP dataset (source: own work)

Figure 5.7: Flood return periods from the extreme value analysis.

5.3 TIMING

The timing section of the results aim to answer research question 3: Could timing of a flood event be obtained from PMRS? To forecast floods, a relational model between upstream observed C/M ratios and downstream C/M ratios at a later time epoch has been established. As relational method, a Quantile Regression model has been chosen (see Ch. 4). The following processing steps were tried out to reach a best results:

- Quantile regression with and without Normal Quantile Transform
- varying the response time between upstream observations and downstream observations
- Shift optimization & probability extraction

Below, the results of these variants is further described.

The Normal Quantile Transform (NQT) pre-processing step transformed each feature (C/M ratio) following a normal or Gaussian distribution. This tends to spread out the most frequent values (Weerts et al., 2011). With the effect of reducing the effect of outliers. The result of the pre-processing step was not ideal. The coefficient of determination showed that the fit without the NQT pre-processed data performed better. The pre-processing step has not been taken into account in the further proceeding of the model.

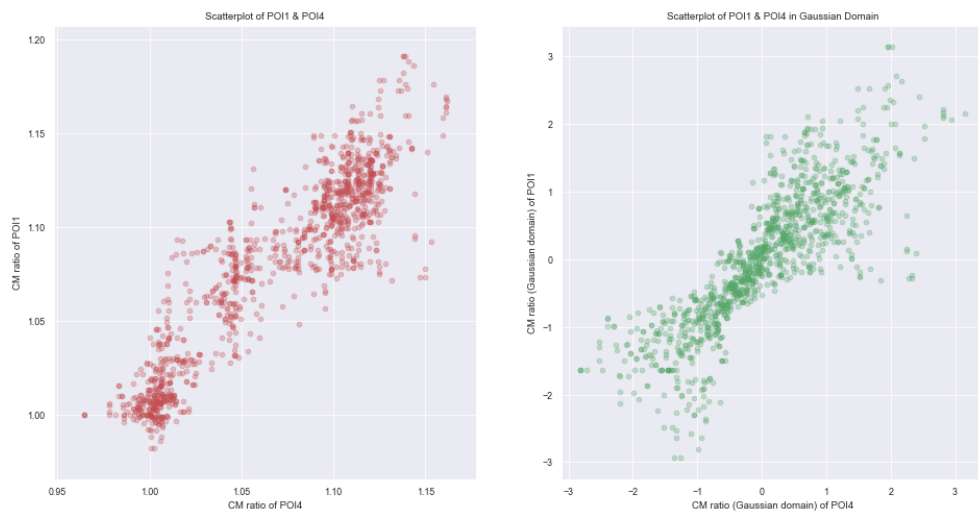


Figure 5.8: Normal Quantile transform. Left: The scattered C/M ratio points. Right: the allocated points to their Gaussian distribution.

Figure 5.9 and 5.10 show the two data sets that are used for Senanga. (the AMSR-E and DSMP data set). For the analysis of the model the DSMP data set is used because of the length of historical data. The DSMP entails a data set of more than 30 years. The 30 year record also provided a more trustworthy extreme value analysis. What can be seen is that output of the C/M ratio changes throughout the year. The width and height peak of the C/M ratio in each flood season differ. However, when comparing the shape of each individual year, one can note that the up- and downstream point show

similarities in width, height and shape. This similarity is of importance because it allows for the upstream location to forecast the C/M-ratio at the downstream location, given a certain probability.

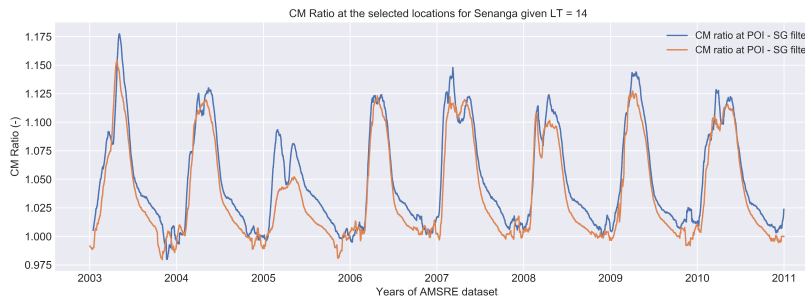


Figure 5.9: C/M ratio at Senanga. AMSR-E data set. Lead time optimized to 14 days. (own work)

Lead time optimization is the time shift in time between upstream point and downstream (forecast) location. This time component is visualized in grey timescale in Figure 4.4 in the methodology.

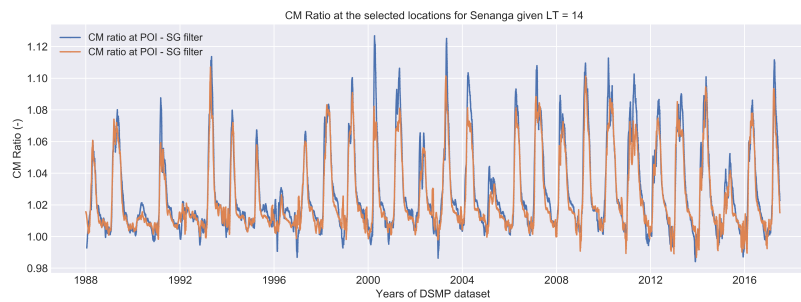


Figure 5.10: C/M ratio at Senanga. DSMP data set. Lead time optimized to 14 days. (own work)

The C/M-ratio data series of the upstream and downstream points are used to find the quantile regression relationship between a point upstream and a point at the area of interest (at Senanga). The relational quantiles are fitted with a linear function to obtain the fits of each quantile. The time-shift between the upstream and downstream point determines the amount of lead time that can be provided by the model. This time shift is optimized using the coefficient of determination in this quantile regression plot. The Figures 5.11 & 5.12 display the quantile regression plot. The quantile regression fit of the up- and downstream points show a clear relation. By obtaining the fits, a probability distribution between the up- and downstream point is established. The 90% quantile corresponds to a probability of exceedance of 10%, as explained in the Chapter 4. The latter is used to implement a probability factor in the forecasting model. For both data sets (ASMR-E and DSMP) the quantile regression is found and optimized.

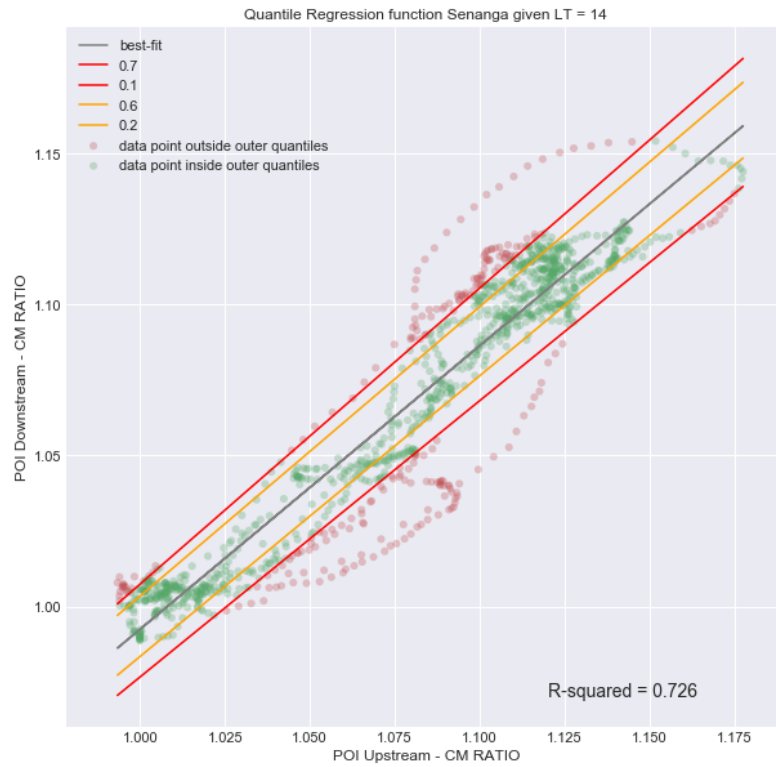


Figure 5.11: Quantile Regression plot between the upstream and downstream point of interest at Senanga. AMSR-E data set. Lead time optimized to 14 days. (own work)

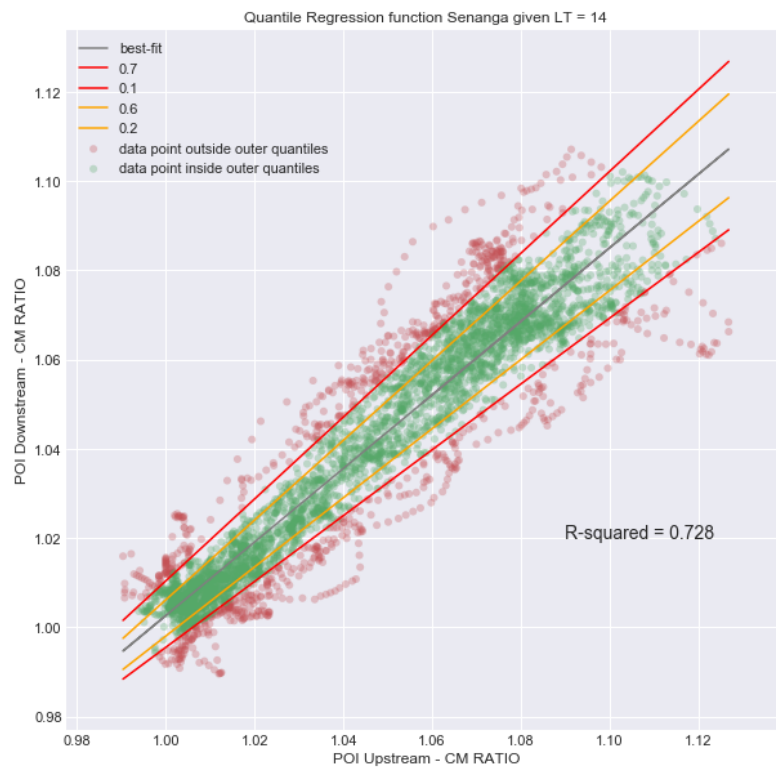


Figure 5.12: Quantile Regression plot between the upstream and downstream point of interest at Senanga. DSMP data set. Lead time optimized to 14 days. (own work)

As stated before, the shift is optimized using the coefficient of determination or the r^2 -value. The optimal shift is found to occur at a shift of 14 days. In other words, the best fit of the up- and downstream C/M-ratio is found after a delay of 14 days. This was expected as the correlation analysis (section 5.2) also showed this time shift as the most optimal. In brief, this means that a rise in flood levels upstream is followed by a rise in flood levels downstream about 14 days later. These 14 days indicate the maximum lead-time that can be generated if the upstream point is used for detection. This lead time is sufficient for response and early action (section 3.4) and is also more than what currently is offered by GloFas (section 2.5).

In the figures 5.13 the shift optimization is displayed. The Senanga lead optimizations show to have a good correlation between up and downstream values. Their correlation allows for the use of the upstream point as a proxy for flood forecasting in the downstream point at Senanga. The relation found in the Lukulu points are not performing. The r^2 -value at Lukulu for the AMSR-E data set is quite low (0.30). For the DSMP data set it is so low (<0.1) that it can be questioned if a relation between up- and downstream points can be drawn. Due to the difference in topographical, geological location of the points at Lukulu, a difference in the output occurs. An important difference is the type of floodplain in Lukulu. For Senanga a clear, wide and annual returning wet floodplain is present. For the Lukulu station, it is less certain that the upstream point shows to inundate when flooding occur at Lukulu. This is also due to the fact that the upstream point at Lukulu contains less of the upstream area of all the water that surpasses Lukulu. Thus flooding at Lukulu is not directly linked to the inundation of the floodplain in the upper Zambezi. Different branches, like the Kabompo river, also play an important role in the flooding of Lukulu. Finally, the floodplain it self is less suitable. It is less wide and the yearly inundation of the wetland is not always occurring. The Lukulu data set is not evaluated in the model as it will only produce effects from noise.

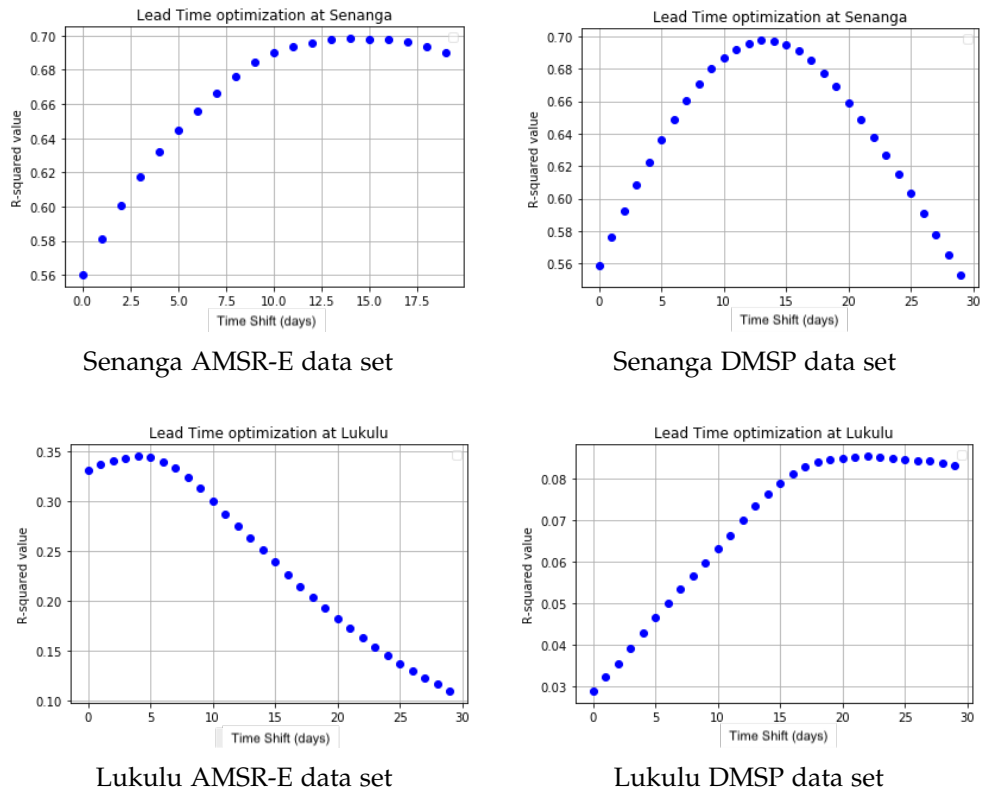


Figure 5.13: shift optimization for the different points of interest and the different satellite types. (source: own work)

From the quantile regression plots, the fits for the quantile relationship are obtained. The probability of exceedance plots are obtained by using the quantile fits and plotting them in the time series. The probability of exceedance graph shows the different exceedance probabilities at each point in the data set. The probability fits between between the upstream C/M ratio series and downstream 14-day shifted C/M ratio are the main input to the model. They are used as the upstream *predictor*.

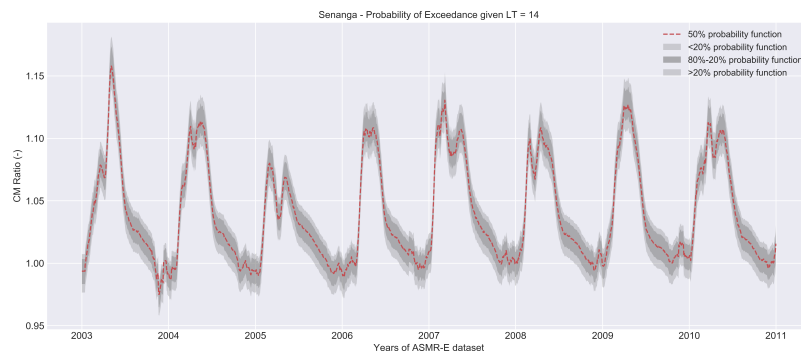


Figure 5.14: Probability of exceedance of certain threshold. Values used to produce contingency table of the model. AMSR-E data set. Lead time optimized to 14 days. (own work)

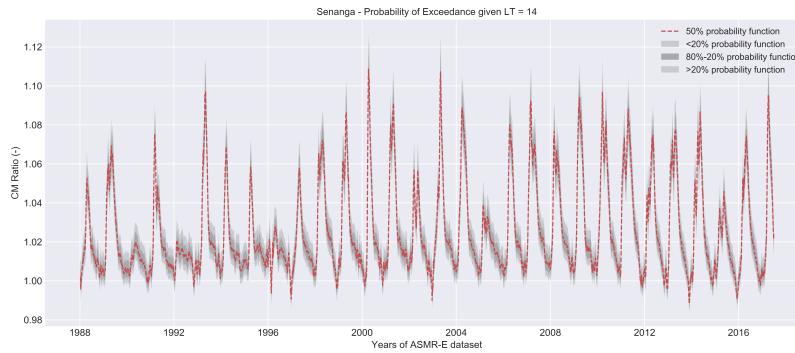


Figure 5.15: Probability of exceedance of certain threshold. Values used to produce contingency table of the model. DSMP data set. Lead time optimized to 14 days. (own work)

The upstream *predictions* of the C/M-ratio values are used as the main input for the model. The downstream *observation* are used to construct the relationship with the upstream prediction and are used to verify the skill of the model. The model workings are explained in the Methodology. The model compares all the different years separately. It is validated by comparing if the actual moment of threshold exceedance is predicted within a given time window. The model is created to compare this moment in time with the prediction, given a certain time window. If the prediction reaches the same threshold within the given amount of days, a hit or correct negative is detected. Otherwise if the prediction and observation do not show the same threshold, given the time window, a false alarm or miss is detected. The skill of the model is tested using these parameters. The skill is tested in the contingency table. The contingency table is interpreted using a ROC diagram. Figure 5.16 displays the performance of the model. On the y-axis the HR is displayed. On the x-axis the FAR (left) or POFD (right) are displayed. As long as the lines stay left of the grey diagonal, the model shows to have skill. The right graph, displaying the HR against the POFD, aims to answer the following question: What is the ability of the forecast to discriminate between the events and non-events? The left graph, displaying the HR against the FAR, aims to answer the question: what is the ability of the forecast to discriminate between hits and false alarms? Both should be taken into account when assessing the skill of a model, as they both interpret the output in a different way. The coloured lines in the ROC curve represent the corresponding probability of exceedance levels. These show that the model performs differently for the different probability of exceedances.

For the higher range of thresholds (C/M-ratio > 1.07) it is not possible to create valid ROC diagrams. There occurs a class imbalance when working with the higher thresholds. The imbalance occurs because one of the classes or thresholds constitutes a small minority of the data. ROC graphs cannot measure well for imbalanced data set (Dataman, 2018). Therefore the output of the ROC curves and contingency table can only be assessed for the lower

thresholds.

For the humanitarian actor it is of importance to have a model that rather detects an exceedance of a threshold too early, rather than no detection. Therefore, warning with a threshold of a 10 year return period is on the high side. It would be better to use such systems to allocate the yearly occurring floods. Which correspond to C/M-ratio thresholds in the range of 1.05-1.07. There does however occur a trade-off between (financial) warning capacity and response frequency of a humanitarian organisation.

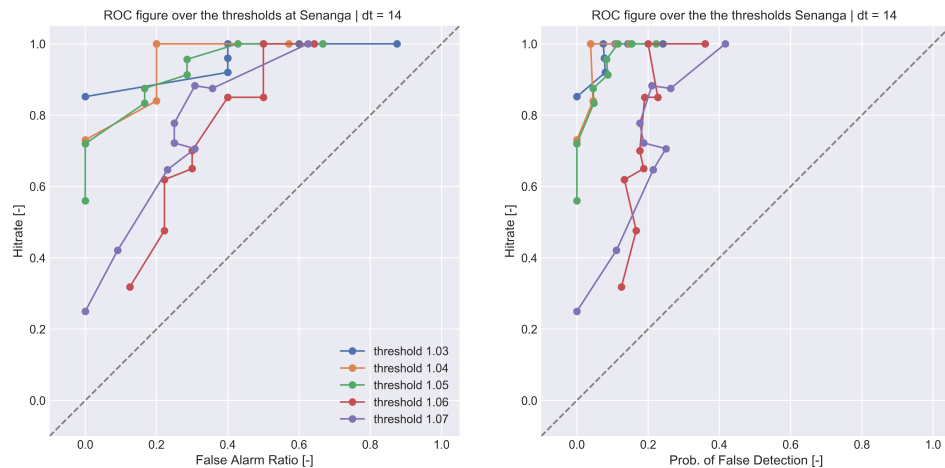


Figure 5.16: Leadtime = 0 days. ROC graph at Senanga for the DSMP data set, $dt = 14$. The threshold has a changing timewindow in which the ROC contingency table is created. (source: own work)

5.4 SKILL ANALYSIS

In this section the aim is to answer research question 4: How does a PMRS based model perform in comparison with GloFas and what skill can a forecast combination with PMRS offer? In the ROC plots given in figures 5.17 to 5.19 the output of the model is tested. The model is tested for 3 different time windows (7, 4 and 0 days lead time).

For clarification, the dt -value is the model time window, the lead time is calculated by subtracting the dt -value from the maximum shift as referred to in E.1. So a model time window of $dt = 7$ days refers to an lead time of: $14 - 7 = 7$ days.

The time windows upon which the model is assessed are related to the time windows used in the GloFas forecast. The corresponding time window is chosen to be able to compare the result to GloFas. It also indicates the ability of combining two systems, as they both show skill for the given lead times. The skill is analysed for all probability of exceedances. This allows

for the discrimination between a given probability and its skill.

In Figure 5.17 the time window of 7 days is implemented. This corresponds to a lead time of 7 days. The 7 day lead time forecast shows skill for most thresholds and probability of exceedances. For the high thresholds (1.06, 1.07) and the lowest probability of exceedance (0% - 20%) the model does not show to have skill. This is also due to the fact that there is an imbalance in the data set for those larger thresholds. Thus a clear conclusion that these probabilities show no skill cannot be drawn. What is noticed is the skill that is seen for all the other plotted points. With a 7 day lead time the model is able to provide skill, thus could be used in combination with GloFas to increase performance.

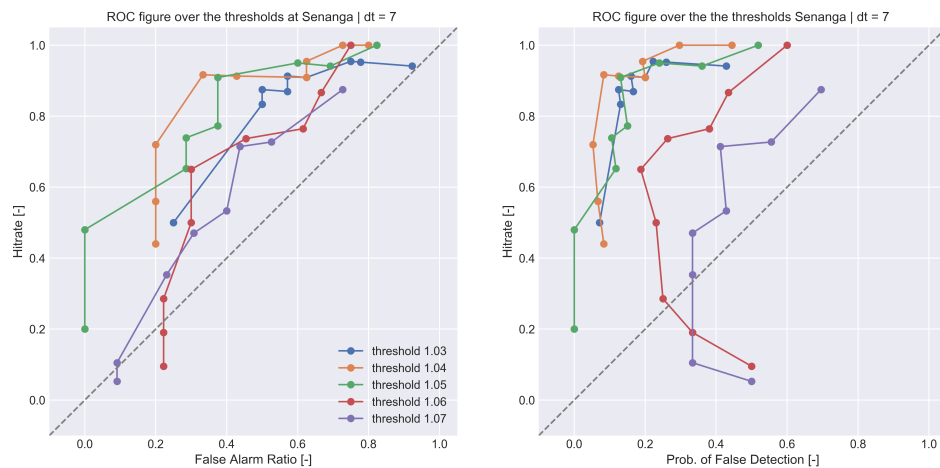


Figure 5.17: Leadtime = 7 days. ROC graph at Senanga for the DSMP data set, dt = 7. The threshold has a changing timewindow in which the ROC contingency table is created.(source: own work)

In Figure 5.18 the performance for the 10 day time window is assessed. This time window corresponds to a 4 day lead time. This is due to the maximal shift of 14 days, thus maximal lead time of 14 days. When subtracting the time window of the model, a lead time of 4 days is created. The 4 day lead time is also chosen as it is one of the lead times used by GloFas. The skill increased when compared to the 7 day forecast. The plot moved up to the left corner. The increased skill is observed. The increase in skill is also expected as the model has more degrees of freedom in its time window.

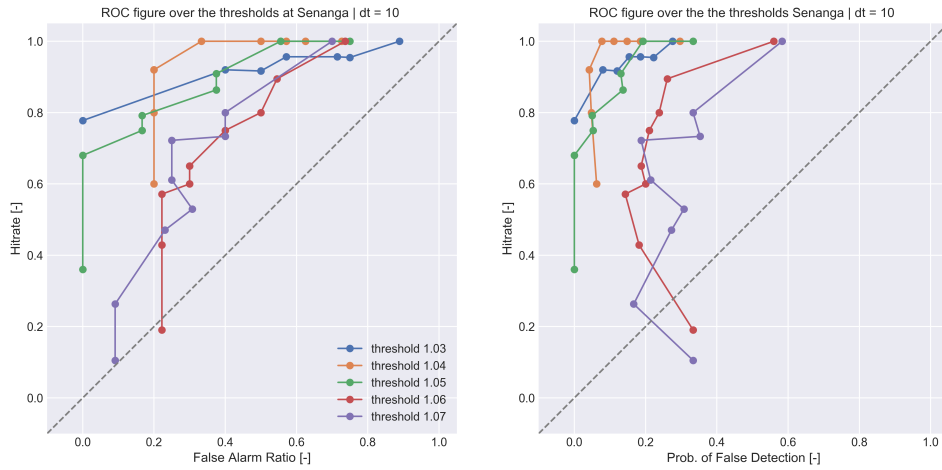


Figure 5.18: Leadtime = 4 days. ROC graph at Senanga for the DSMP data set, $dt = 10$. The threshold has a changing time window in which the ROC contingency table is created. (source: own work)

Finally, in Figure 5.19 the 0 day lead time is predicted. These graphs indicate that the model has a lower uncertainty when the time window increases. This is also expected as the model is allowed to find a prediction threshold in a bigger time-bound.

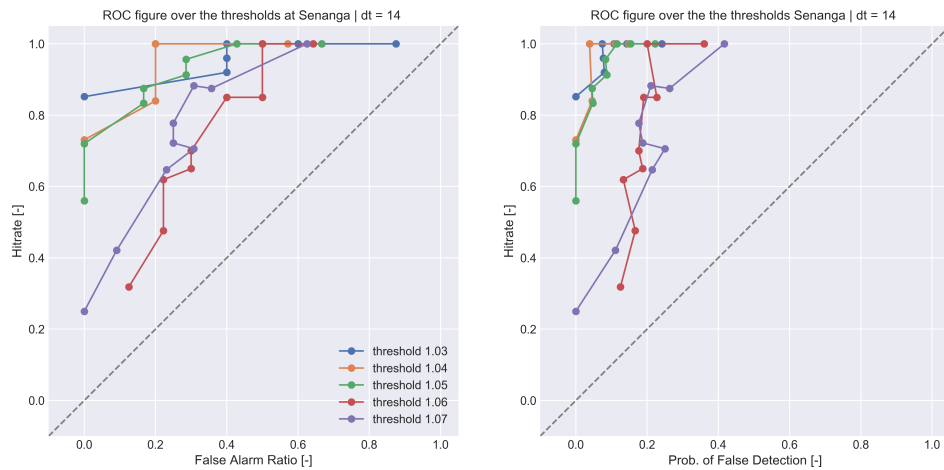


Figure 5.19: Leadtime = 0 days. ROC graph at Senanga for the DSMP data set, $dt = 14$. The threshold has a changing timewindow in which the ROC contingency table is created. (source: own work)

The results are also generated for the different thresholds that are obtained from the return periods. Because of the limit of the ROC plots, floods with a return period of 2 years can only be displayed. In Figure 5.20 the flood return period of 2 years is displayed based on the discharge records. In Figure 5.21 the flood return period of 2 years is displayed based on the C/M-ratio

records.

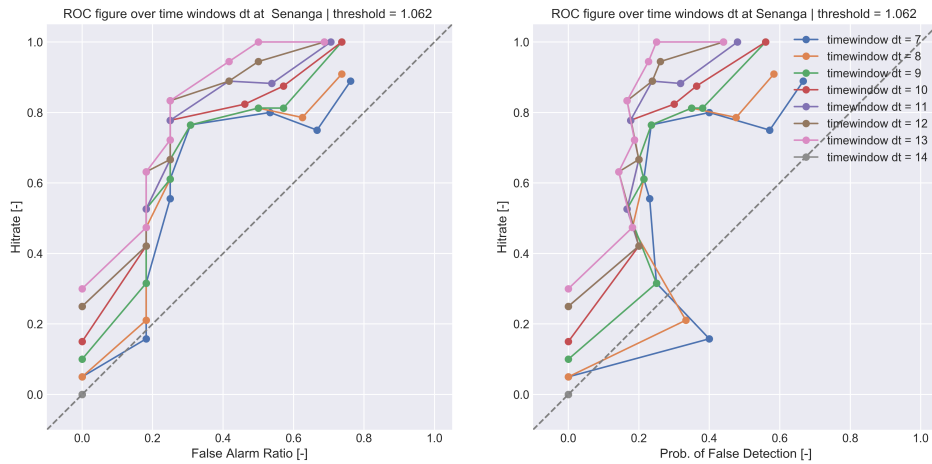


Figure 5.20: Senanga DMSP data set with threshold = 1.062. ROC graphs at Senanga for the DSMP data set. The threshold is set at one specific level and the ROC curve is changed over different time windows (dt).(source: own work)

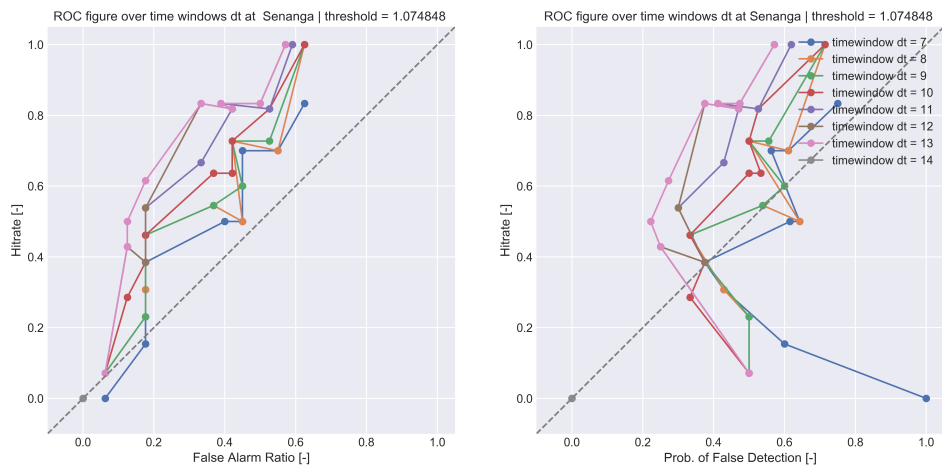


Figure 5.21: Senanga DMSP data set with threshold = 1.07. ROC graphs at Senanga for the DSMP data set. The threshold is set at one specific level and the ROC curve is changed over different time windows (dt). (source: own work)

What can be noted is that most of the probabilities and time window show predictive value. The difference outcomes for the return period of the discharge and C/M ratio are expected because the threshold set by the discharge 2 year return period flood is much lower. For the C/M ratio 2 year return period it is noted that the ROC are just not able to accommodate for the interpretation of the outcome. The dt=7 time line shows strange behaviour due to the imbalance in the result set. The results of the ROC curves based on the 5 and 10 year return periods can be found in appendix C. The skill that is shown by the PMRS model indicates its effectivity in forecasting

a flood. It is interesting to compare the products with each other and see how they both can contribute in lowering the uncertainty bound or pushing the lead time.

5.4.1 Comparison with GloFas

The model output will be compared to the ground truth data and the GloFas data. This is done by assessing the work with a contingency table that is created for the Senanga station. The GloFas contingency table is computed in a different way. GloFas is equipped with a 4 or 10 day lead time. The prediction and observation are compared based on their annual exceedance of the 10 year return period flood threshold. It is not taken into account at what moment the observation indicates a flood. In other words, a time window is not taken into account. This is because there is no exact impact data set that can relate one moment in time to a flood. Thus only the extreme value analysis is included (10 yr return period) and the actual moment of flooding is excluded. For this the PMRS model needs to be slightly adjusted. The time window is enlarged in such manner that one full wet season is taken into account. The results can be found in Figure 5.22. The Figure shows that for all thresholds and for all quantiles (probability of exceedances) the models shows to have good skill. The skill that was acquired by the EAP for a GloFas virtual station to be classified as *trustworthy* is: $HR > 0.70$ & $FAR < 0.30$. For all the different probability of exceedances this is the case. Thus the model would be classified as *trustworthy* for forecasting by the regulations of the EAP. It must be noted that this is the performance of the PMRS model based on the normal to high flows. This does not include extremes that have a return period of 5 or 10 years. However, the ROC cannot model those outputs because of the imbalance in the data set. This is later discussed upon in the Discussion.

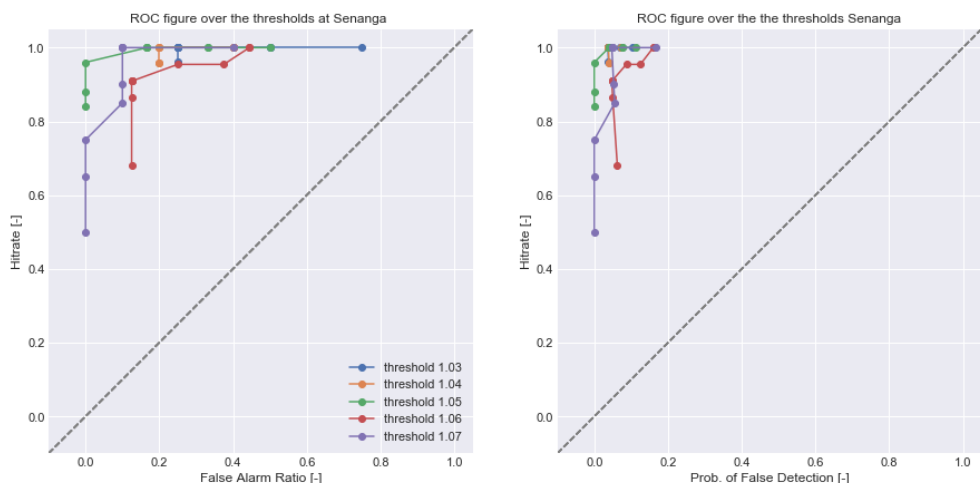


Figure 5.22: Senanga DMSP data set that compares to the GloFas data set. Effects of the time window not included.(source: own work)

5.5 "FOLLOW THE FORECAST" ANALYSIS

In this section the aim is to display the results that are found for research question 5: What is the intervention window created by the Early action Protocol for flood protection in Zambia? This section entails a three fold of different techniques used to assess the different parts of the FFWRs.

5.5.1 Geo-Intelligence workflow

In this section the lead time that is acquired by the model is set into perspective to the geo-intelligence workflow that has to be done to acquire those results. By assessing the time it takes to go from measurement to forecast, one can find the final intervention window used for taking action.

The results of the PMSR model are obtained using ASMR-E and DSMP satellite data sets. This data is historical, as it entails a large 30-year data set. Both data sets have global a 99% global coverage with a day- and night-overpass. The full geo-intelligence workflow can be found in Figure 5.23. Insights into the geo-intelligence workflow inside the model can be found in appendix E. The geointelligence workflow shows that the process is split up into different time steps (de Groeve, 2010). The time steps are given for downloading the AMSR-E data from the JAXA satellite mission. For real application of this method, a currently running satellite mission should be selected. This is just an indication of the timescale for the ASMR-E data set. The timescale is divided into 5 different steps. Starting from the actual measurement of the instrument to the moment the trigger is sent out.

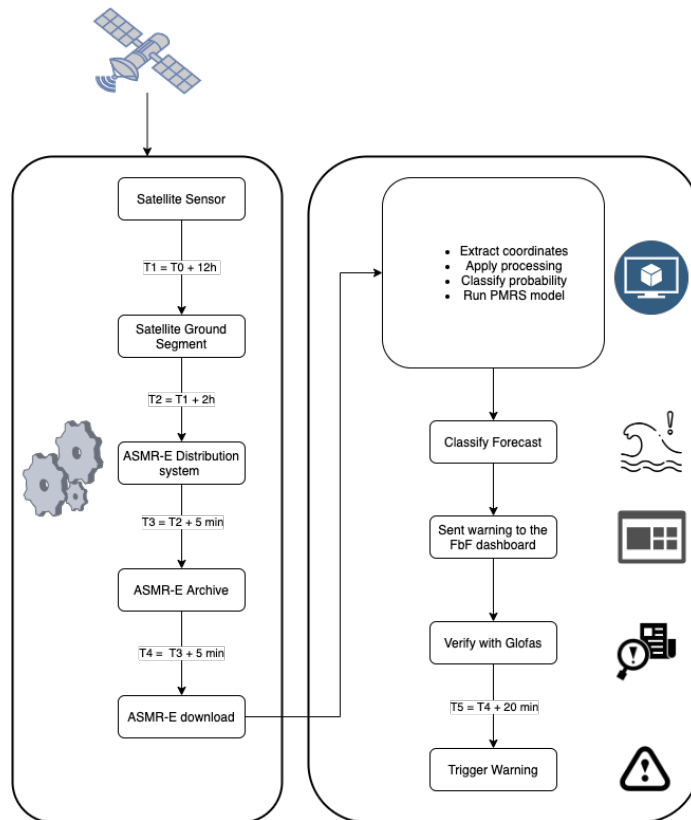


Figure 5.23: Geo-intelligence workflow for the ASMR-E data set (source: own work)

The largest amount of time is found in the satellite overpass that has a full coverage. As de Groeve et al. identified, “the average time between a flood event and flood alert is between 2.5 and 24 hours” (de Groeve, 2010). This is due to the overpass that occurs twice a day. With an average of 12 hours. The 2.5 hours that is defined largely by the time it takes for the data to be published (2 hrs) and then processed to find a trigger (0.5 hrs). The processing time of a signal differs for the amount of locations extracted, computing power and model optimization. The results indicate that the minimal time it takes from flood alerts to come in is 2,5 hours. If the satellite has a full coverage of the Zambezi plain, it surpasses twice a day, with the descending node (night overpass) being the most favorable overpass for brightness temperature extraction. As the satellite has 99% global coverage, there could be instances that satellite data is acquired with a T1 of 24 hours. This is due to the first overpass to miss the area, thus having to wait another day for the descending overpass. The minimal and maximal lead time and the intervention windows are displayed in Table 5.4.

	T ₁	T ₅	Intervention Window Time
Minimal	0 h	2,5 h	(PMRS model lead time) + 2.5h
Average	12 h	14,5 h	(PMRS model lead time) + 14.5h
Maximal	24 h	26,5 h	(PMRS model lead time) + 26.5h

Table 5.4: Intervention window calculation, T-values refer to Figure 5.23

The model workflow (Appendix E) displays the steps that are taken to go from an input NetCDF data file to the actual trigger. The colored green parts show the possibility for integration or combination with a GloFas trigger. By combining the GloFas trigger with the PMRS trigger the decision making structure is based on two input sources. This can lower the uncertainty when making Early Action Response decisions, thus leading to quicker decision making. The speed at which the decision making process is executed has an influence on the intervention window.

5.5.2 Flow of the Forecast

The flow of the forecast is obtained from the analysis of the EAP, see Figure 5.24. The current decision making process is not set in concrete as the EAP is still under construction. The decision structure is let by the TWG. This working group is allowed to structure and decide on the applied disaster response. The tasks are executed and disseminated to the allocated branches at regional, district and community level. In general, the actions are executed by the ZRCS in cooperation with the DMMU. Decision making is based on the input from trigger, the Zambian Meteorological Department (ZMD), WARMA and the DMMU. In the HVS section a more in-depth insight into the decision making process is provided.

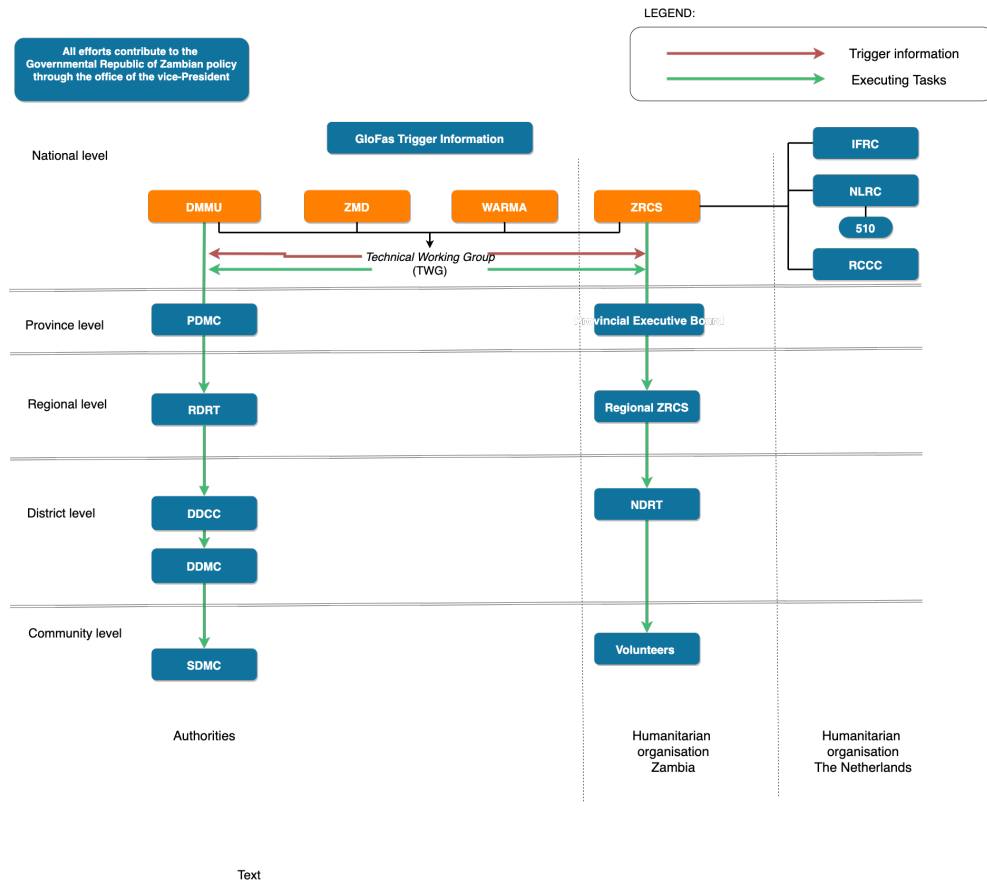


Figure 5.24: Organogram of the flow of forecast information for the EAP in Zambia (source: own work)

5.5.3 Humanitarian Stream Map

The Humanitarian (Value) Stream is mapped using the outputs from the EAP and the outputs of the interviews with the people from the ZRCS. The decision making flow of the EAP is visualized in Figure 5.25. There are a few important outcomes of the interviews that are described in the following paragraphs.

Pre-disaster actions

From the interviews held with the members of the ZRCS, specific actions have been identified as important in the pre-disaster phase. These actions are described in the EAP but have not all been put into action in Zambia. The implementation of the EAP is not yet fully put into action in Zambia. Not all pre-disaster preparation actions have been executed. Thus, they are noted here to stress the importance of the preparation phase. The green blocks in Figure 5.25 are the pre-disaster steps.

In the interviews with the ZRCS it became known that the actions described in the EAP are also largely dependent on the preposition strategy and status. As agreed upon, with the financial abilities that are supplied through the FBF strategy, the ZRCS is able to fully preposition goods in the different branches. The propositioning of goods, such as tentages and chlorine tablets, have an enormous effect in the ability of the ZRCS to act on forecasted floods. They allow regional branches of the organisation to quickly act without having to wait for further supplies. Setting up the preposition in a correct way was noted to be the most important element for ensuring a well working disaster response.

Furthermore, it was noted by an interviewed ZRCS member that it is of importance to fully inform the people in the vulnerable regions of all the effects of natural disasters. Sensitization in general is an important topic, in the humanitarian stream it is split out into multiple subjects. The sensitization has to happen in the fields of WATER Sanitation and Hygiene (WaSH), shelter provision, disease burden and food security. By making sure the public is aware of the risks, their vulnerability can lower because the people will have an increased coping capacity. With the right knowledge locals can also be trained on what to do in case of a disaster.

Lastly, it was noted that an identification of the most vulnerable would benefit the ability to react quickly to a disaster. By identifying the ones in need, the disaster response teams can target their time more wisely. This can, partly, be done in the preparation phase of the event.

Intervention time

The intervention time is between the moment the trigger is sent out and the actual flood happens. This intervention time is visualized in Figure 5.25 by

the blue and yellow blocks. The yellow blocks show the latter discussed opportunities, the blue blocks are the actual taken actions in disaster response. (as defined in the EAP)

First of all, it was noted by the interviewees that it is actually possible to execute all the actions that are stated in the EAP and in Figure 5.25 in the **seven** days of intervention time. This can only be ensured if the pre-positioning process in the pre-disaster phase is executed. But if this is secured, the 7 day intervention as supplied by Glofas and the PMRS model is enough to act on the forecasted floods.

The interviewees were also asked what possibilities additional lead time would give them. Additional lead time would have the benefit of people from the ZRCS branches to go into the affected site and identify the damage by sight, identify the ones most in need, and specify their actual current needs. They stated that it can be hard to visit the damaged site in time to make a first damage assessment. This is due to the bad road conditions, mostly influenced by heavy rain. This pre-assessment can be of importance to better target the actions taken. Also reducing the risk of not being well prepared when taking appropriate actions. The yellow blocks identify these identification processes that could be better executed with extra lead time. The PMRS model could be pushed to supply even more lead time, giving the disaster response teams extra time to execute this pre-assessment. This could be done by increasing the resolution, optimizing up- and downstream relations and combining multiple forecasts in one forecast to create more certainty.

Decision Making

The question arises, what can a decision maker, or in this instance the ZRCS do with such a system? The PMRS model is an extremely lightweight daily forecasting model that runs on a probability distribution. The model is now fitted for Senanga. But flood indication at Senanga is also valuable for flood warnings downstream. The TWG could use such a model to create more certainty in their flood warning. Now, the model has an effect on district / region level. But potentially this research could be extended to other areas that confirm the requirements. In the discussion section some suggestions are given to push the lead time even further by using a combined model.

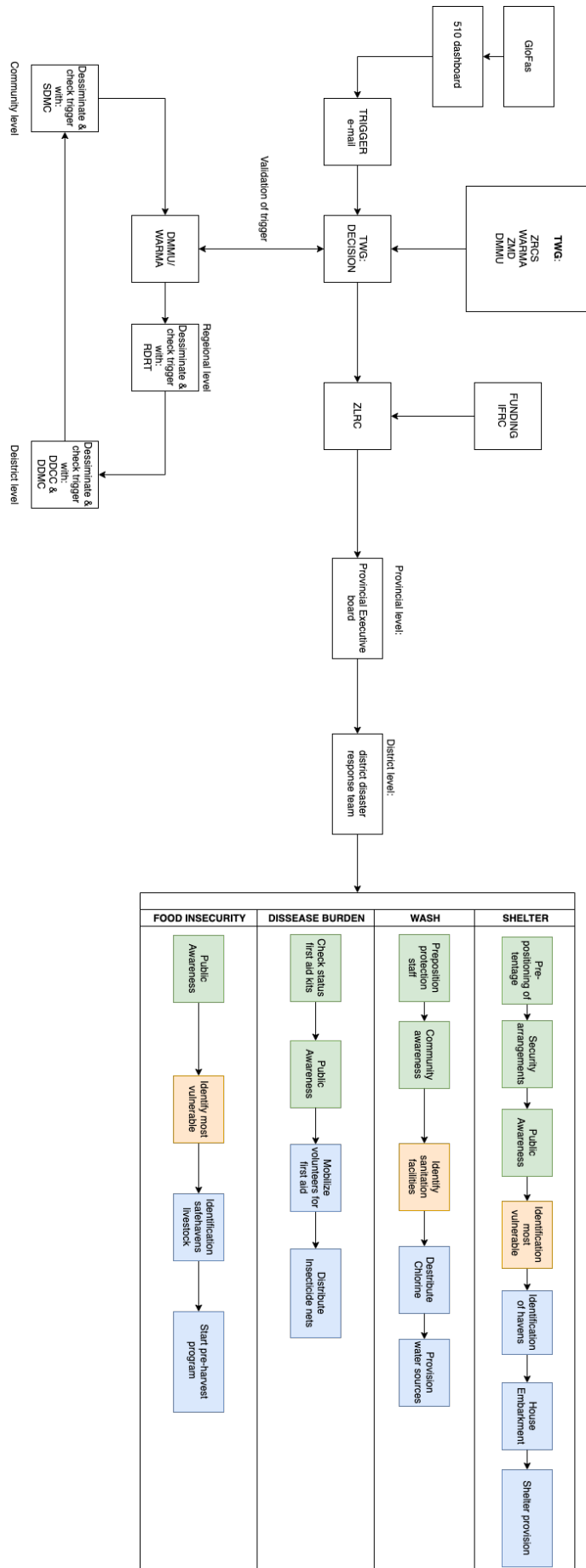


Figure 5.25: Overview of steps. Nomenclature on next page for easy reading (source: own work)

For easy reading the nomenclature of the Humanitarian Value stream map supplied:

Nomenclature:

- GloFas - Global Forecasting Awareness System
- TWG - Trigger Working Group
- ZRCS - Zambia Red Cross Society
- WARMA - Water Resources Management Authority
- ZMD - Zambia Meteorological Department
- DMMU - Disaster Management Mitigation Unit
- IFRC- International Federation of the Red Cross and Red Crescent Societies
- RDRT - Regional Disaster Response Team
- DDMC - District Disaster Management Committee
- SDMC - Satellite Disaster Management Committee
- DDCC - District Development Management Coordinator

In this chapter the outcomes of the research will be discussed and are set into perspective. The chapter is subdivided into six main parts, all touching upon a different part of the research. First the hydrological complexities of the system will be touched upon. Following a discussion about the model and its performance. The discussion is continued with insights about the satellite uncertainty. Finally the decision making and implementation strategy are discussed. The limitations are displayed at the end of the chapter.

6.1 HYDROLOGICAL COMPLEXITIES

Care should be taken with defining the sites that are monitored. There are a variety of explanations for a C/M-ratio to show insufficient predictive power. Generally speaking, when the discharge variations lead to water level changes without the inundation over the river banks, the PMRS data is mostly based on noise and flood magnitudes are useless. A solution for this problem would be to allocated river segments as input, rather than one cell. This would eliminate some of the random noise variations. A river segment could be extracted if the a combination of higher resolution pixels are used. Additional satellite products can be used to obtain higher resolution in the pixel. This could allow the user to extract river segments and combine multiple inputs in a multi-quantile regression approach.

River systems are fluid and ever changing systems. Their geography changes over time. The C/M-ratio measurement cell must always be taken in the middle of the river, to overcome problems of non-detection of inundation. The system could be improved by automatically finding an ideal location within the floodplain. This could be done by extracting river locations using optical data. It must be stated that the Zambezi river with its Barotse floodplain is the most ideal location for using PMRS data. The width, river type and clear annual inundation and the slow hydrological response, make sure the PMRS model is allowed to forecast with a specific lead time. Scalability of the product is extremely dependent on the geographical location and topography of the area.

The C/M-ratio is a measure of the comparison of two brightness temperatures. It does not entail actual discharge but rather recognizes a flooded area in-pixel. It is used to mimic the floods by looking at the percentage of the pixel that is filled with water. Therefore, a specific type of river width is required. To use such technology in different catchments, a classification of

the river-bank and -width must be made in advance.

The relative size of the contributing basin at the upstream point is a point of discussion. At Senanga, the POI's covered a very large portion of the basin that lies upstream of Senanga. In other POI's, such as upstream at Lukulu, that is not the case. A PMRS-model could be extended with a multi-quantile regression of several points or other probability methods using multiple points in several branches upstream.

A source of random noise is the effect of local heavy rain. This does not fully influence flooding but can cause local pools of water. They do not contribute to the inundation or flooding of a river, but do appear to be present/visual in the brightness temperature. In Figure 5.9 and 5.10, it can be noted that every wet season starts with a flashy signal, showing lots of noise. This noise can partly be explained because of this latter described effect of heavy rain or pools. These heavy rains can locally affect the brightness temperature and will shortly create peaks in the brightness temperature. This might change very quickly as the pools also quickly disappear due to the evaporation and infiltration.

Another point of discussion is the amount of the wetland being covered in the pixel. If the river system is not confined in a large part of the pixel and inundation patterns are not covered by the pixel, the C/M ratio signal may not be commensurate with the river flows. As stated before, combining river lengths or multiple pixels could be a way of overcoming this under-performance.

Combining the hydrological settings of a specific river system, it can be noted that there occur a wide variety of sizes, flow rates, climate conditions which influence the performance of the PMRS. As every river system differs, it is important to check the performance of each system based on the hydrological conditions that are present.

6.2 MODEL

For this model the Savitsky Golay filter is used with a polynomial degree of 1 and a window of 15 days. This SG filter allows for pre-processing of the data, without disturbing the actual output. It must be noted that the optimization of the polynomial and window is now only assessed on the best outcomes of the ROC figures. Extensive optimization of the SG filter parameters has not been performed in this study.

New satellites missions with different sensors should be tested to compare its difference to the DSMP data set. Differences were noticed in the comparison between the AMSR-E and DSMP data set. The inter-platform relations and differences are to be studied before using different satellite products.

The ROC curve measures the ability of the PMRS forecast model to discriminate between a flood or not a flood. Thus, it measures the resolution or classification performance in some way. It solely interprets the results of model. The ROC does not include any bias in the forecast, however the bias is canceled by using a regression model. The ROC does not say anything about the reliability of the PMRS model in terms of durability or stability. The ROC curve should rather be used to consider the potential usefulness of the product. To test the stability, it is advised to include a stability analysis of the system.

The model evaluates every flood year independently and then conclusions are drawn from the output of all those years combined. The latter assumes that each flood event is part of a set of independent time series. However, the characteristics of the floodplain are not taken into account. Characteristics like soil moisture or precipitation rates, can influence a system over a longer period of time. Previous high magnitudes in floods are not correlated with each other in time, while this information could be useful to estimate floods better.

The model is trained to find the C/M-ratio at a specific location. This is done by comparing the brightness temperature of the Measurement and the Calibration cell. To find the Calibration cell, the model finds the surrounding point with the highest correlation in terms of brightness temperature. However, it is not said that this cell contains no water. It just does best compared to the other surrounding 8 cells.

The imbalance in the data, at the high thresholds, resulted in uninterpretable ROC graphs. In order to overcome this problem, a solution for this imbalance should be found in a longer data set. This could be done by creating a long series of synthetic discharges (e.g. simulated with a hydrological model). From this simulated discharges, a C/M-ratio can be extracted. This simulated C/M-ratio should have the same statistical characteristics as the observe C/M-ratios, shorter in time span. The level of noise and the statistical characteristics can be obtained from a simulated discharge that is produced by a hydrological model specified to the area.

The GloFas contingency table is computed differently than the PMRS model. In the PMRS model, an extra time component is included. This time component entails the first moment a threshold is exceeded and allows the model to find a prediction given a predefined time interval. The integration of this time component is done because of its importance to forecasting. By not including the time window between the prediction and the observation, the actual forecast skill is not assessed in a way that follows the manner in which the forecast is used for decision making. With the consequence that the GloFas model is tested on the ability to locate a flood, rather than forecast the timing.

However, the choice for not integrating this in the GloFas forecast is also logical. As there is no exact (to date) impact data available, it is hard to

combine the threshold exceedance to a date. GloFas is equipped with a given lead time. This is not acquired from an upstream point in the floodplain. This difference between the PMRS and GloFas model can also be used as an advantage. When the time window of the PMRS model is set to 7 days lead time, there is also a possibility that a flood is detected before the actual 7 days. Thus the detection of a flood can also occur for example in 3 days. Giving the Senanga prediction 11 days lead time. (14 day *shift* - 3 day *time window*) This allows for a earlier trigger, giving additional information to the forecast system when combined.

6.3 SATELLITE DATA UNCERTAINTY

This research did not include a uncertainty analysis, however it provides probabilistic predictions, that are based on the uncertainty between the relationship of upstream and downstream observations. In that manner, the uncertainty is taken into account empirically. However, some of the following aspects play a role in assessing the uncertainty. For example, the sensor at the satellite has a specific sensitivity. This is stated to be 1 K. This must be taken into account when comparing with regions where the actual difference with the 'C' and 'M' cell are less visible. Some other sources of uncertainty that occur are implicitly and empirically taken into account by using fits through quantiles rather than some mean.

This research is based on the pre-set grid in the MEAsURes database where both the ASMR-E and DSMP data are given. The points of interest were selected in specific grid cells that are located within a floodplain. Depending on the locations of the grid cells, it is questionable if this research can be applied to other locations. Furthermore, the grid cells in the MEAsURes database are processed and re-gridded before uploaded to the database. It is not known what the effect is of the re-gridding and processing algorithms on the actual data.

6.4 DECISION MAKING

The GloFas product is an automated, operational product, which makes it a reliable product for humanitarian organisations. It allows to forecast and detect floods in regions where in-situ measurements are limited. However, GloFas also comes with its limitations, much experience is still to be gained (Revilla-Romero et al., 2015). It is of importance that the end user is aware of its skill and its limitations. By utilizing multiple forecast sources, it is possible to mitigate the risk and lower the uncertainty of the forecast.

Another important point to take into account when deciding which (combination of) system to use is the fact that systems are also dependent on their continuity. Flood forecasting systems rely on specific remote sensing products, satellite missions or specific funding. It is important to diversify

the inputs as there might not be a guarantee that all services will continue on the long run.

In the theoretical background, the theory of adaptive signal monitoring systems is touched upon. For an EAP conform to the adaptive planning strategies, one needs to research the implementation of such signal monitoring systems in the EAP. These strategies built on the described pillars in section 2.6. The robustness and future adaptive behaviour of the EAP can be improved by assessing such a monitoring system.

The EAP actually structures the decision making process in the pre-disaster stage quite well. By implementing this Technical Working Group (TWG), a lot of governance is regulated. The actions that are taken given a certain trigger are described well. There is not a lot of discrepancy between the trigger and the actual action to be taken. It is also quite clear who is responsible for what action. If well prepared, the response to a flooding is performed in an orderly manner. Two factors do play an important role for the future and are not included in the current EAP:

- **Population growth in vulnerable areas:** As discussed in Chapter 3 there is an expected population growth found in Zambia. By the increase of people living in vulnerable areas, the effect of a flood will increase. A problem to be tackled is the urbanisation of these vulnerable areas in the Barotse Floodplain. The government of Zambia should actively take action to overcome this problem of urbanisation. This can increase the coping capacity of the area.
- **Climate Change:** Climate change is currently stressing the coping capacity of the Zambian people. Currently, they are dealing with both extreme flooding and extreme droughts in the country. The increase in extremes has a negative influence on the effects of riverine flooding. The more intense wet seasons will stress the system even more. However, on the other side, the droughts will also negatively influence the floodplain characteristics. The ability of the soil to take up water will lower with an effect that a sudden riverine flooding will cause more harm. A well structured FFWRs can make sure the effects of climate change are taken into consideration.

6.5 IMPLEMENTATION

An important question to ask is, what would be needed in order to implement this method in the current flood forecasting system in Zambia. The PMRS model provides a flood forecast that is comparable to the GloFas product. Both models are equipped with a certain probability range. They are capable of providing a 4 and 7 day forecast on a daily basis. In other words, the systems are equivalent in the information they provide (i.e. similar lead times, both using probabilistic forecasts, both using threshold based

triggers.). The manner of forecasting is in fact very different. One uses a hydrological/hydraulic model fed with precipitation forecasts, the other uses solely upstream Earth Observation (EO). It requires super little infrastructure to run, a serious benefit for low resource environments. A server as light as a Raspberry Pi connected to a moderate internet connection. Creating a super light weight system.

Both models can provide a 4 and 7 day forecast on a daily basis. As found in the HVS results, the lead times are enough to apply all the actions in the different vulnerable areas in Zambia. The models are suited to work in cooperation to enlarge the certainty bound of a forecast system. By integrating both triggers in one final trigger, the uncertainty can be lowered. The PMRS model could be integrated by the geo-intelligence workflow as supplied in the results. This geo-intelligence workflow could run on a (light!) server and would be integrated behind the FBF dashboard. Thus, the end user will still be notified in the same manner.

6.6 LIMITATIONS

There are a few limitations that are stated to take into account when passive microwave radiometry is applied for flood forecasting. First of all, this research worked with the MEAsURes data set of NASA. This data set includes a hindcast of the data that is acquired by multiple satellite missions. The integration with a real-time data source is not tested as they are not openly available. Currently running AMSR-E or DSMP datasets are not publicly available. It can be questioned that those products can be provided by a company without charging costs. As the current EAP is run on a product which is freely available, this might become a problem when combining the GloFas product with the real-time PMRS data set.

This model has now been tested for the Barotse floodplain, which is perfect for this method in terms of topographical location and hydrological characteristics. It is still questionable if smaller floodplains also react in the same manner to this signal. Also, it is questionable if a smaller size flood can be identified by the system.

The pre-selection of the flood prone are validated using optical imagery. However, the inundation extent could be mapped in order to validate and verify the output of the PMRS model. For example, by collecting impact data through an inundation extent survey. This would be a new source of information to actually link the impact data to the output of the PMRS model. There are also possibilities for extracting flood extents from optical satellite imagery. There is a trade-off between accuracy of local input and data accessibility in satellite created products. Furthermore, manual calibration on the processing parameters (eg. SG - filters) is performed by the modeler and is based on the experience of the modeler. Additional automatic calibration and parameter estimation could increase the performance of the model (Zhang et al., 2013).

Flood forecasting is an important aspect in the disaster risk management cycle. Flood forecasting in data-scarce areas can be challenging due to the complexity in data collection and software sustenance. This research combined a method to identify floodings (Passive Microwave Radiometry) with a use-case in flood forecasting. The main research question to be answered is: "Can Satellite Passive Microwave Remote Sensing be used as a trigger for inundation Early Warning System in the Zambezi River, Zambia?" The current chapter concludes on the findings and answer on the research question.

Identification

Can Passive Microwave Remote Sensing be used to identify inundations?

The first part of this research explored the possibility of identifying and forecasting floods. Detection of inundation is found using the DSMP and AMSR-E passive microwave radiometry data sets. The brightness temperatures were acquired using a 37 GHz, horizontal polarization on the descending node. By obtaining 25 km grid cells, the brightness temperatures are converted into the C/M-ratio to identify inundation in the floodplain. Points of interest were successfully identified by taking into account various technical and geographical characteristics of the PMRS system. Clear up- and downstream signals are extracted to create the input for the PMRS model. In conclusion, the passive microwave radiometry is able to identify and forecast a flood in the Barotse floodplain.

Multi Annual Analysis

To what extent can multi-annual trends in PMRS be related to discharge records?

The multi-annual analyses of the C/M-ratio and discharge records were conducted. By combining both data sets, a polynomial relationship between the discharge and C/M-ratio is found. The strong correlation, as classified by Kendall Tau & Spearman's Rank, shows the ability to describe river flow dynamics with C/M ratio. Flood return periods are obtained for both the discharge as the C/M-ratio data sets. The return period analysis allows for the estimation of the maximum annual return periods (1,2,5 or 10 years). The high return periods that are found in the analysis, for example for the 2009 flood, correspond to a 30 year return period flood. As the return periods for the C/M-ratio and discharge records do not fully correspond, it is questionable if a relatively short data set is able to say something about high extremes beyond the length of the observation series.

Timing

Could the timing of a flood event be obtained from PMRS?

Within this sub-question, the goal was to create a model that could provide

a flood forecast, given a certain lead time and a probability distribution, based on upstream observations. Both are requirements for comparability and compatibility with current flood forecasting products. The quantile regression analysis and probability analysis led to the outcome of a flood forecasting model. Through the integration of a time window, the model was trained to only assess the **first** moment a flood occurred. An important result of this research, is the ability of the PMRS model to forecast a flood, given a lead time and probability index. It should be noticed that good flood forecasting results are obtained using low C/M-ratio threshold. This shows that a model with relatively little input data is able to forecast a flood downstream from a signal upstream. Although good results are obtained, it should be stressed that the model is not tested against actual impact data. For that, the temporal resolution of the impact data was a too coarse .

Skill Analysis

How does a PMRS based model perform in comparison with GloFas and what skill can a forecast combination with PMRS offer?

In the skill analysis, the outcomes of the model were tested for the return periods. It turned out that using the ROC graphs at high thresholds, an imbalance in the data set occurred. Nonetheless, the results for predicting exceedances of the 1 to 2-year return period flood show to have skill. The PMRS model is benchmarked against GloFas. The product showed to meet the regulations for GloFas to be qualified as a 'trustworthy' measurement station. These qualifications are $POD > 0.70$ & $FAR < 0.30$ in all probability ranges (ZRCS, 2019). Combined with the fact that the PMRS model provides equivalent information to GloFAS, there is potential to combine two systems to create more lead time and lower uncertainty levels.

Follow the Forecast

How can the lead time of (a combination of) forecasting systems be optimized to enable a maximum implementation time for the actions in an EAP?

The 'follow the forecast' part of this research focused on the timing and decision making in the FFWRs. Following from the geo-intelligence workflow, an implementation set-up of this system is provided. The system is able to run behind the FBF dashboard, thus little extra knowledge is required for the end-user. The lowering of uncertainty could speed up the decision making process. It is stated that extra lead time will not result in extra actions. However, the accuracy and effectivity of the actions can be improved by extra lead time. With this extra lead time the ZRCS and DMMU are able to better identify magnitude of the flood, identify the most vulnerable and allow for the right allocation of humanitarian goods.

To conclude on this research, the technology assessment and "follow the forecast" questions are combined to draw a final conclusion. The question to answer is whether it is possible to use passive microwave radiometry as a means for flood forecasting in the Zambezi river system in Zambia. The passive microwave radiometry provides an easy and, most important, *available* means of flood forecasting in data scarce environments. The satellite data can be combined with relatively simple flood forecasting models to supply

a probabilistic flood forecast. Especially in the Barotse Floodplain, this research has shown that the method is capable of predicting a flood, given a specific lead time and probability level. The system has shown to lower the uncertainty of a forecast. This is important in the decision making process of the EAP. Although no extra early actions would be implemented with a larger intervention window, the ZRCS and the TWG can surely benefit from an increase in certainty. It can increase the decision making process and therefore enlarge the intervention window to act. In Chapter 6, multiple limitations and uncertainties are set-out. The most important limitation is the implementation strategy for this product, further investigation is needed to fully integrate such a model into the EAP. In the light of climate change and population growth, it is favourable to increase the intervention window and lower the uncertainty of a flood forecast. Especially in the Zambezi floodplain at Senanga, the passive microwave radiometry has shown to provide extra skill to a combined forecast with GloFas.

Summing up, the PMRS allows for automated, global-covered creation of grid-based flood forecasts which are independent to cloud coverage. This thesis showed that the PMRS model can create low spatial resolution flood forecasts combined with a probability bound in just hours after satellite detection. The PMRS model has a high global potential for data scarce flood-prone river basins with similar topography and river characteristics as seen in this research.

7.1 RECOMMENDATION FOR FURTHER RESEARCH

This section includes the recommendations for future search. It is based on the noted limitations and points of discussion that are found during this research. By integrating this work in future research, the technology that is used for PMRS flood forecasting can be raised to a higher level.

First of all, it is advised to further extent on the functioning and robustness of the PMRS model. By integrating bootstrapping techniques that statistically produce a probabilistic data set, the robustness of the model's skill can be better tested, even though time series are short. The integration of the model with a current flood forecasting product such as GloFas is not tested extensively. Further research can investigate the possibilities of the different forms of cooperation that can be set up between the two models.

Secondly, it is advised to investigate the relationship between accuracy of flood detection and river characteristics. The river characteristics such as width, size or contributing catchment area only an important role in the forecasting capacity of the PMRS model. This could be investigated by finding the relation between the accuracy of the identification and forecasting and comparing this with the preciously described river characteristics. Typical widths and upstream catchment areas used in this research can be found in Table 5.1. River characteristics can be obtained in multiple ways, of which optical satellite imagery is a good starting point.

In addition, to better inform the selection of the forecast threshold, it would be interesting to further set this research into perspective using accurate impact data. By acquiring a flood extent survey and interviewing local river deputies, a more in-depth impact analysis can be collected. Additional discharge data could also lead to better insights in the relation between the CM-ratio and the discharge. By further integrating river authorities in the research, such records might be obtained. This can help to better fit the model to the actual needs of the end-user. Extra data types allow for an in-depth sensitivity and uncertainty analysis of the product.

As satellite products constantly improve, it will be interesting to see how the resolution and quality of the passive microwave radiometry will change over the years. For example, enlarging the scanning capacity of the sensor would lower the time to get a full covered PMRS profile over the earth. This can impact the intervention window time. Changes in the quality of the data can also have an impact on the spatial scalability of the product.

Finally, future research could explore the potential of using PMRS data to model hydrological processes that can also be extended to other environmental domains, such as droughts. Would it be possible to use this observational approach to complement on drought indicators? PMRS could be used in areas where river runoff and rainfall statistics largely influence the drought indicators of an area. Additional PMRS data could be beneficial to such systems.

BIBLIOGRAPHY

- FORECAST-BASED FINANCING. Technical report, German Red Cross National Headquarters, Berlin,.
- ADPC. Total disaster risk management: Good practices. Technical report, Asian Disaster Preparedness Center (ADPC), 2005.
- A. Alaoui. Mapping soil vulnerability to floods under varying land use and climate. In *Soil Mapping and Process Modeling for Sustainable Land Use Management*, pages 365–373. Elsevier, 2017.
- G. R. Brakenridge, S. V. Nghiem, E. Anderson, and R. Mic. Orbital microwave measurement of river discharge and ice status. *Water Resources Research*, 43(4):1–16, 2007. ISSN 00431397. doi: 10.1029/2006WR005238.
- K. M. Carsell, N. D. Pingel, and D. T. Ford. Quantifying the benefit of a flood warning system. *Natural Hazards Review*, 5(3):131–140, 2004.
- CIMSS. Spatial analysis, 2015. URL https://cimss.ssec.wisc.edu/sage/remote_sensing/lesson3/concepts.html.
- Coface. Economic-Studies-and-Country-Risks. <https://www.coface.com/Economic-Studies-and-Country-Risks/Zambia>, 2020. [Online; accessed 10-March-2020].
- M. Dale, J. Wicks, K. Mylne, F. Pappenberger, S. Laeger, and S. Taylor. Probabilistic flood forecasting and decision-making: an innovative risk-based approach. *Natural hazards*, 70(1):159–172, 2014.
- D. Dataman. Why can't I just Use the ROC curve. <https://towardsdatascience.com/sampling-techniques-for-extremely-imbalanced-data-281cc01da0a8>, 2018.
- T. de Groeve. Flood monitoring and mapping using passive microwave remote sensing in Namibia. *Geomatics, Natural Hazards and Risk*, 1(1):19–35, 2010. ISSN 19475705. doi: 10.1080/19475701003648085.
- T. De Groeve. Flood monitoring and mapping using passive microwave remote sensing in namibia. *Geomatics, Natural Hazards and Risk*, 1(1):19–35, 2010.
- T. De Groeve and P. Riva. Global real-time detection of major floods using passive microwave remote sensing. Technical report. URL <http://www.gdacs.org/floods>.
- T. De Groeve and P. Riva. Early flood detection and mapping for humanitarian response. Technical report, 2009a.

- T. De Groeve and P. Riva. Global real-time detection of major floods using passive microwave remote sensing. In *Proceedings of the 33rd international symposium on remote sensing of environment, Stresa, Italy*, pages 4–8, 2009b.
- European Space Agency (ESA). What is remote sensing, 2015. URL http://www.esa.int/SPECIALS/Eduspace_NL/SEM7YBE3GXF_0.html.
- J. Gaillard and J. Mercer. From knowledge to action, bridging gaps in disaster risk reduction. *Progress in Human Geography*, 37:93–114, 2013.
- GRC. Forecast-based financing, a new era in humanitarian help. Brochure, 2017. URL <https://www.forecast-based-financing.org/>.
- M. Haasnoot, S. van 't Klooster, and J. van Alphen. Designing a monitoring system to detect signals to adapt to uncertain climate change. *Global Environmental Change*, 52:273–285, 9 2018. ISSN 09593780. doi: 10.1016/j.gloenvcha.2018.08.003.
- IFRC. Early Warning, Early Action. <https://media.ifrc.org/ifrc/document/early-warning-early-action/>, 2008. [Online; accessed 10-March-2020].
- IFRC. Manual Forecast Based Financing. <https://media.ifrc.org/ifrc/fba/>, 2008. [Online; accessed 10-March-2020].
- I.N. Streefkerk. Linking Drought Forecast Information to Smallholder Farmers's Agricultural Strategies and Local Knowledge in Southern Mali. Technical report, TU Delft, Delft, 2020.
- K. E. Joyce, K. C. Wright, S. V. Samsonov, and V. G. Ambrosia. Remote sensing and the disaster management cycle. *Advances in geoscience and remote sensing*, pages 317–346, 2009.
- R. Kawsar. Water resource management and remote sensing, a prospective issue that requires considerable attention. blog, 2015. URL <https://geoawesomeness.com/water-resource-managment-and-remote-sensing-a-prospective-issue-that-requires-considerabl>
- A. M. Kinoshita and T. S. Hogue. Spatial and temporal controls on post-fire hydrologic recovery in southern california watersheds. *CATENA*, 87(2):240 – 252, 2011. ISSN 0341-8162. doi: <https://doi.org/10.1016/j.catena.2011.06.005>. URL <http://www.sciencedirect.com/science/article/pii/S0341816211001196>.
- R. Lemmens, B. Toxopeus, L. Boerboom, M. Schouwenburg, B. Retsios, W. Nieuwenhuis, and C. Mannaerts. Implementation of a comprehensive and effective geoprocessing workflow environment. *International Archives of the Photogrammetry, Remote Sensing & Spatial Information Sciences*, 42, 2018.
- B. D. Macdonald. The greenhouse gases and infrared radiation misconceived by thermoelectric transducers. *Update*, 2019:05–11, 2019.
- M. Martina, E. Todini, and A. Libralon. A bayesian decision approach to rainfall thresholds based flood warning. 2006.

- Neisingh, W. Unveiling inundations. Technical report, TU Delft, Delft, 2018.
- OCHA. Humanitarian Response, Disasters, Zambia. <https://www.humanitarianresponse.info/en/disaster/fl-2020-000007-zmb>, 2020.
- Ohuru R. A Method for Enhancing Shareability and Reproducibility of Geoprocessing Workflows. Case Study: Integration of Crowdsourced Geoinformation, Satellite and In-Situ Data for Water Resource Monitoring. Technical report, TU Twente, 2019.
- M. Owe and A. A. Van de Griend. Comparison of soil moisture penetration depths for several bare soils at two microwave frequencies and implications for remote sensing. *Water Resources Research*, 34(9):2319–2327, 1998. doi: 10.1029/98WR01469. URL <https://agupubs.onlinelibrary.wiley.com/doi/abs/10.1029/98WR01469>.
- D. Parker and M. Fordham. An evaluation of flood forecasting, warning and response systems in the european union. *Water Resources Management*, 10(4):279–302, 1996.
- B. Revilla-Romero, F. Hirpa, J. Pozo, P. Salamon, R. Brakenridge, F. Pappenberger, and T. De Groeve. On the Use of Global Flood Forecasts and Satellite-Derived Inundation Maps for Flood Monitoring in Data-Sparse Regions. *Remote Sensing*, 7(11):15702–15728, 11 2015. ISSN 2072-4292. doi: 10.3390/rs71115702. URL <http://www.mdpi.com/2072-4292/7/11/15702>.
- R. N. Rodriguez and Y. Yao. Five things you should know about quantile regression. In *Proceedings of the SAS global forum 2017 conference, Orlando*, pages 2–5, 2017.
- R. Šakić Trogrlić and M. van den Homberg. Indigenous knowledge and early warning systems in the lower shire valley in malawi. 2018.
- R. Šakić Trogrlić, G. B. Wright, M. J. Duncan, M. J. van den Homberg, A. J. Adeloje, F. D. Mwale, and J. Mwafulirwa. Characterising local knowledge across the flood risk management cycle: a case study of southern malawi. *Sustainability*, 11(6):1681, 2019.
- L. L. Salvadó, M. Lauras, and T. Comes. Humanitarian Value Stream Mapping: Application to the EBOLA outbreak. *ISCRAM 2015 Conference Proceedings - 12th International Conference on Information Systems for Crisis Response and Management*, 2015-Janua, 2015.
- G. J. Schumann, J. C. Neal, N. Voisin, K. M. Andreadis, F. Pappenberger, N. Phanthuwongpakdee, A. C. Hall, and P. D. Bates. A first large-scale flood inundation forecasting model. *Water Resources Research*, 49(10):6248–6257, 2013. ISSN 00431397. doi: 10.1002/wrcr.20521.
- T. Teule. Assessing Two Methods to Potentially Improve the Flood Early Warning System in Malawi. Technical report, 2019. URL 510.global/research.

- V. Thiemig, B. Bisselink, F. Pappenberger, and J. Thielen. A pan-african medium-range ensemble flood forecast system. *Hydrol. Earth Syst. Sci*, 19 (8):3365–3385, 2015.
- J. Timberlake. *Biodiversity of the Zambezi basin*. Biodiversity Foundation for Africa Bulawayo, Zimbabwe, 2000.
- UNDRR. Zambia: Risk-sensitive Budget Review. Technical report.
- UNFCCC. Economic Losses, Poverty and Disasters. Technical report.
- United Nations. United Nations Dataset. http://data.un.org/CountryProfile.aspx/_Images/CountryProfile.aspx?crName=Zambia, 2015. [Online; accessed 10-March-2020].
- United Nations. *National Report Zambia*, 2016. URL https://sustainabledevelopment.un.org/content/documents/dsd/dsd_aofw_ni/ni_pdfs/NationalReports/zambia/Drought.pdf.
- United Nations, ISDR. Developing Early Warning Systems: A Checklist. Technical report, 2017. URL <https://www.unisdr.org/2006/ppew/info-resources/ewc3/checklist/English.pdf>.
- J. Verkade and M. Werner. Estimating the benefits of single value and probability forecasting for flood warning. *Hydrology & Earth System Sciences Discussions*, 8(4), 2011.
- A. Weerts, H. Winsemius, and J. Verkade. Estimation of predictive hydrological uncertainty using quantile regression: examples from the national flood forecasting system (england and wales). *Hydrology and Earth System Sciences*, 15(1):255, 2011.
- X. Yang, T. M. Pavelsky, G. H. Allen, and G. Donchyts. Rivwidthcloud: An automated google earth engine algorithm for river width extraction from remotely sensed imagery. *IEEE Geoscience and Remote Sensing Letters*, 2019.
- Y. Zhang, Y. Hong, X. Wang, J. Gourley, J. Gao, H. Vergara, and B. Yong. Assimilation of passive microwave streamflow signals for improving flood forecasting: A first study in cubango river basin, africa. *Selected Topics in Applied Earth Observations and Remote Sensing, IEEE Journal of*, 6:2375–2390, 12 2013. doi: 10.1109/JSTARS.2013.2251321.
- ZRCS. Early Action Protocol, Flood Hazard. Technical report, 510.global, IFRC, Zambia, 2019.

APPENDIX A

A | POLARISATION COMPARISON

Brakenridge et al. (2007) defined the H(orizontal) polarization to be the most optimum for its sensitivity to surface water (water fraction) and the soil moisture percentage. Described in the Figure A.1.

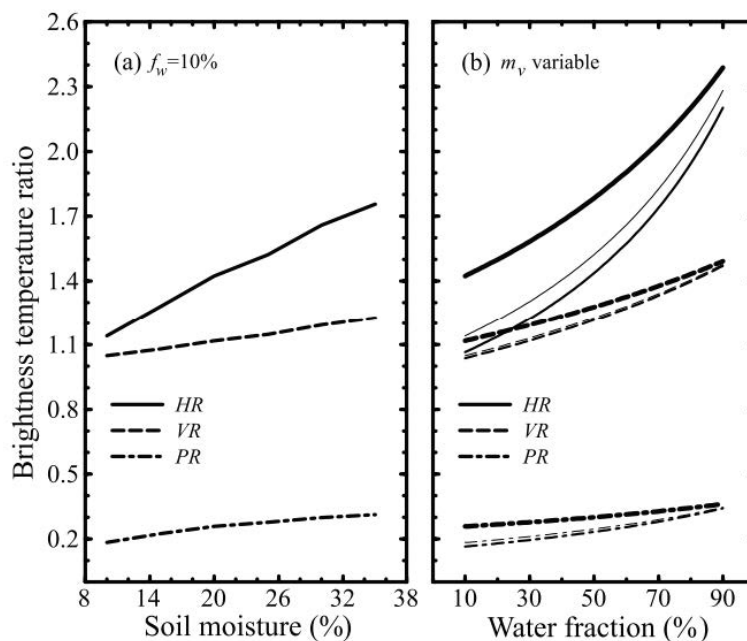


Figure A.1: Brightness temperature change for a silt-loam soil type. Comparison to see how the TB changes with water fraction and soil moisture percentage. The HR polarisation shows to be the most preferable (Brakenridge et al., 2007)

APPENDIX B

B | ZAMBEZI RIVER INFORMATION

This Appendix includes some visualizations of Barotse floodplain located in the Zambezi river catchment in Zambia. It entails different figures that show the flood extent and average precipitation.

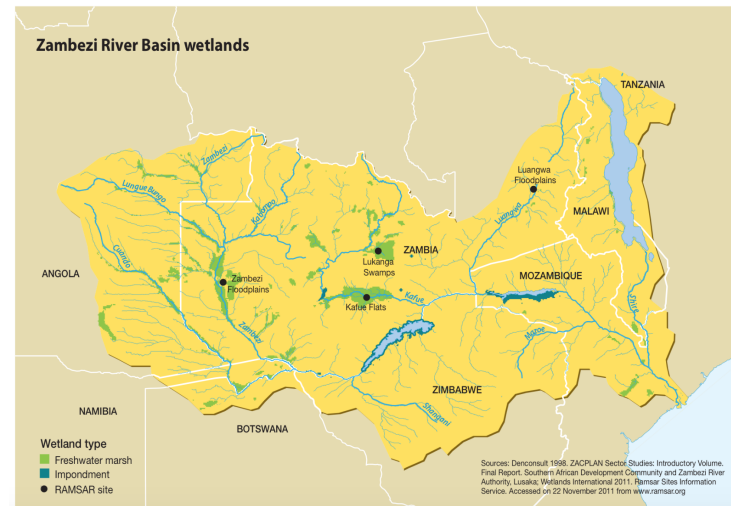


Figure B.1: Zambezi catchment area (source: Denconsult)

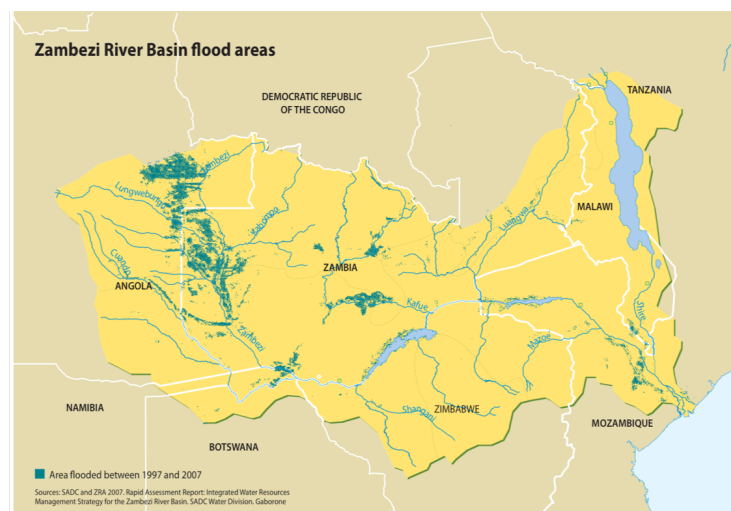


Figure B.2: Zambezi catchment area, flood extent (source: Denconsult)

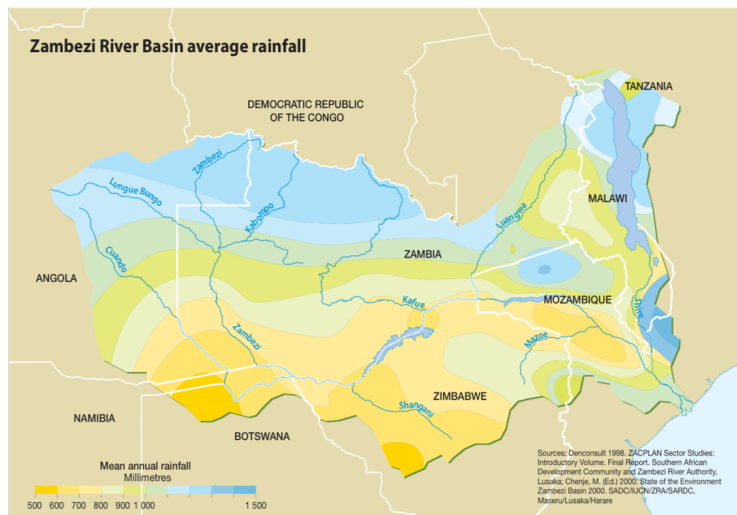


Figure B.3: Zambezi catchment area, precipitation rates (source: Denconsult)

APPENDIX C

C | DISCHARGE VS C/M-RATIO RELATIONSHIP

The discharge levels at Senanga are compared to the CM ratio values at the same geographical location. Few interesting things seen in the graphs. First of all, the onset of the peaks occurs at the same time. This indicates that the CM ratio and the Discharge both show the same flood occurring at the same moment in time. The CM ratio showed a different behaviour in the end of the rain season. At the end of the season it is seen that the CM ratio keeps higher values, although the ground-truth discharge data lowers. This is due to the fact that the CM ratio measured the surface water levels. In wetlands it is more common for water to stay on the land in smaller pools. This effect of wetlands was clearly seen in the CM ratio.

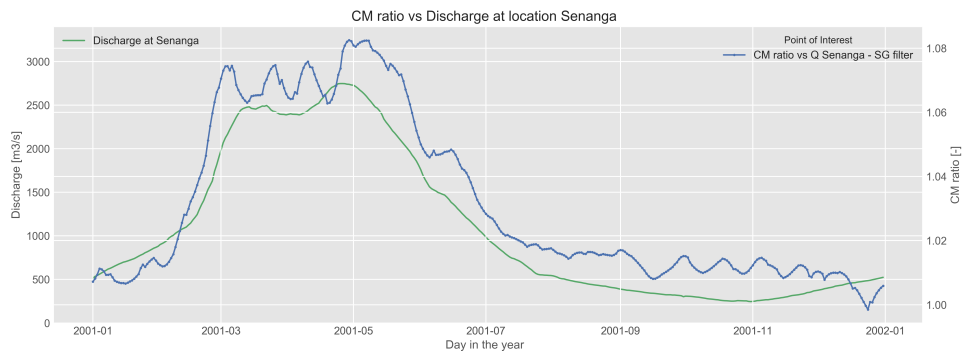


Figure C.1: Discharge - CM ratio relationship at Senanga in 2001 - DSMP dataset (source: own work)

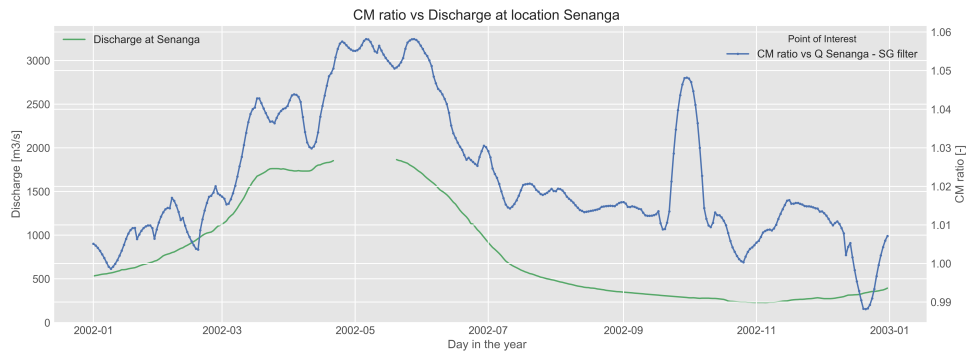


Figure C.2: Discharge - CM ratio relationship at Senanga in 2002 - DSMP dataset (source: own work)

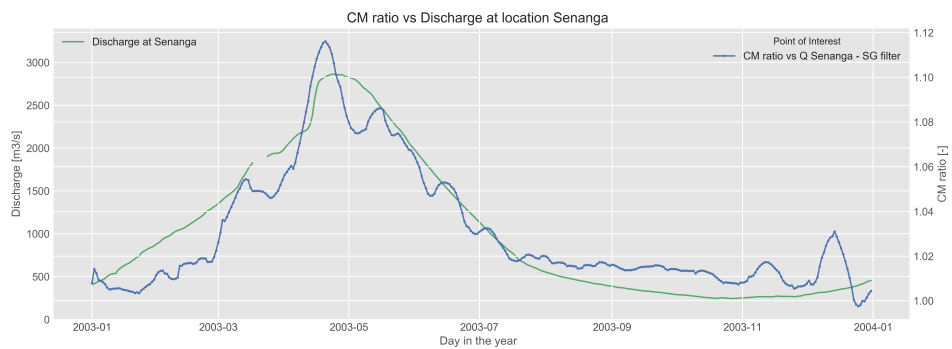


Figure C.3: Discharge - CM ratio relationship at Senanga in 2003 (source: own work)

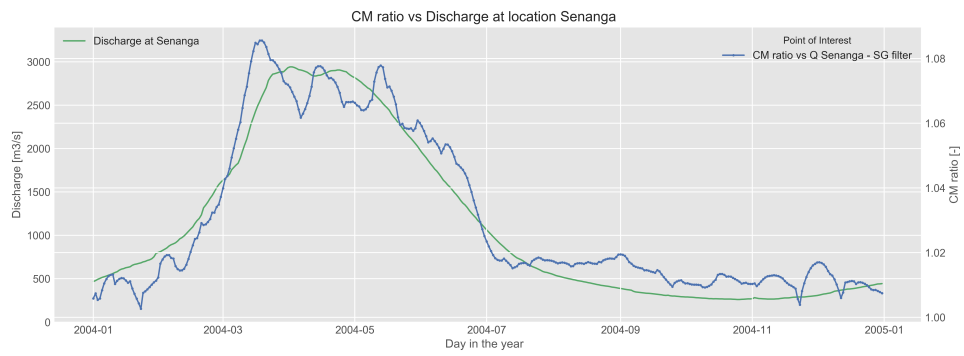


Figure C.4: Discharge - CM ratio relationship at Senanga in 2004 - DSMP dataset(source: own work)

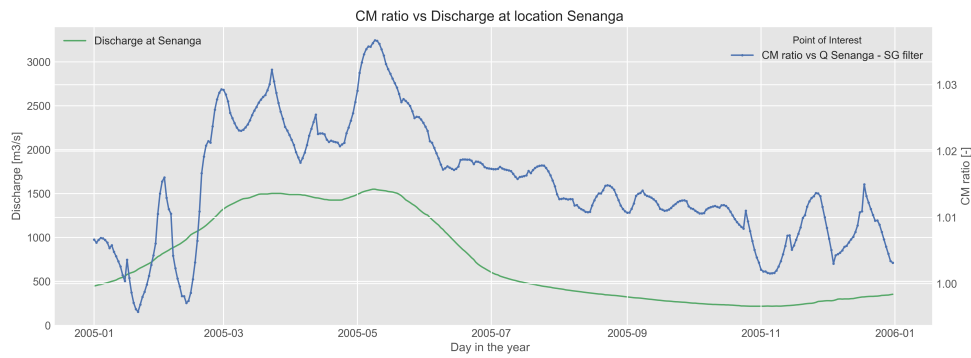


Figure C.5: Discharge - CM ratio relationship at Senanga in 2005 - DSMP dataset(source: own work)

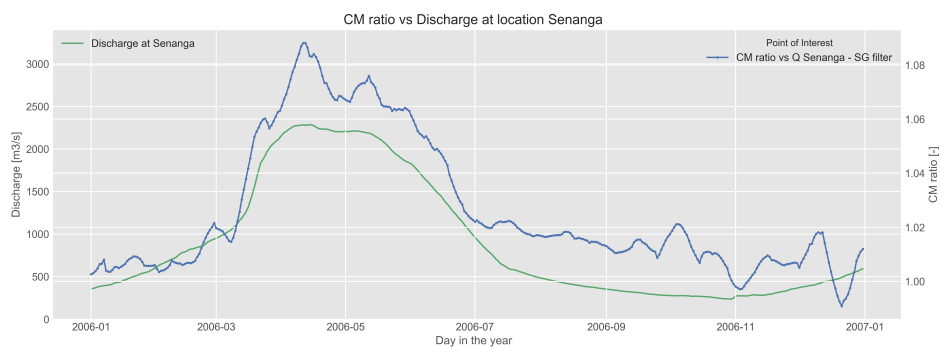


Figure C.6: Discharge - CM ratio relationship at Senanga in 2006 - DSMP dataset(source: own work)

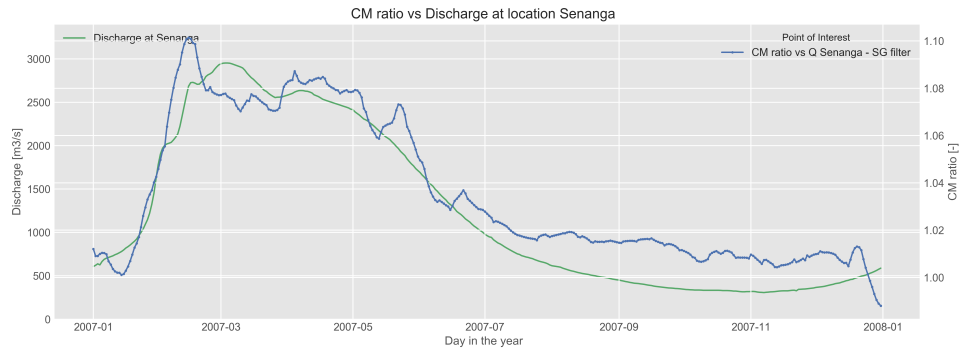


Figure C.7: Discharge - CM ratio relationship at Senanga in 2007 - DSMP dataset(source: own work)

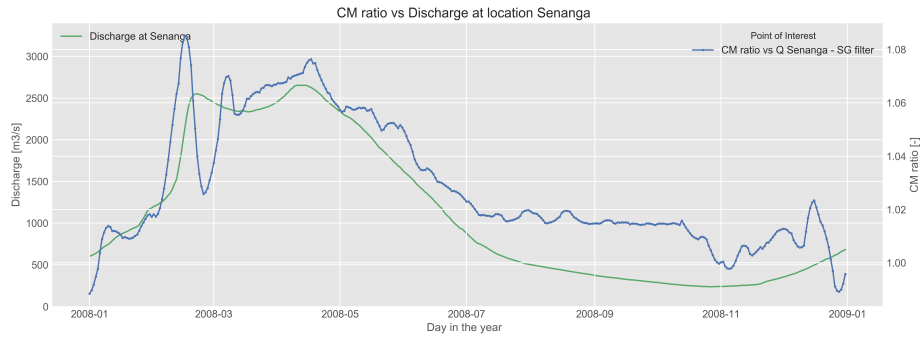


Figure C.8: Discharge - CM ratio relationship at Senanga in 2008 - DSMP dataset(source: own work)

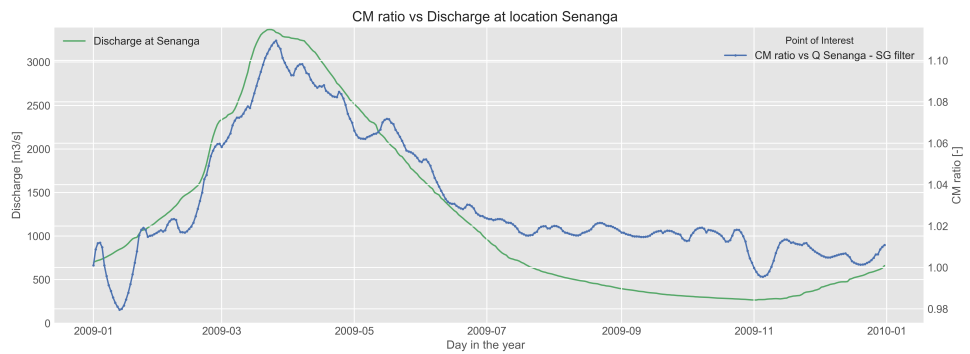


Figure C.9: Discharge - CM ratio relationship at Senanga in 2009 - DSMP dataset(source: own work)

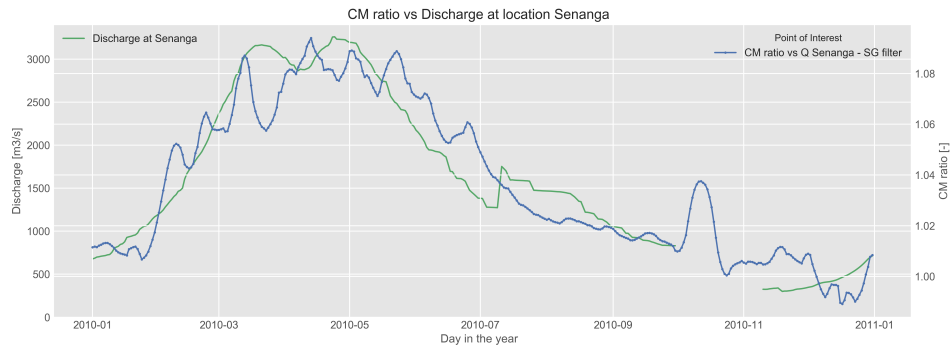


Figure C.10: Discharge - CM ratio relationship at Senanga in 2010 - DSMP dataset (source: own work)

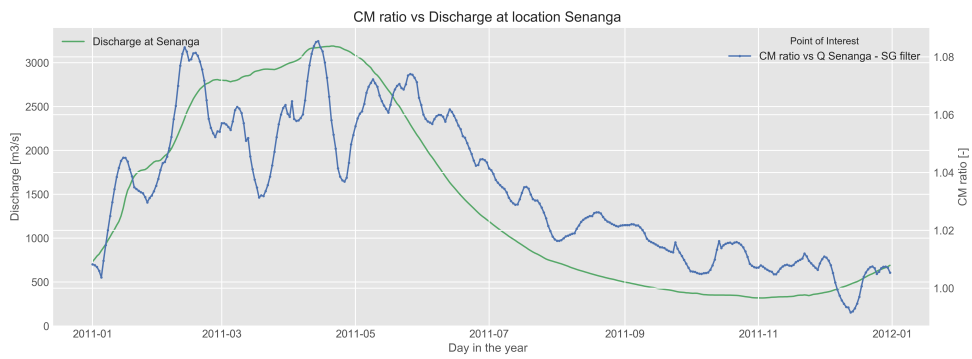


Figure C.11: Discharge - CM ratio relationship at Senanga in 2011 - DSMP dataset (source: own work)

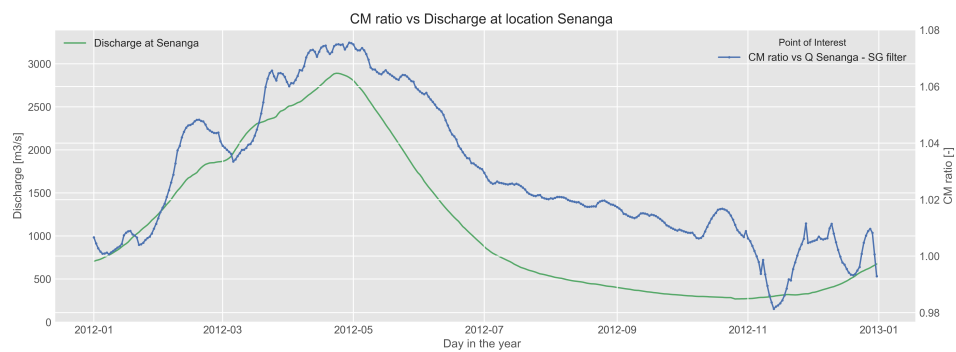


Figure C.12: Discharge - CM ratio relationship at Senanga in 2012 - DSMP dataset (source: own work)

APPENDIX D

Di | IDENTIFICATION OF UP- AND DOWNSTREAM AREAS

This Appendix entails the work done for the identification of the different Points of Interest and provides more ROC graphs. The work is part of the Chapter 5.

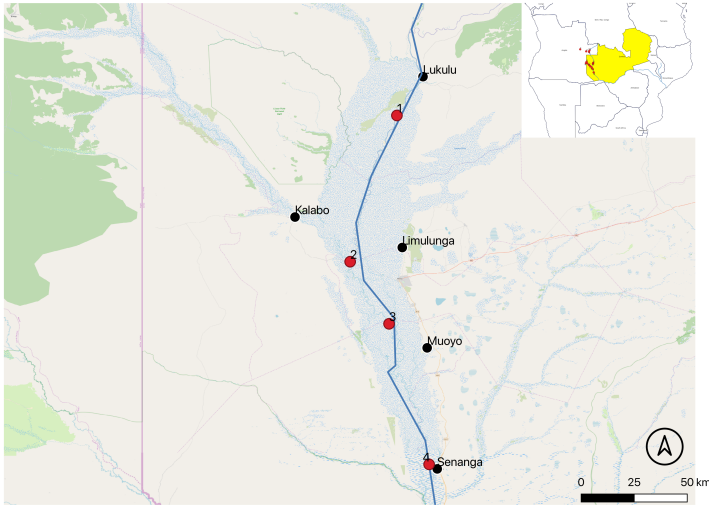
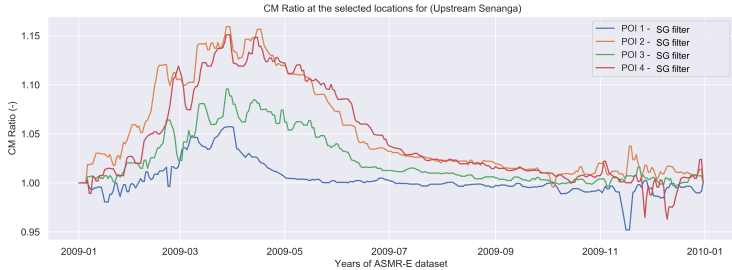


Figure D.i.1: Upstream POI's at Senanga in the Barotse floodplain (source: own work)

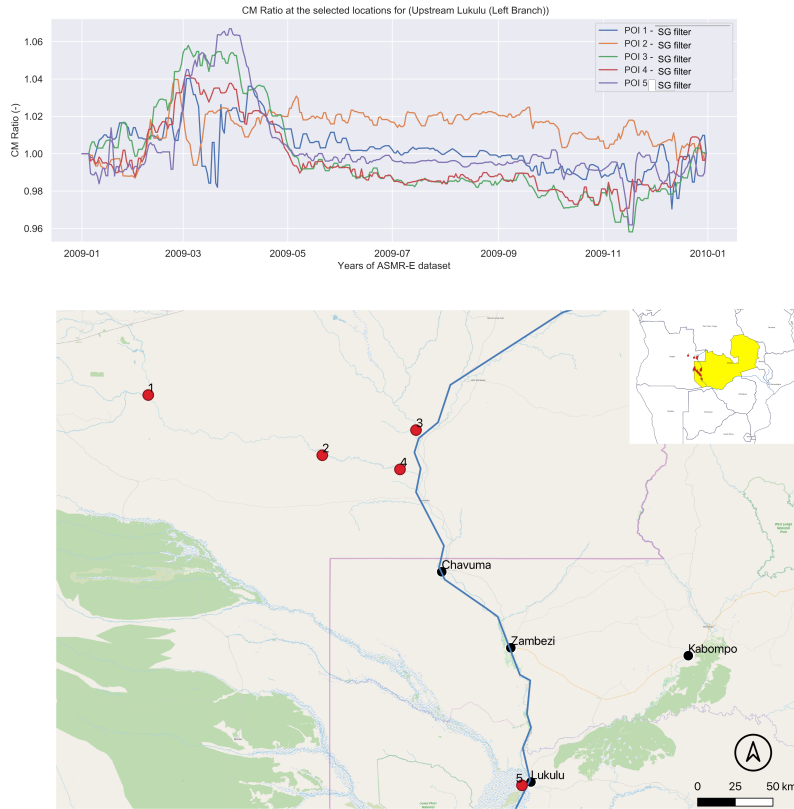


Figure D.i.2: Upstream POI's North/West of Lukulu (source: own work)

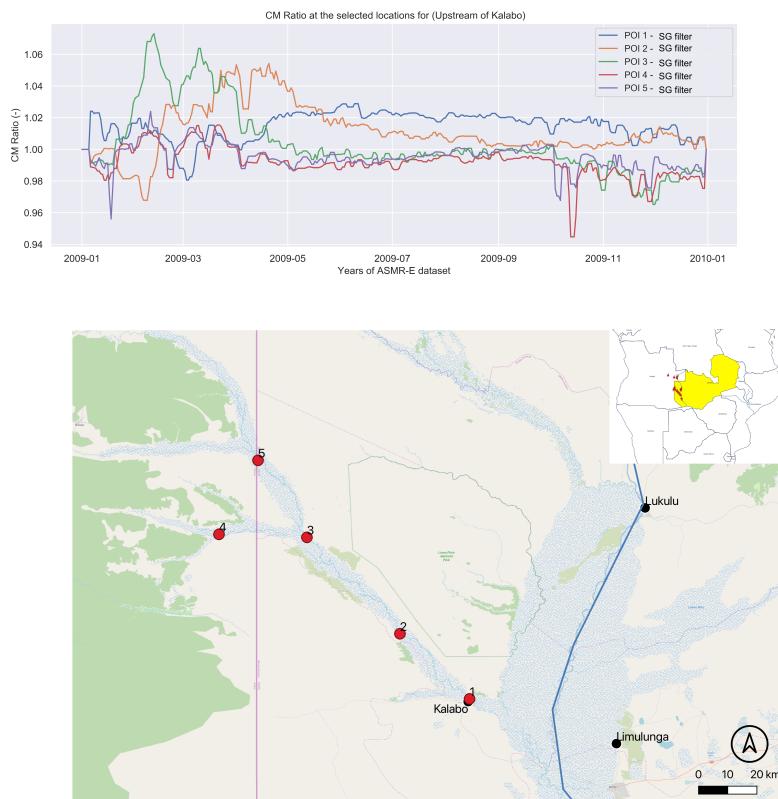


Figure D.i.3: Upstream POI's West of Kalobo (source: own work)

ROC plots for the thresholds that correspond to the 10 and 5 year return period. The ROC figures are not valid as there occurs an imbalance in the dataset. Explanation for the used ROC figures can be found in Chapter 5.

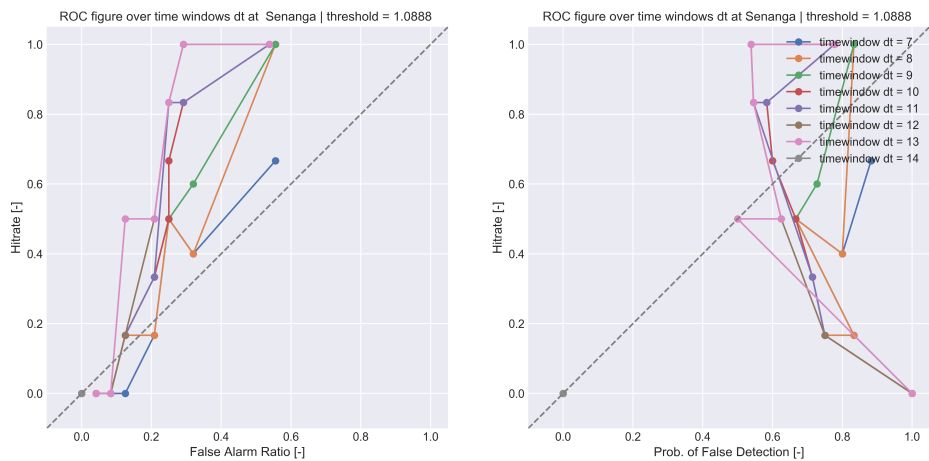


Figure D.ii .1: Senanga DMSP dataset with threshold = 1.07. ROC graphs at Senanga for the DSMP dataset. The threshold is set at one specific level and the ROC curve is changed over different time windows (dt).(source: own work)

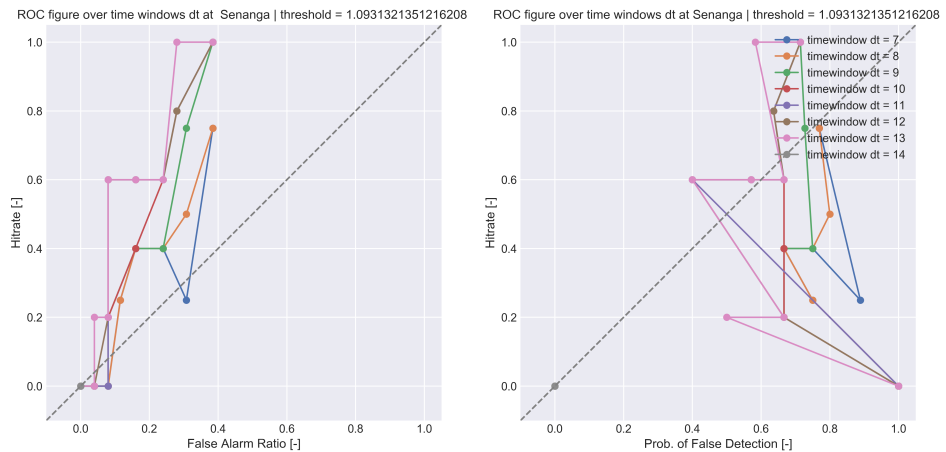


Figure D.ii .2: Senanga DMSP dataset with threshold = 1.09. ROC graphs at Senanga for the DSMP dataset. The threshold is set at one specific level and the ROC curve is changed over different time windows (dt).(source: own work)

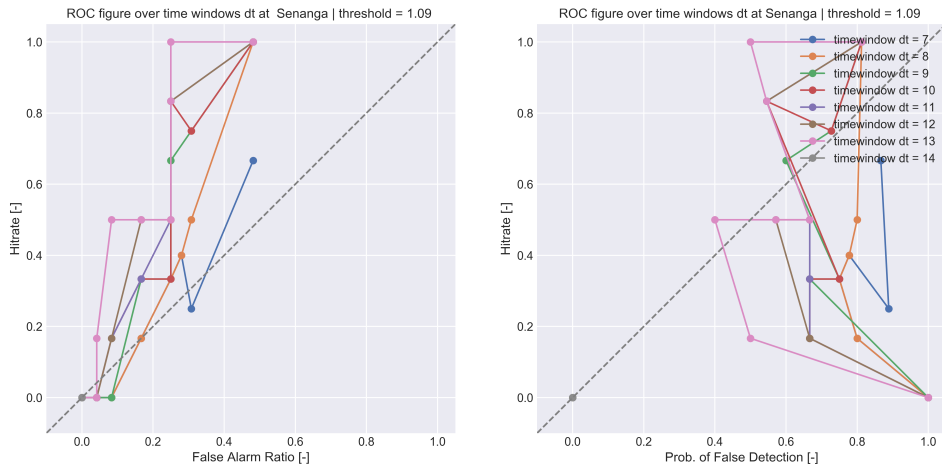


Figure D.ii .3: Senanga DMSP dataset with threshold = 1.09. ROC graphs at Senanga for the DSMP dataset. The threshold is set at one specific level and the ROC curve is changed over different time windows (dt).(source: own work)

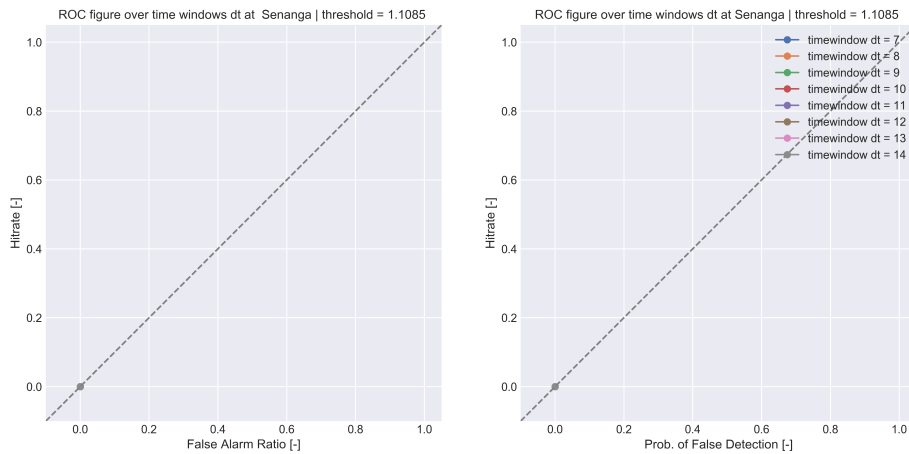


Figure D.ii .4: Senanga DMSP dataset with threshold = 1.11. ROC graphs at Senanga for the DSMP dataset. The threshold is set at one specific level and the ROC curve is changed over different time windows (dt) No output can be generated at this threshold. (source: own work)

APPENDIX E

E | GEO-INTELLIGENCE MODEL STRUCTURE

In this Appendix the geo-intelligence workflow of the model is visualized.

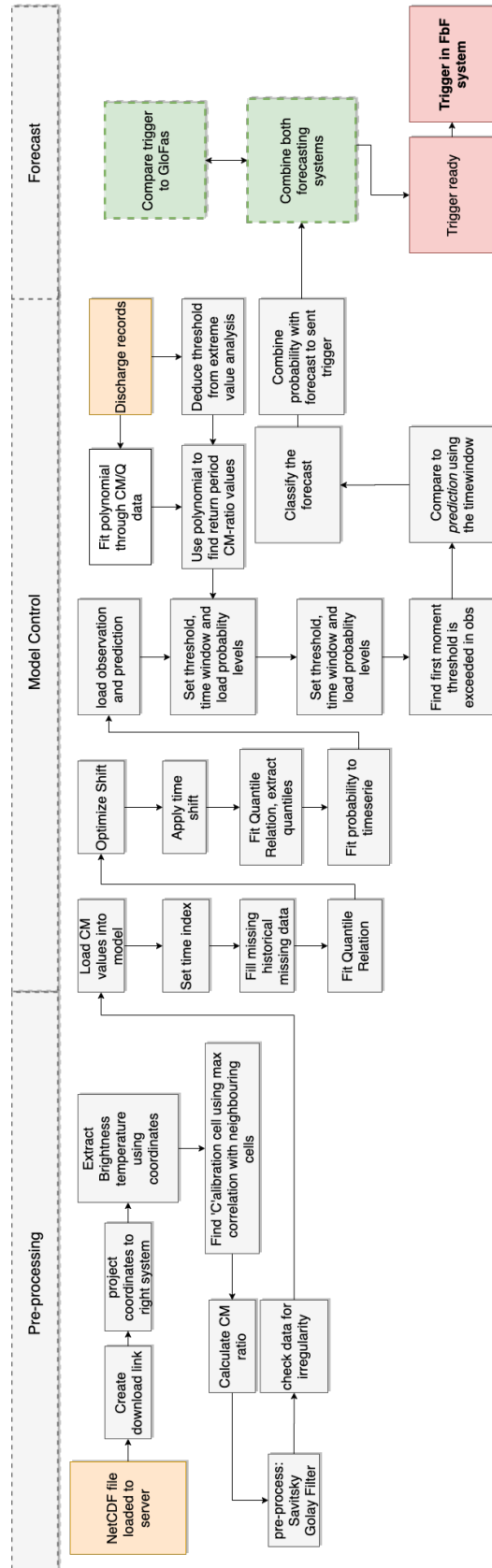


Figure E.1: Geo-intelligence workflow inside the model. Inputs are given in yellow (source: own work)

COLOPHON

This document was typeset using L^AT_EX.

